Analysis of natural eye movements to assess visual field loss in glaucoma

Daniel Sileshi Asfaw

A thesis submitted for the degree of Doctor of Philosophy

Division of Optometry and Visual Science
School of Health Sciences

March 2020

Contents

Contents iii

List of Tables vii

List of Figures ix

List of Abbreviations xvii

Acknowledgements xix

Declaration xxi

Thesis Abstract xxiii

1 Introduction 1
- 1.1 Preamble and Motivation . . . 1
- 1.2 Glaucoma and visual function . . . 2
  - 1.2.1 Glaucoma . . . 3
  - 1.2.2 Visual function . . . 4
  - 1.2.3 Binocular visual field . . . 9
- 1.3 Eye movements . . . 9
  - 1.3.1 Types of eye movements . . . 10
  - 1.3.2 What drives eye movements when viewing a scene? . . . 12
- 1.4 Eye tracking . . . 15
  - 1.4.1 History of eye tracking methods . . . 16
  - 1.4.2 Eye movement recording methods . . . 17
- 1.5 Some key challenges regarding the use of eye-movements to detect or quantify vision loss . . . 19
- 1.6 Objectives . . . 20

2 Eye movements in glaucoma: A literature review 23
- 2.1 Introduction . . . 23
- 2.2 Methods . . . 24
  - 2.2.1 Data Sources and Search Strategies . . . 24
  - 2.2.2 Screening of citations . . . 24
- 2.3 Results . . . 33
  - 2.3.1 Driving . . . 33
  - 2.3.2 Reading . . . 35
  - 2.3.3 Mobility . . . 36
  - 2.3.4 Free viewing . . . 36
  - 2.3.5 Visual search . . . 37

2.3.6 Other tasks . . . 37
2.4 Discussion . . . 39
2.5 Conclusions . . . 41

3 Does glaucoma alter eye movements when viewing images of natural scenes? A between-eye study 43
3.1 Introduction . . . 43
3.2 Methods . . . 45
3.2.1 Participants . . . 45
3.2.2 Clinical testing . . . 45
3.2.3 Apparatus . . . 48
3.2.4 Stimuli . . . 48
3.2.5 Procedure . . . 48
3.2.6 Eye movement analysis . . . 49
3.2.7 Statistical analyses . . . 52
3.3 Results . . . 53
3.4 Discussion . . . 54
3.4.1 Comparison with previous findings . . . 55
3.4.2 Relationship between eye movements and common clinical measures . . . 57
3.4.3 Implications and future work . . . 57
3.5 Conclusions . . . 58

4 Using eye movements to detect visual field loss: a pragmatic assessment using simulated scotoma 59
4.1 Introduction . . . 59
4.2 Methods . . . 62
4.2.1 Task overview . . . 62
4.2.2 Participants . . . 62
4.2.3 Stimuli and Study design . . . 65
4.2.4 Procedure . . . 66
4.2.5 Eye movement analysis . . . 67
4.2.6 Statistical analyses . . . 70
4.2.7 Further analysis to improve separation performance . . . 70
4.2.8 Receiver operating characteristics (ROCs) analysis . . . 73
4.3 Results . . . 74
4.3.1 Statistical analysis results . . . 74
4.3.2 Receiver operating characteristic (ROC) analysis results . . . 76
4.3.3 Improving separation performance . . . 78
4.4 Discussion . . . 80

5 Detecting glaucomatous visual field loss using a novel spatiotemporal analysis of eye movements 83
5.1 Introduction . . . 83
5.1.1 Participants . . . 84
5.1.2 Clinical Vision Tests . . . 85
5.1.3 Raw gaze data . . . 87
5.1.4 Processed eye movement data . . . 87
5.2 Experimental design, materials and methods . . . 88
5.2.1 Apparatus . . . 88
5.2.2 Stimuli . . . 89

5.3 Methods . . . 91
5.3.1 Pre-processing of the eye movements data . . . 91
5.3.2 Reference methods . . . 91
5.3.3 Novel spatiotemporal analysis (Index method) . . . 92
5.4 Results . . . 97
5.5 Discussion . . . 100
5.5.1 Significance of results . . . 100
5.5.2 Prior work on using machine learning classifiers to analyse eye movements . . . 102
5.5.3 Effect of video content . . . 102
5.5.4 Potential limitations and future work . . . 103

6 Overview and future work **105**
6.1 Update to systematic review . . . 107
6.2 Thesis contributions . . . 107
6.3 Limitations and future work . . . 108

A Images used for the experiment in Chapter 3 **113**

B Supplemental material for Chapter 4 **115**

C Supplemental material for Chapter 5 **119**
C.1 Analysis using summary eye movement measures for dataset in Chapter 5 119
C.1.1 Saccade amplitude 119
C.1.2 Saccade rate 119
C.1.3 The spread of fixations: Bivariate contour ellipse area (BCEA) . . 120
C.1.4 Fixation duration 120
C.1.5 Kernel density estimate (KDE) of gaze fixations 120
C.1.6 Saccadic reversal rate 120

References **123**

List of Tables

Table 2.1 Summary of literature reviewed showing sample size, eye movement parameters used for comparison and task involved. The sign (↑) is used when eye movement parameters are larger/more frequent (statistically significant) in patients with glaucoma than in control subjects; conversely, the sign (↓) indicates that eye movement parameters are smaller/less frequent (statistically significant). The sign (-) represents a finding of no difference between patients and control subjects. For completeness, task performance measures used are included. 26

Table 3.1 Patient information and demographics. Patient IDs colours correspond to marker colours used subsequently in Figures 3.1 and 3.6. 46

Table 3.2 Comparison of the difference between worse and the better eyes in different eye movement features. Statistically significant p values are marked with an asterisk and highlighted in bold. 54

Table 3.3 Spearman's rho correlations comparing between-eye differences in saccade amplitude, BCEA, and SRR with clinical measures and age. Statistically significant associations are marked with an asterisk and highlighted in bold. (Following Bonferroni correction for four comparisons, the criterion for significance was $p < 0.013$.) 54

Table 5.1 Sample clinical information of participants. The complete tables for both patients and controls are uploaded in a spreadsheet file. The tables have eight fields: participants' ID, the eye used for the study, age, sex, MD measurements (for both left and right eyes), binocular VA, and CS measurements. Participants were assigned a unique ID, G001–G044 for patients and C001–C032 for controls. Shown here are the data from the first five patients. 86

Table 5.2 Sample sensitivity values for each of the 54 test points in the 24-2 VF test. The results provided are for every participant/eye. The data for G007 is also shown graphically in Figure 5.1. 87

Table 5.3 Description of fixation and saccade fields contained within the 'processed eye movement data' CSV files. Five events (trial name, eye, start time, end time, and duration) are similar for both fixation and saccade events. Saccade and fixation positions are expressed using four (Start X, Start Y, End X, and End Y) and two (X and Y) fields, respectively. In addition, each saccade has two additional fields that describe the size and speed of the saccade. 88
Table 5.4 Details of the stimuli (three video clips) used in the experiment. . . . 89

List of Figures

Figure 1.1 Schematic of an eye illustrating the impact of raised intraocular pressure on the fluid pathway and optic nerve. Glaucoma can partially or completely block the outflow of aqueous fluid through the trabecular meshwork. Based on the angle (between the iris and cornea), it can be open-angle or closed-angle glaucoma. The image is from https://nearsay.com accessed in January 2020. 5

Figure 1.2 Example of VF showing point-wise sensitivity levels in dB, GHT, MD, and PSD. 8

Figure 1.3 A greyscale plot of Humphrey 24-2 fields from the left and right eyes are merged point by point to produce the simulated IVF. The maximum sensitivity from the left and right eye VF corresponding points are used to estimate the sensitivity values in the stimulated IVF. 10

Figure 1.4 The eye tracker used by Guy Buswell in 1935 in his study of picture viewing. A) The subject, with head restrained, views the picture on the screen to the left. B) An eye scan of one of the pictures used in the studies, 'The Wave' by Hokusai. 17

Figure 2.1 Flow of articles selection process in the systematic review. 24

Figure 2.2 The frequency of published papers and the citation received over time grouped by task involved in the study. 33

Figure 3.1 HFA Greyscales of monocular visual fields for all 15 participants measured using the 24-2 algorithm (SITA). HFA MD values (dB) are given for each image, and were used to classify the eye as Better or Worse. The worse eye in each image is indicated by asterisk. 47

Figure 3.2 Stimuli, Apparatus and Procedures (a) Participants were seated 60 cm from the screen (distance constrained using the chin-/head-rest), and viewed the stimuli monocularly. An eye tracker was mounted below the monitor, and recorded eye movements during test trials. Participants used a computer keyboard to initiate each trial. (b) The stimuli were displayed for a random duration between 3 and 5 seconds. Before each trial a black central fixation point, on a white background, was presented, (c) During each run a patient watched 120 images monocularly, and each patient completed two runs (one per eye). 49

Figure 3.3 Computation of the novel saccadic reversal rate (SRR) (a) Example eye movement data from a single trial. White dots represent fixations, and vectors represent saccades. The arcs represent θ_{diff}: the angular difference between successive pairs of saccades. (b) Illustration of how θ_{diff} values were computed (measured anticlockwise relative to the horizontal) (c) Polar Histogram of θ_{diff} values (same data as panels (a) and (b)). For example, on two occasions θ_{diff} fell within 165°–195°, while on one occasion the angular difference was very small (close to zero). The saccadic reversals are highlighted in red. Coloured dots around the periphery of the histogram show each of the individual θ_{diff} values computed in panel (b). Note that for illustration purposes, the bins shown here are 30° wide, and include data from a single trial only. However, in the final analysis bins of 20° were used, and data were concatenated across all 120 trials. 50

Figure 3.4 SRR analysis (left eye of patient id K). The upper row illustrates the raw scanpaths for individual trials (fixations and saccades represented as points and vectors, respectively). The bottom row shows the corresponding distribution of θ_{diff} values. SRR was computed at the end of a run, and was defined as the proportion of θ_{diff} values that fell in the red bin to the total count of θ_{diff} (Shown here: SRR = 0.13). 51

Figure 3.5 BCEA computation across a run (left eye of patient id k). The upper row illustrates the raw scanpaths for individual trials (fixations and saccades represented as points and vectors, respectively). Each saccade is coloured uniquely to match the plots at the bottom. The bottom row shows the aligned saccades/fixations. BCEA was computed at the end of a run Based on the best fitting ellipse (red dashed line). 52

Figure 3.6 Plots of difference between the better and worse eye in (a) median value of a saccade amplitude (b) SRR (c) BCEA. The black solid line in each plot marks the null hypothesis ('no difference between the eyes'). 55

Figure 3.7 Scatter plots depicting relationships between (a) between-eye differences in SRR and VA, $p = 0.01$ (b) between-eye differences in BCEA and 24-2 MD values, $p = 0.01$. 56

Figure 4.1 Apparatus, stimuli, and procedure. (a) The experiment apparatus consisted of an LCD monitor (51 x 25.5 cm; 1,920 x 1,080 pixels; 60 Hz) with an integrated eye tracker. Participants viewed the screen binocularly and were seated at approximately 60 cm away from the eye tracker without a head/chin rest, meaning that the screen subtended at a visual angle of 46° x 24°. Study participants were only required to look at the screen during test trials (no explicit response) and a keyboard was provided between trials on which to indicate their readiness to continue. Changes in viewing distance were monitored using the eye tracker and the size of the artificial VF loss was dynamically adjusted. (b) The stimuli consisted of two video clips and three static images, the latter of which were displayed for 60 seconds each. The two videos were presented for their full duration of 301 seconds and 307 seconds, respectively. The resolution of video and the images were presented at a resolution of 1,280 x 720 pixels and the frame rate of the two videos were 30 frames/second. All stimuli were displayed in a full-screen mode (resolution of 1,920 x 1,080 pixels). Stimulus order was randomised between participants. 64

Figure 4.2 IVFs and example screenshots from the three simulated-VF loss conditions: (a) no VF loss. (b) moderate VF loss. (c) advanced VF loss. The impairments were constructed on monocular field data from a single real patient. The IVF was estimated by taking the maximum sensitivity from corresponding points in the left- and right-eye VFs. Note that the simulated VF loss moved depending upon the observer's current point of gaze (white cross), and so remained approximately static in retinal coordinates. 66

Figure 4.3 Four methods of eye movement analysis. (a) Example eye movements obtained from a single participant, during free-viewing of one of the static images. The colour of the scanpath codes time. (b) Histogram of the saccades, computed from (a). The median amplitude was used as the summary measure. (c) Aligned plots of the saccades in the VF. The BCEA is the area of the ellipse (grey shaded region). (d) Saccadic movements in the direction of/landed on the pre-saccade VF loss location (black dots falling in the grey shaded region) for the moderate and advanced group. (e) An illustration of KDE analysis of gaze data for the frames of the videos. The KDE model was used to compute the probability score of a test point (average gaze position in a frame for a given participant, shown in blue dot). 69

Figure 4.4 Method of extracting features from saccadic movements. (a) Example of a scanpath from a participant who watched VIDEO 2. (b) Each saccade is mapped to a new planned by setting their starting position to as (0,0). (c) Scatter plot, showing the end location of each saccade in polar coordinates. Saccades that landed in the same bin are shown using the same color. Each bin measures 3° (radial) and by 30° (angular). In total, there were 84 bins (resolution of seven in the radial direction and 12 in the angular direction). The extracted features represent the number of saccades that landed in each bin. For example, the first bin represents the saccades that were greater than 0° and less than 3° in amplitude and executed in a direction between 345° and 15°. 72

Figure 4.5 Median values (±95% confidence intervals) for (a) median saccade amplitude, (b) bivariate contour ellipse area (BCEA), (c) proportion of saccades landing on the pre-scotoma locations (SLV), and (d) kernel density estimation (KDE) probabilities, split into experimental conditions (no VF loss, moderate, and advanced) and stimulus type (VIDEO 1, VIDEO 2, and IMAGES). Statistically significant differences are denoted with an asterisk (* for $p < 0.05$ and ** for $p < 0.001$). 77

Figure 4.6 ROC curves and the AUC scores showing the separation between (a) the no VF loss and moderate (b) the no VF loss and advanced simulated VF losses for the measures described in Figure 4.5. The separation was best between no and moderate VF loss in terms of the SLV and KDE probability score, and between no and advanced VF loss in terms of saccade amplitude and BCEA. 78

Figure 4.7 KDE analysis of fixation data, including KDE probability scores as a function of time for (a) VIDEO 1 and (b) VIDEO 2. The solid lines show the median values for each group. The shaded regions indicate the interquartile ranges. The average (median) probability score for the participants in the moderate group was smaller than for the no VF loss group ($p < 0.05$). This difference was more substantial in the grey shaded region of VIDEO 1. . . 79

Figure 4.8 ROC after analysing multiple eye movement parameters to separate (a) no VF loss and moderate VF loss group, (b) no VF loss and advanced VF loss. 80

Figure 5.1 Sample 24-2 VF greyscale plots and the corresponding numeric VF map (for participant G007). The 54 sensitivity values in the VF map are vectorized and stored in a comma separated file (see Table 5.1). The vectorization was performed by concatenating sensitivity values starting from first row (top) to the last row (bottom). The same vectorization procedure was applied to the sensitivity values of both eyes. 86
Figure 5.2 Sample frames excerpted at a specific time from the three video clips used in the experiment. 89
Figure 5.3 Saccadic-movement representation using tokens. The underlying scanpath is from a single participant in the control group watching VIDEO A. (a) Frames from the clip and raw saccades made at a given time while watching the clip. (b) Scanpath of saccades made until the given time in the video. (c) Centralised saccades plotted by setting the start of all saccades to the centre (0,0). (d) Tokens (letters and their combination) used to encode saccadic movements based on the direction and size of the saccade. For illustration, the size of each bin in the polar grid is of size 3° in the radial and 30° in the angular coordinate. The token highlighted in red corresponds to the saccade (e.g., the first column represents a saccade of 10° in size and executed at an angle of 190°) highlighted in the same colour as in (c). (e) Example of a wordbook that stores each term that encodes a series of saccades. 93
Figure 5.4 Architecture for the Novel Spatiotemporal Analysis (Index method). The workbook from each participant, sequential eye movement representation as illustrated in Figure 5.1 were encoded using TF-IDF, with the first and resulting matrix reduced using principal component analysis (PCA). The extracted static features include counts of saccades that land on each bin in the polar histogram, and other common eye movement metrics, such as saccade amplitude, were serialised. Kernel PCA (KPCA) was used to reduce the dimension of the extracted static features. The resulting features from static and sequential features were serialised and fed into a support vector machine (SVM) classifier. 94
Figure 5.5 Median values (95% confidence interval) for (a) saccade amplitude, (b) saccade rate, (c) spread of fixations as measured using BCEA, (d) fixation duration, (e) KDE probabilities and (f) fixation duration split into experimental conditions (glaucoma and controls) and video type (VIDEO A, VIDEO B, and VIDEO C). 98
Figure 5.6 ROC curves based on the proposed analysis of sequential and static features and their combination for (a) VIDEO A (b) VIDEO B and (c) VIDEO C. 99

Figure 5.7 ROC curves and the AUC scores showing the separation between glaucoma and control groups for the measures described in Fig 5.5 for (a) VIDEO A (b) VIDEO B and (c) VIDEO C. 99

Figure 5.8 Evaluation of the proposed method (a) ROC curves for separation between controls and glaucoma patients for three video clips. For each video stimulus, 10-fold cross-validation was performed to evaluate the classifier, and this was repeated 100 times to estimate the mean and 95% CI of the sensitivity and the specificity of the classifier. The coloured ROCs represent results based on the Index method, while the grey ROC is based on the Reference method. 101

Figure 6.1 ROC curves and the AUC scores showing the separation between glaucoma and AMD combined vs. control groups using the proposed Index method for the three videos described in Chapter 5. 110

Figure A.1 All the 120 images used in the experiment. Images were presented sequentially in random order. 113

Figure B.1 Rank sum tests comparison results (statistics, p-value) between no VF loss and moderate and no VF loss and advanced in SA, BCEA, SLV and KDE probability scores. Statistically significant associations are marked with an asterisk and highlighted in bold. 115

Figure B.2 Saccade amplitude function of time for VIDEO 1 and VIDEO 2 and IMAGES. For each participant in each group, the median saccade amplitude in every second was computed. The solid lines show the median values for each group. The shaded regions indicate the interquartile ranges. 116

Figure B.3 Feature extraction from saccadic movements. (a) Example of a scan-path from a participant who watched VIDEO 2. (b) Each saccade is mapped to a new planned by setting their starting position to as(0,0) position. (c) Scatter plot of the end of the saccades in (b) shown in a polar plane. Saccades that landed in the same bin (sector) are shown using the same color. Histogram of the saccades both in the radial and angular directions are computed to extract the number of saccades landing in each bin. Each bin measures 3° (radial) and by 30° (angular). In total, there were 84 bins (resolution of seven in the radial direction and 12 in the angular direction). The extracted features represent the number of saccades that landed in each bin. For example, the first bin represents the saccades that were greater than 0° and less than 3° in amplitude and executed in a direction between 345° and 15°. 117

Figure C.1 Integrated VF (IVF) of the patients. IVF estimates of the binocular VF from the two monocular (left and right eye) VFs. The sensitivity values for each point in the IVF were computed by taking the maximum sensitivity from corresponding points in the left and right eye VFs. The IVF was generated with a bespoke computer program written in MATLAB (MATLAB R2017a (MathWorks, Inc., Natick, MA, USA). 121
Figure C.2 Histogram of saccades for each video clip for each participant in the control group. 122
Figure C.3 Histogram of saccades for each video clip for each participant in the glaucoma group. 122

List of Abbreviations

AMD Age-related macular degeneration
ANOVA Analysis of variance
AUC Area under curve
BCEA Bivariate contour ellipse area
CI Confidence interval
CS Contrast sensitivity
ETDRS Early Treatment Diabetic Retinopathy Study
HPT Hazard perception test
HFA Humphrey field analyser
IDF Inverse document frequency
IOP Intraocular pressure
IVF Integrated visual field
IQR Interquartile range
KDE Kernel density estimation
LogMAR Log minimum angle of resolution
MD Mean deviation
MEAMS Middlesex elderly assessment of mental state
ONH Optic nerve head
POAG Primary open-angle glaucoma
RNFL Retinal nerve fiber layer
SAP Standard automated perimetry
SD Standard deviation
SITA Swedish interactive thresholding algorithm
SRR Saccdic reversal rate
SVD Singular value decomposition
SVM Support vector machine
TF Term frequency
RGC Retinal ganglion cells
ROC Receiver operating characteristic curve
VA Visual acuity
VF Visual field

Acknowledgements

All the credit goes to the almighty God who made me able to come this far. My sincere and heartfelt thanks go to my supervisors David Crabb and Pete Jones for providing me with all the guidance, encouragements and also for having faith in me. I would like to appreciate their tolerance for my abysmal writing and their invaluable help in producing something readable.

I also want to express my sincerest gratitude to the participants of my study for taking part in my research. I would like to regard all the members of Crabb Lab (both past and present), who had been incredibly supportive and wonderful to work with and motivating for finishing this work. Also, I would like to thank Nick Smith for making his implementation available and his dedication for referring his old codes to answer my questions.

This project has received funding from the European Union's Horizon 2020 research and innovation program under Marie Sklodowska-Curie grant agreement No. 675033.

Finally, to my family and friends for their constant love and inspiration. Without your support and patience, this whole journey would not have been possible.

Declaration

The work contained within this thesis was completed by the candidate, Daniel S. Asfaw. All references and contributions have been stated. This thesis has not been submitted for any other degrees, either now or in the past. Previously published work has been clearly stated in the text. The University Librarian of City University London is permitted to allow the thesis to be copied in whole or in part without further reference to the author. This permission covers only single copies made for study purposes, subject to normal conditions of acknowledgement.

In Chapter 3, data collection was performed by Vera M. Mönter under the supervision of Nick Smith and David Crabb. Data analysis and writing of the manuscript was performed by Daniel S. Asfaw.

In Chapter 4, study design, data collection, analysis and reporting were performed by Daniel S. Asfaw.

In Chapter 5, data was extracted and reorganised by Daniel S. Asfaw from an archive of data prepared in part by Nicholas D. Smith. Daniel S. Asfaw conceived, developed and tested all of the analyses presented in the second half of the chapter.

Thesis Abstract

Diagnosis and monitoring of glaucoma, an age-related eye conditions that can cause irreversible loss of vision, relies on assessment of the visual field (VF). In this thesis, I develop novel methods of detecting visual field loss from natural eye movements when watching videos or looking at pictures. I present data from a literature review and three empirical studies.

In the literature review, I identified and examined 26 papers that investigated eye movements of glaucoma patients while performing tasks such as reading, driving, and visual search. The review indicated eye movements are altered by glaucomatous visual field (VF) loss but identified inconsistency in how these alternations manifest between studies.

The first study investigated empirically whether glaucoma produces measurable changes in eye movements. Fifteen glaucoma patients with asymmetric vision loss viewed 120 images of natural scenes monocularly; once each with the better and worse eye. Eye movements were recorded using a remote eye tracker, and key eye-movement paramet-ers were computed and compared between eyes (better eye versus worse eye). These parameters included conventional metrics (saccade amplitude [SA], fixation counts and duration, and bivariate contour ellipse areas [BCEA]), as well as a novel metric I designed to measure saccadic sequences: the saccadic reversal rate (SRR). In the worse eye, SA and BCEA were smaller ($p < 0.05$), while SRR was greater ($p < 0.05$). There was also a significant correlation between the between eye difference in BCEA, and differences in mean deviation (MD; a measure of VF loss severity) values ($p = 0.01$), while differences in SRR were associated with differences in visual acuity ($p = 0.01$). Furthermore, between-eye differences in BCEA were a significant predictor of between-eye differences in MD: for every 1 dB difference in MD, BCEA reduced by 6.2% (95% confidence interval [CI]: 1.6–10.3%).

The second study investigated whether changes in eye movements due to glaucoma are large enough to be clinically useful. I developed a gaze-contingent simulated VF loss paradigm, in which participants experienced a variable magnitude of simulated VF loss, based on a real glaucoma patient. Fifty-five people with healthy vision watched two short videos and three pictures, with either: no VF loss; moderate VF loss; or advanced VF loss. Eye movements were recorded using a remote eye tracker, and key eye-movement parameters were computed (SA; spread of saccade endpoints as quantified using BCEA; location of saccade landing positions, and the similarity of fixations locations among participants as quantified using kernel density estimation). There were statistically significant di˙erences between conditions, but these measures—alone or in combination—were not capable of identifying VF loss with sufficient diagnostic precision compatible with assumed clinical utility, when considered against a reference standard for measuring the VF (automated perimetry). I do, however, suggest ways in which performance could be improved.

The third study had two parts. First, I curated a dataset of eye movements of 46 patients with glaucoma and 32 controls, which I made available online for other researchers. Second, I presented a novel spatiotemporal saccadic movement analysis using a machine learning method, which I validated on the dataset. My novel method involved translating individual saccades into one of N values, based on its size and direction, and then using the relative presence of different permutations of saccadic sequences to classify individuals as patients or controls. This 'n-gram' approach has been successfully applied previously in other technical domains, such as automatic speech recognition. I evaluated the sensitivity and specificity of my method using ten-fold cross-validation. Areas under the ROC curve (AUC) for the novel approach was 0.78 (95% CI 0.75–0.81), compared to 0.63 using simple eye movement summary statistics (e.g., SA), and AUC = 0.70 (95% CI: 0.66–0.74) using a published current reference standard.

Overall, results from this thesis provide more evidence for eye movements being disrupted by VF loss, that these changes are related to changes in clinical measures, and that it is possible to extract and process these measures using some novel methods automatically. In future, assessment of natural eye movements could be analysed to help detect glaucomatous VF loss, and in the Discussion, I outline what steps are required to reach this goal.

Chapter 1

Introduction

1.1 Preamble and Motivation

Eye movements are one of the most frequent voluntary actions we make. Wherever we look we generate saccadic eye movements. Saccades rapidly move the eyes from one point to another and are interspersed by fixations where the eye is stable. Scanpaths (or gaze patterns) describe sequence of fixations and saccades. My hypothesis is that scanpaths collected non-invasively during a period of time that a person is, for example, simply engaged in looking at a film or image, could provide an 'eye movement fingerprint' that could be used to detect if a person has a problem with their vision.

The work in this thesis considers in particular vision loss characteristics of glaucoma, an age-related eye disease characterised by progressive retinal ganglion cell death and visual field (VF) loss. Glaucoma is the leading cause of irreversible blindness worldwide, and the second most common cause of blindness in England and Wales (Quartilho et al., 2016). With the world's population ageing, the number of people with glaucoma is expected to increase. Loss of peripheral vision, VF loss, is the functional characteristics of the condition. Yet, many patients with glaucoma remain undiagnosed because it can be asymptomatic until a relatively late stage (Weinreb et al., 2014). Large scale studies have reported that a large proportion of patients remain undiagnosed. For example, one-third of primary open-angle glaucoma (POAG) patients are undiagnosed in the United Kingdom (UK) (Chan et al., 2017). It would, therefore, be helpful to develop a novel method that can better test and monitor VF loss efficiently.

The overall working hypothesis of this thesis is that dysfunction in vision (VF loss) can turn up in the form of tell-tale differences in a person's gaze and can be measured by

eye movement tracking, including novel analysis of patterns of saccades as a person watches a film or a slide show of pictures. Departures from a typical 'eye movement fingerprint' could indicate significant visual impairment, and the method might be ideal for detecting or monitoring patients' VF loss. With the rapid development of eye tracking technologies, eye movement research is attracting widespread interest to investigate the effects of ocular, neurodegenerative, and psychiatric disorders (see Willard and Lueck (2014) for review). This is partly due to the fact that eye movement measures are relatively easy to obtain, and the experimental tasks tend to be short and simple for participants, including even young children and elderly adults (Noiret et al., 2017). The availability of a range of affordable and portable eye trackers has also allowed researchers to study eye movements of patients under a wide range of scenarios: for example, while patients perform tasks in front of a computer (e.g., reading and watching videos) or tasks in a natural environment (e.g., walking and driving).

The work in this thesis was motivated by a series of studies that have considered eye movements and their relationship to VF loss in glaucoma (Smith et al., 2012; Crabb et al., 2014; Smith et al., 2014). Specifically, the thesis describes experiments and analytical work motivated by the proof-of-principle results published in Crabb et al. (2014). These authors developed a novel methodology to extract and quantify features from extensive maps of saccades. Elderly people with healthy vision and patients with a clinical diagnosis of glaucoma viewed three unmodified film clips on a computer set up incorporating the Eyelink 1000 eye tracker (SR Research, Ontario, Canada). Eye movement scanpaths were plotted using novel methods that first filtered the data and then generated saccade density maps. Maps were subjected to novel data analysis. This proof-of-principle work successfully differentiated a large group of patients with a clinical diagnosis of glaucoma from a group of age-similar visually healthy people. This thesis aims in part to further develop works of Crabb et al. (2014) to improve the separation between patients with glaucoma from controls.

1.2 Glaucoma and visual function

The aim of this PhD thesis was to investigate naturalistic eye movements of patients with glaucoma. This section provides a brief background on glaucoma and visual function. The interested reader can find more detail about glaucoma in Prum et al. (2016) and Weinreb et al. (2014).

1.2.1 Glaucoma

Glaucoma is a group of irreversible, progressive optic neuropathies characterised by clinically visible changes to the optic nerve head (ONH) and leading to functional changes to the VF (Foster et al., 2002; Davis et al., 2016; Weinreb et al., 2014). These changes are sometimes due to elevated intraocular pressure (IOP), inducing collapse and compression of the optic nerve, which leads to axonal transport disturbance and the death of retinal ganglion cells (RGCs) (Quigley, 1996; Johnson et al., 2000)—cells responsible for receiving visual information from photoreceptors and transmitting this information via their axons to the optic nerve. There are two main types of glaucoma: open-angle glaucoma (OAG) and angle-closure glaucoma (ACG) (Barkan, 1938). The two types of glaucoma differ in the anatomical structure of the angle of the eye, the junction between the iris and cornea, where the trabecular meshwork drains aqueous humor. In OAG the angle remains open as the trabecular meshwork is unblocked by iris tissue. While in ACG, the angle is narrow and the iris obstructs normal aqueous outflow. An increase in intraocular pressure marks both open- and closed-angle glaucoma. In ACG, well-marked symptoms are often observed; however, other forms of chronic glaucoma are largely asymptomatic (Greco et al., 2016). Glaucoma can be either a primary or secondary disease, depending on the condition that causes the increase in IOP. In the latter, IOP is elevated during the disease and finds a cause; in the former, if the IOP is ever elevated, no cause is found (Casson et al., 2012).

Glaucoma affects more than 70 million people worldwide (Quigley and Broman, 2006; Weinreb et al., 2014), and incidence rates are predicted to rise significantly in the future due to an ageing population (Quigley et al., 2001; Tham et al., 2014). The worldwide prevalence of OAG is estimated to be higher than ACG (1.96% vs. 0.69%)(Quigley and Broman, 2006), and the prevalence of both types of glaucoma for people aged 40–80 years is 3.54%. However, the prevalence of glaucoma subtypes varies among races and countries. For instance, the prevalence (proportion of patients to population size) of primary angle-closure glaucoma (POAG) is highest in Africa (4.20%), and the prevalence of PACG is highest in Asia (1.09%) (Tham et al., 2014). In the United States and Europe, the number of people with POAG is approximately seven times greater than those with ACG (Quigley and Broman, 2006). Generally, POAG is the most common type of glaucoma, and most glaucoma cases are in Asia, representing 60% of all glaucoma cases (Tham et al., 2014).

Numerous studies have identified the risk factors associated with POAG (Prum et al., 2016). Elevated IOP is an important risk factor for POAG (Dielemans et al., 1994; Leske et al., 1994; Quigley and Broman, 2006; Chan et al., 2017). However, there is no single IOP cutoff value that can be used to detect POAG (Chan et al., 2017). For instance,

setting 21 mm Hg IOP as a cutoff value (the threshold used for ocular hypertension) could detect only around half of the people with glaucoma (Sommer et al., 1991). Older age is another risk factor of POAG. In people under 40 years of age (Tham et al., 2014), the prevalence of POAG is below around 1% and is around 8% in people over 80 years of age. The prevalence of POAG among elderly is highest for people in Latin America and the Caribbean (12% at the age of 80). In people from Europe or with European ancestry who are older than 80 years old, the prevalence of POAG is less than 5% (Tham et al., 2014). Other risk factors of glaucoma include a family history of glaucoma and genetics (Brandt et al., 2001; Ramdas et al., 2011; Hysi et al., 2014; Springelkamp et al., 2017), thinner central corneal thickness (Brandt et al., 2001; Dueker et al., 2007), being male (Gordon et al., 2002; Rudnicka et al., 2006), cup-disc ratio (Gordon et al., 2002), blood pressure (Mitchell et al., 2005), diabetes (Flammer et al., 2001), migraines (Wang et al., 1997), and age-related macular degeneration (Le et al., 2003).

Raised IOP is a major modifiable risk factor for POAG (Leske et al., 2007), but detecting glaucoma based on the measurement of IOP alone is a poor method (Casson et al., 2012). Clinical diagnosis of glaucoma requires observation of characteristic ONH features or consistent, characteristic VF changes (Weinreb et al., 2016). Examinations are repeated over time to assess the optic nerve head for neuroretinal tissue loss and to detect the development of VF scotomas (Weinreb and Khaw, 2004). Functional defects are assessed primarily by using standard automated perimetry. Slit-lamp biomicroscopy is commonly used for the evaluation of the ONH and the retinal nerve fibre layer (RNFL) to diagnose glaucoma. Digital imaging technologies have provided a more objective, quantitative and efficient approach to quantify RNFL thickness changes. Confocal scanning laser ophthalmoscopy, scanning laser polarimetry, and optical coherence tomography are widely used imaging techniques for the evaluation of the ONH and RNFL structures.

1.2.2 Visual function

Simply put, visual function describes how well the eyes and wider visual system are operating. Functional tests are very useful to understand how patients with eye conditions like glaucoma perceive their visual world. In glaucoma, visual function measures typically used in a clinic include visual acuity (VA), contrast sensitivity (CS), and VF. The latter, measured using perimetry, is paramount in the assessment of visual function in glaucoma. This section briefly describes VA, CS, and VF examinations. It is not meant to be a detailed description but is written to aid the reader who knows little about these measurements.

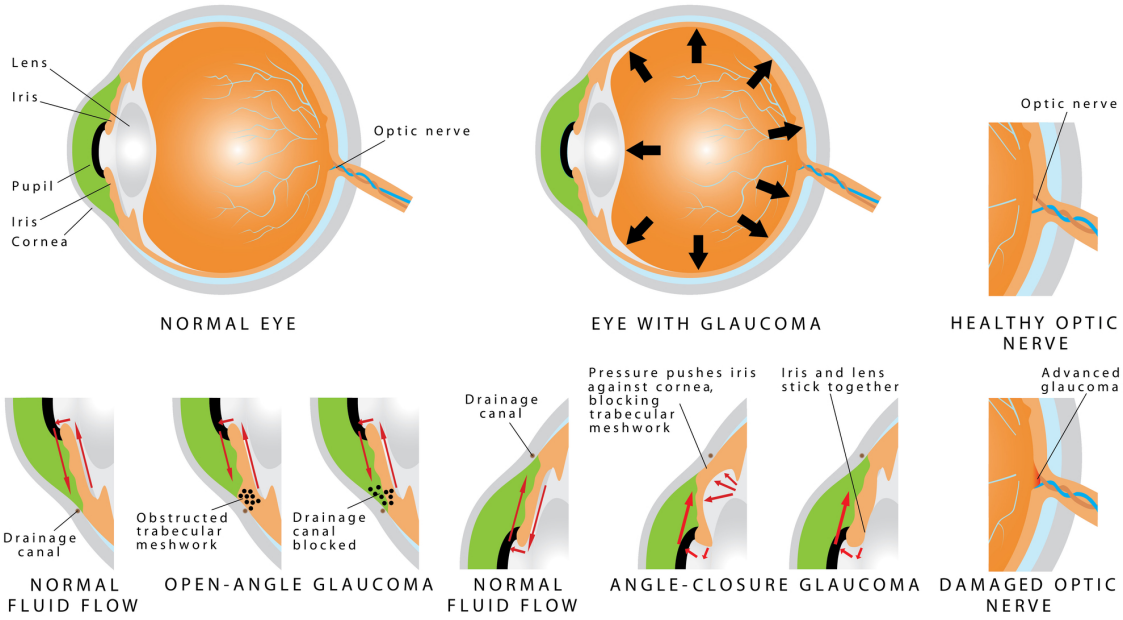

Figure 1.1: Schematic of an eye illustrating the impact of raised intraocular pressure on the fluid pathway and optic nerve. Glaucoma can partially or completely block the outflow of aqueous fluid through the trabecular meshwork. Based on the angle (between the iris and cornea), it can be open-angle or closed-angle glaucoma. The image is from https://nearsay.com accessed in January 2020.

1.2.2.1 Visual acuity

VA estimates the level of finest detail that can be detected or identified. The traditional method of measuring acuity, for those who can report what they see, is with acuity charts of high contrast black targets presented on a white background (Bennett et al., 2019). VA is reported in units relative to a visually healthy observer's performance at 6 meters (~20 feet) using Snellen notation, where normal visual acuity is reported as 6/6 (or 20/20). This translates to a minimum angle of resolution (MAR) of 1.0, the logarithm of which (logMAR) is 0.0.

Several types of optotype acuity charts have been developed to test VA (reviewed elsewhere (Bailey and Lovie-Kitchin, 2013)). The Snellen acuity and the Early Treatment Diabetic Retinopathy Study (ETDRS) are the two most widely used in clinical practice. The Snellen chart has several limitations (Kaiser, 2009). One limitation is the difference in the difficulty on different rows (vision levels); different rows have significantly different numbers of letters, spanning from one (top) to eight (bottom) characters per row. Visual acuity for a target optotype can be affected by the proximity of adjacent letters or optotypes (Lalor et al., 2016). This spatial interaction effect on target resolvability, also referred to as crowding, can be affected due to inconsistent decrease in letter size in Snellen charts (where the spacing between letters is relatively wide at the top of the chart compared to the bottom). The ETDRS chart was developed to address

the limitations of the Snellen chart, especially in the low VA range. The ETDRS chart has an equal number of characters per row, an equal logarithmic decrement between successive rows, and relatively uniform legibility across character types (Bailey and Lovie, 1976).

1.2.2.2 Contrast sensitivity

CS usually refers to the ability to detect luminance increments with central vision (McKendrick et al., 2007). Reduced contrast sensitivity often is a characteristic of glaucoma, and it is believed that much of the visual disability is caused by this reduction (Bambo et al., 2016). The standard sensitivity test, which is also used throughout this thesis, is the Pelli-Robson chart. The test includes 8 lines and 16 levels of horizontal capital, with two triplets per line. Each set of triplet letters on the chart becomes progressively lower in contrast relative to the background (Pelli et al., 1988). The first triplet on the chart (top left) is of the highest contrast and the last triplet (bottom right) is of lowest contrast and is most difficult to read. Pelli-Robson measures CS using a fixed target size/spatial frequency and varied contrast. Other tests use fixed contrast and varied spatial frequency (e.g., the Bailey-Lovie high and low contrast acuity charts, (Bailey and Lovie, 1976), and some assess contrast sensitivity at a range of stimulus sizes/spatial frequencies (e.g., the Vistech chart, (Ginsburg, 1984) and the Arden grating test (Arden and Jacobson, 1978)). The Mars contrast sensitivity chart (Arditi, 2005) is similar to of the Pelli-Robson chart (a near test), although it is smaller in size (Mars charts measure 23cm x 35.5cm compared to up 84cm x 59cm of the Pelli-Robson chart) and is held normally at 50cm from the patient.

1.2.2.3 Visual Field

VF is the area on which light can reach the retina, while the eye is steadily fixating. This light stimulates the rod and cone cells on the retina, which is processed by the ganglion cells within the inner retina. The fovea is the central part of the VF. It contains the highest concentration of cones, and in healthy eye is the area of highest sensitivity. In a visual-healthy subject, the VF covers the 60° superiorly, 70° inferiorly, 90° temporally and 60° nasally (Wong and Plant, 2015; Henson et al., 2000). The blind spot is a location of the optic nerve head: an area with no photoreceptors located in the temporal part of the VF.

The VF test is an integral tool in glaucoma diagnosis and management. Traditionally, a VF test is performed using perimetry to localise the site of visual dysfunction and track its progression. Perimetry has employed achromatic (white) test targets that are presented as luminance increments against an achromatic adapting field, measuring

increment thresholds at locations throughout the VF. Dynamic or static techniques are employed to assess VF. In dynamic or kinetic VF measurement, an achromatic target of a specific size and luminance is moved along a radial line from the far periphery towards the point of fixation. This is done either manually (e.g., Goldmann) or on an automated machine (e.g., Octopus). While in static perimetry, the increment threshold for a briefly flashed test target is measured at a number of fixed locations throughout the VF.

The commonly used automated VF perimetry test is often named standard automated perimetry (SAP). This involves the assessment of a subject's light-difference sensitivity at various locations of their field of view. The Humphrey VF Analyser (HFA, Carl Zeiss Meditec, Dublin, CA) is the most commonly used SAP machine, although there are also other machines (Wong and Plant, 2015). In the experiments throughout this thesis, the HFA was used to assess VF and as such the focus of discussion will be based upon HFA results. Humphrey tests can be configured to test the central 24° ('24-2'), 30° ('30-2'), and 10° ('10-2'). The most common set up is the 24-2, which assesses with a 54-point grid.

A typical output from an automated static perimeter is a grid of numbers and an interpolated greyscale visualisation, as illustrated in Figure 1.3. The results are generally presented in terms of dB attenuation (tenths of a log unit), such that the highest numbers represent the highest sensitivity. The low sensitivity areas (locations of visual dysfunction) are represented in dark in the greyscale. The full output from HFA also contains a comparison of the patients' values to age-matched normative data. Probability maps provide data on points in the VF that are significantly abnormal (i.e., that have a probability of occurring in less than 5% of the normal population). Summary statistics that are provided by the HFA include the mean deviation (MD), which is the mean reduction in sensitivity over the VF, and pattern standard deviation maps (PSD), which refers to the difference in VF shape from the normal hill of vision. The glaucoma hemifield test (GHT) gives a measure of whether the VF has glaucomatous traits by comparing differences between the superior and inferior hemifields (Åsman and Heijl, 1992).

To measure the reliability of the VF test, different indices are reported. Fixation loss is estimated by positive responses to stimuli that are projected within the physiologic blind-spot, although some recently automated perimeters are equipped with eye tracking devices. Fixation losses of more than 20% will be categorised as poor reliability. False-positive errors are estimated by the number of positive responses to a long pause between stimuli being projected. False-negative errors are those in which

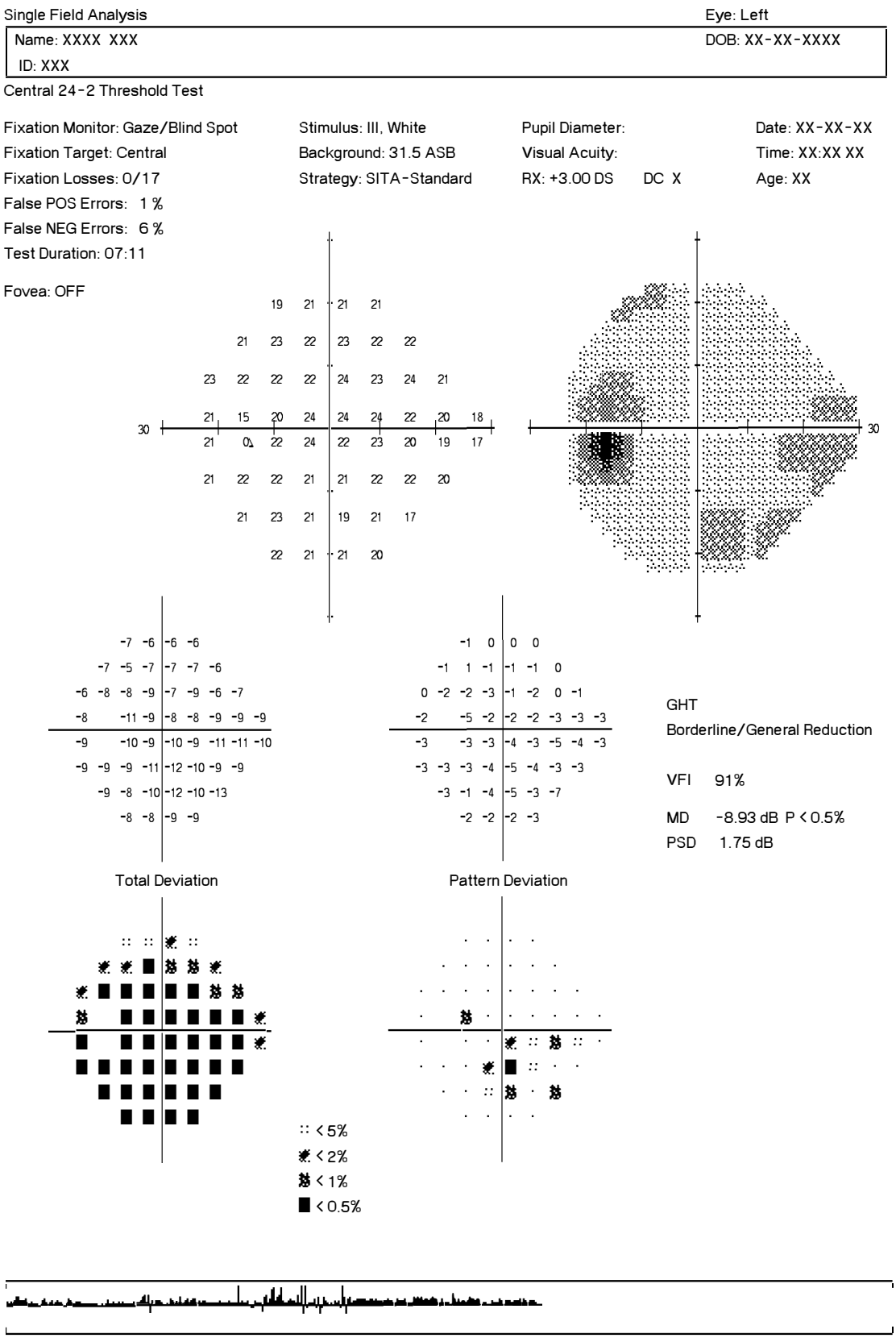

Figure 1.2: Example of VF showing point-wise sensitivity levels in dB, GHT, MD, and PSD.

super-threshold stimuli are missed at locations for which a threshold has been estimated. In an abnormal VF, false negatives can represent increased functional variability in affected areas of the field rather than poor compliance. Tests with false-negative or false-positive percentages above 33% of the VF are classified as being of poor reliability.

Other perimetric technologies have been developed to improve the sensitivity and test duration. A detailed discussion of these is given elsewhere (Turalba and Grosskreutz, 2010; Sethi et al., 2013).

1.2.3 Binocular visual field

VF is commonly measured in clinics monocularly to diagnose or monitor the progression of VF loss. Yet monocular measurements are less informative of patients' visual functioning since both eyes contribute to the visual perception process.

The binocular VF can be characterised approximately using the Esterman VF test (Esterman, 1982; Mills and Drance, 1986). The Binocular Esterman VF test can be measured using a perimeter (Humphrey Field Analyzer; Zeiss-Humphrey Systems, Dublin, CA) and a Goldmann perimeter (Octopus 900; Haag-Streit, Koniz, Switzerland). The Esterman VF test measures the 130° horizontal field of view, with 120 test points and is performed on an automated perimeter using a suprathreshold test strategy, which means each point is tested at a fixed brightness.

Binocular VF testing is rarely performed in clinics. The integrated VF (IVF) offers an alternative assessment of a patients' binocular VF severity (Crabb et al., 1998; Coleman et al., 2007). The IVF is estimated from monocular results, taking the best sensitivity values from corresponding VF locations from the two monocular measurements. The IVF has been shown to agree closely with the Esterman test in identifying patients with glaucomatous central defects (Crabb et al., 1998) and has also been used to predict patients with glaucoma who are fit to drive (Crabb et al., 2004; Owen et al., 2008). In this thesis, a custom application is developed to compute IVF (Figure 1.3).

1.3 Eye movements

Our eyes continuously sense the visual world by shifting positions in their orbits. The VF subtends approximately 180° visual angle horizontally and 130° vertically, but at a single glance the visual system can only process the visual information that falls on the fovea, the highest acuity central portion of the retina (1° of the VF). Consequently, eye movements direct the fovea to sample the visual information that

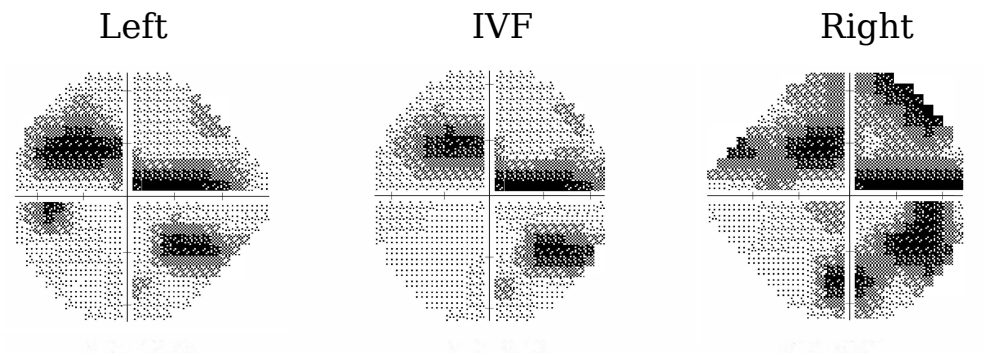

Figure 1.3: A greyscale plot of Humphrey 24-2 fields from the left and right eyes are merged point by point to produce the simulated IVF. The maximum sensitivity from the left and right eye VF corresponding points are used to estimate the sensitivity values in the stimulated IVF.

falls in the peripheral VF. Eye movements also enhance visual acuity by keeping images stabilised on the retina during self-motion (head and eye movements) with respect to the visual environment.

1.3.1 Types of eye movements

What follows is a summary of the movements made in a human eye. This thesis work mainly studies saccades and fixations, but an overview of other eye movements is presented for completeness. For more detail, the interested reader is directed elsewhere (Tatler et al., 2011; Duchowski, 2017; Krauzlis, 2013).

1.3.1.1 Saccades

Saccades are rapid eye movements that redirect the eye to a new point of fixation. They are required since we need to move our eyes to centre our fovea on the location of interest (Tatler et al., 2011). The size of a saccade (typically 1° to 20° of the visual angle) can vary depending on the task; for example, small saccades are made while reading and much larger saccades are made while gazing around a room. Saccadic eye movements are ballistic, and once a saccade begins, it is not possible to change its destination or path. If the target moves during this time (which is on the order of 15–100 ms), a second saccade must be made to correct the error (Purves et al., 2001). On average, a saccade lasts 30–120 ms. There is a 100–300 ms delay before the saccade occurs (the initiation period) (Liversedge et al., 2011).

1.3.1.2 Fixation

Fixations are periods of stability in which an object of interest remains relatively stationary on the retina. A stable gaze is required for fixation since the photoreception process is slow, requiring 20 ms to respond to step changes in light (Friedberg et al.,

2004). Fixations typically last between 200 and 600 ms, after which another saccade will occur (Liversedge et al., 2011). During fixations, the eye constantly makes several types of small motions, usually within a one-degree radius: tremors, drifts, and microsaccades (Krauzlis et al., 2017). Ocular tremors are high frequency (40–100 Hz) oscillatory eye movements with very low amplitudes of about six arc-seconds (approx. 0.0017°). Ocular drifts, on the other hand, are meandering movements at a relatively lower frequency (< 40 Hz) that produce much larger shifts in eye position (Cherici et al., 2012; Rucci and Poletti, 2015). By drifting the retinal image, smooth ocular drift transforms the visual input in ways that increase spatial acuity. Microsaccades are the largest of these fixational eye movements, controlled by the same neuronal mechanisms that generate larger saccades, and share functional properties with larger saccades (see Martinez-Conde et al. (2009)). One commonly described function of microsaccades is to correct the drifts made during fixations (Krekelberg, 2011).

1.3.1.3 Smooth pursuit movements

Smooth pursuits are slow and continuous eye movements, used to track any visual target in motion. Smooth pursuit movements minimise retinal slip and the resultant blur. Smooth pursuit eye movements can track moving objects at velocities of about 15°/s. If a target moves above this speed, the saccades are usually made in the direction of the moving target. Compared to saccades, smooth pursuit movements are slower (<100°/s), smoother and more continuous. In addition, smooth pursuit movements require visual feedback to track the moving object (Krauzlis, 2013; Purves et al., 2001; Liversedge et al., 2011).

1.3.1.4 Vergence movements

Vergence movements are eye movements that align the fovea of each eye with targets located at different distances from the observer. Unlike other types of eye movements (such as saccades and smooth pursuits, which are conjugate eye movements), during vergence movements, both eyes move in opposite directions (deconjugate); they involve either convergence (inward rotation) of the lines of sight of each eye to see an object that is nearer or divergence (outward rotation) to see an object that is farther away (Krauzlis, 2013; Purves et al., 2001; Liversedge et al., 2011).

1.3.1.5 Vestibulo-ocular and optokinetic reflexes

These are other types of eye movement that stabilise the eyes relative to the external world and maintain the position of the visual image in the retina. Unlike saccadic, smooth pursuit and vergence eye movements, vestibulo-ocular movements are used when the head is moving. These eye movements automatically compensate for rapid

head movements by moving the same distance but in the opposite direction. The optokinetic reflexes complement the vestibulo-ocular reflexes using full-field visual information about self-movement of images across the retina to compensate for the perturbation of the visual world on the retina (Krauzlis, 2013; Purves et al., 2001; Liversedge et al., 2011).

1.3.2 What drives eye movements when viewing a scene?

We constantly make eye movements to scan our visual surroundings. How we select the next fixation target has been one of the central topics in eye movement research. Generally, there are two main factors that drive spontaneous eye movements: the 'bottom-up' and 'top-down' factors. Several works, including pioneers of eye movement research, Buswell (Busswell, 1935) and Yarbus (Yarbus, 1967), have been arguing for the importance of both top-down and bottom-up factors (reviewed in (Henderson, 2003; Rothkopf et al., 2007)). This section provides a very brief overview of the main factors that drive our eye movements.

1.3.2.1 Bottom-up salience

Under free-viewing conditions (i.e., where no instruction is provided), eye movements are driven primarily by the salience of the image. Salient parts of the image capture visual attention known as overt attention, in which the shift in attention from one object to the next is accompanied by an eye movement (Itti et al., 1998). Given the relationship between attention and eye movements, salience refers to the properties of an image that first cause the deployment of overt attention. These features are also referred to as 'pre-attentive' since overt attention has yet to be activated, i.e., the pre-attentive features are responsible for saccade initiation.

The role of pre-attentive features of an image in eye movements has been explained using the salience map model, a computational model developed to predict eye movements (Itti et al., 1998; Itti and Koch, 2001; Peters et al., 2005). Visual saliency maps are frameworks based on computer vision algorithms that define portions of a scene that 'stand out' from the background as potential points of interest. The framework first extracts features (intensity, colour, and orientation) from the input image at different spatial scales in parallel and are combined to create a saliency map. This is followed by a winner-take-all network that detects the most salient location, resembling neural information processing in the early stages of visual processing (Itti and Koch, 2000, 2001). Several studies have proposed different image features that contribute to the salience map (Einhäuser and König, 2003; Baddeley and Tatler, 2006; Frey et al., 2007; Onat et al., 2007; Jansen et al., 2009). Under free-viewing of static images, it has been

reported that low-level image features differ significantly at fixation location, characterised by high edge density (Mannan et al., 1996, 1997; Tatler et al., 2005; Henderson et al., 2007), local contrast (Parkhurst and Niebur, 2003; Tatler et al., 2005), texture (Parkhurst and Niebur, 2004), and mid-level visual features including corners (Barth et al., 1998; Zetzsche et al., 1998). The overall level of the predictive power of these features remains low, indicating that salience-based models (Itti and Koch, 2001; Torralba and Oliva, 2003; Deco and Rolls, 2004) that concentrate on bottom-up image features have modest power to explain the full eye movement behaviour of observers. Although the salience map is based upon biologically plausible principles of feature extraction, it has certain drawbacks. For instance, salience-based models have failed to explain different aspects of eye movements: repetitive scanpaths on reviewed images, saccade sequences, and variability of fixation durations. Interested readers are referred to (Land and Tatler, 2009; Tatler et al., 2011) for more drawbacks of the silence models.

Several algorithms have been proposed to improve traditional saliency models, for example by exploiting structural information in images (Erdem and Erdem, 2013) and by incorporating oculomotor biases (saccade amplitudes and saccade orientations) (Le Meur and Liu, 2015). Recently, machine learning techniques have been proposed to predict the fixation locations (Cornia et al., 2016; Kruthiventi et al., 2017; Cornia et al., 2018). Unlike the traditional salience models, which depend purely on low level image features, these algorithms automatically 'learn' how people direct their gaze from eye tracking data in a supervised fashion (Zhao and Koch, 2013).

1.3.2.2 Effect of task

Early eye movement research by Busswell (1935) and Yarbus (1967) demonstrated that eye movements were influenced by top-down instructions, and not purely by the properties of a picture. Several subsequent works have found that the spatio-temporal deployment of eye movements are influenced by tasks being performed in a real-world setting such as making tea (Land et al., 1999) or sandwiches (Land and Hayhoe, 2001), various sports activities like playing cricket (Land and McLeod, 2000) or catching a ball (Hayhoe et al., 2005), as well as under laboratory conditions such as moving an object around an obstacle (Johnson et al., 2000), copying an arrangement of blocks (Ballard et al., 1995), simply grasping an object (Brouwer et al., 2009); or reading (Legge et al., 1997; Rayner, 1998; Engbert et al., 2005). These studies have shown that low-level object features (salience-based eye movement models) play a small role in the eye movements of observers while executing tasks; rather, observers' gaze behaviour was mainly driven by task-relevant objects (Land et al., 1999; Land and Hayhoe, 2001). For instance, eye movements when free-viewing an object compared to grasping showed

a clear difference in fixation locations; fixations were clustered around the centre of the object during free-viewing, compared to biased fixation around the contact point of the object and hand when grasping (Brouwer et al., 2009).

1.3.2.3 Other factors

Although the bottom-up (Influence of stimulus properties) and top-down (task related factors) have been discussed as the two main factors that drive our eyes, there is a general census that other factors can also affect fixation locations (Williams and Castelhano, 2019; Schütz et al., 2011). Here, I have summarised those factors as 'other factors'. Higher-level strategies, such as looking at particular objects, are argued to be better predictors of eye movements (fixation locations) than low-level image properties (Einhäuser et al., 2008). Using receiver characteristic curve analysis, Einhäuser et al. (2008) found that objects predict more than features (around 65% vs 60%). Nuthmann and Henderson (2010) also found that the saccadic landing position was close to the centre of the objects. Features, specifically of faces, have been reported to capture observers' gaze even when no specific instruction is given to recognize a person (Cerf et al., 2009). An investigation into the role of faces on saccade control has also shown that saccades to faces can be even faster, with an average latency of 147 ms (Crouzet et al., 2010). Other studies have shown that eye movements are influenced by the merits of looking at a specific target in a scene. Gaze selection could be influenced by whether information gain is maximised (Najemnik and Geisler, 2005) or whether looking at a specific location is rewarding (Sohn and Lee, 2006), arguing that eye movements are continuously evaluated by brain circuitry responsible for evaluating our actions. Recently, an eye movement model has been proposed that considers reward maximisation and uncertainty reduction 116 to explain the complex aspect of fixation selection better than the salience-based models.

Another factor that affects eye movements is oculomotor bias. For example, when viewing an image or movie, the most interesting objects are often located at the middle, so that observers are biased to fixate at the centre of the screen (Bindemann, 2010). Vincent et al. (2009) estimated that up to 34–56% of eye movements are due to the central bias of fixations, and a model based on oculomotor biases alone performs better than the standard salience model (Tatler, 2007). There is also a tendency of observers to select nearby locations more frequently than distant locations as targets for their saccades (Bahill and Stark, 1975; Pelz and Canosa, 2001; Gajewski et al., 2004). Other studies have also reported that other unconscious observer biases affect eye movements. For example, when viewing pictures horizontal saccades dominate (e.g., Lee et al. (2002); Moeller et al. (2004); Bair and O'keefe (1998)), and the saccade amplitude distribution is heavily skewed towards medium-sized saccades (Foulsham

and Kingstone, 2012; Tatler and Vincent, 2009).

1.3.2.4 Eye movements when viewing videos

Although the majority of studies on scene perception have used static images to understand the factors that drive eye movements, static images are less representative of the real-world visual scene (Smith and Mital, 2013). Videos contain continuously changing visual and auditory information that guides the spatiotemporal deployment of eye movements (see Smith (2013) and Williams and Castelhano (2019)) for review). Professionally edited video clips may be designed to focus viewers' attention by manipulating visual features such as lighting, colour, focal depth, central framing, and motion elements. In the research throughout this thesis, professionally edited video clips were used in Chapters 4 and 5, as such the main focus of the discussion will be based upon this. Several factors related to the characteristics of the stimulus are reported to affect eye movements when watching videos. Including features such as motion and flicker into computational visual salience model has increased the prediction accuracy of fixation targets when watching videos (Mital et al., 2011; Carmi and Itti, 2006b,a; Vig et al., 2009). For example, Mital et al. (2011) have shown that when watching short clips of movies, motion features are strong predictors of fixation locations rather than other low-level features, such as luminance, colours, edges and corners.

When viewing videos, unlike static images, there is high consistency in gaze allocation across observers (Dorr et al., 2010; Smith and Mital, 2013; Goldstein et al., 2007). However, the degree of consistency depends on the content and composition of the video. For example, Dorr et al. (2010) reported that eye movements when watching Hollywood movies are significantly more consistent than those for natural scene movies (unedited real-world scenes), suggesting that consistency in eye movements could be due to the implicit gaze-guidance strategies of movie producers. In addition to motion and flickers, centre bias is another factor that elicits similar eye movements across subjects when watching videos, especially professionally edited video clips (Dorr et al., 2010; Goldstein et al., 2007). Tseng et al. (2009) found that under free-view of professionally edited video clips, the presentation of conspicuous elements of the scenes at the centre by the photographer was a strong contributor to centre bias.

1.4 Eye tracking

Eye tracking refers to a process of capturing eye movements by converting the eye movement signal into a 2D coordinate, describing where an observer is looking at a certain time on the visual scene. Following recent technological advances in afford-

able eye trackers, there is a growing interest in using eye trackers to understand eye movements in the scientific community. The geometric and temporal characteristics of the eye movements have been investigated to understand the effect of different neurodegenerative (Anderson and MacAskill, 2013), psychiatric (Armstrong and Olatunji, 2012), and ocular disease (Kasneci et al., 2017) on a day-to-day activity of patients.

1.4.1 History of eye tracking methods

Investigation of eye movements emerged as early as the 18th century, using afterimage techniques (Porterfield, 1737). Javal (Javal, 1878) used a technique employing a rubber tube connected to the conjunctiva and both ears, a technique that converts eye movements into a sound and used to detect saccades during reading. Early eye movements recording started at the end of the 19th century (Delabarre, 1898; Huey, 1898), using devices consisting of a lever attached to a plaster eyecup. Eye-trackers used in early eye movement research were highly invasive and uncomfortable (see the history of eye movement recording techniques in (Wade et al., 2005), and (Eggert, 2007)). A variant of eye trackers, which used wire coils embedded with contact lenses, were developed to track eye movements with very high precision and accuracy. The first of these eye trackers that used magnetic search coil was introduced by Robinson (Robinson, 1963), and Collewijn (Collewijn et al., 1975), was later developed to measure 3D eye and head movements (Kasper and Hess, 1991). Another variant of eye tracker monitor light reflected from a mirror attached to the surface of an eye (Ditchburn and Ginsborg, 1952). Yarbus (1967), in his landmark study of eye movements, used records of light reflected from a mirror attached to a rubber suction cap attached to the eye.

A breakthrough in eye tracking technology was the development of the non-invasive eye tracking apparatus in the early 1900s by Dodge and Cline (Dodge and Cline, 1901), which recorded the corneal reflection of a bright vertical line on a moving photographic plate. Corneal reflection based eye trackers were used in the early study of eye movements while observers viewed pictures (Busswell, 1935) (Figure 1.3). Recently developed eye trackers widely use the method of tracking the light reflected from the cornea with pupil tracking (Wade et al., 2005). For tasks that involve mobility, portable eye trackers that can be used to measure eye movements in the real environment were first developed in 1948 (Hartridge and Thomson, 1948). Other researchers were able to improve the flexibility of the portable eye tracker (Mackworth and Thomas, 1962; Davis and Shackel, 1960). More recently, Land and Lee (1994) developed a head-mounted portable eye tracker to explore eye movements while making tea, driving (Land et al., 1999) and playing cricket (Land and McLeod, 2000). Modern portable eye trackers record eye movements using pupil tracking (some additionally use corneal reflection) techniques, but the sampling rate remains low compared to remote eye trackers.

a) b)

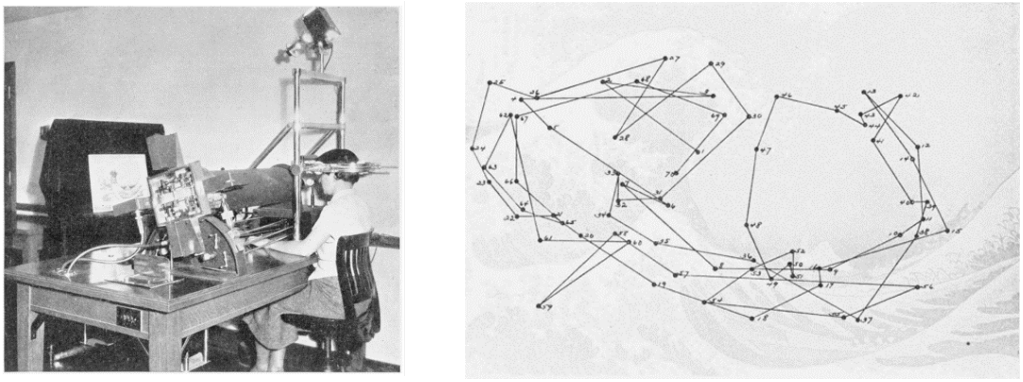

Figure 1.4: The eye tracker used by Guy Buswell in 1935 in his study of picture viewing. A) The subject, with head restrained, views the picture on the screen to the left. B) An eye scan of one of the pictures used in the studies, 'The Wave' by Hokusai.

1.4.2 Eye movement recording methods

As mentioned previously, by far the most common eye trackers are video-based, and the experimental chapters in this thesis used such eye trackers. There are, however, several alternative techniques to record eye movements. These are briefly discussed in the sections below. Interested reader can refer Klein and Ettinger (2019) for detail on eye tracking techniques.

1.4.2.1 Scleral search coil

The scleral search coil eye tracker measures the electrical potential difference between coils (two or more) which is induced by rapidly rotating magnetic fields. Soft coils moulded to have a ring shape are attached to the eyeball (details are discussed in (Eggert, 2007)). Scleral search coil eye movement measurement methods have high precision, with a high signal-to-noise ratio. However, the method is intrusive, as it involves attaching a reference object mounted on a contact lens which is then worn directly on the eye (Klein and Ettinger, 2019). This technique has been improved using a modern contact lens despite the contact lens being large, extending over the cornea and sclera. The other drawback of this method is that wearing a search coil for a long period of time could potentially lead to the drying and deformation of the cornea (Irving et al., 2003). Currently, search coils are rarely used in humans, but they are often used in non-human primates.

1.4.2.2 The Electro-oculogram (EOG)

Another technique to measure eye movement is to model the human eye as an electrical dipole; the retina is more negative than the cornea. Retinal photoreceptors and

neurons produce an electrical potential difference (6mv) because of electrical activities (Klein and Ettinger, 2019). When the eye rotates, a small electric potential difference is created at the surface of skin depending on the eye position. EOG has few advantages compared to video-based eye trackers. First, changing lighting conditions have a limited impact on EOG signals, and it is the only method that allows eye movements to be recorded during sleep (Smith et al., 1971; Penzel et al., 2006). Second, it does not require a high-end signal processing machine and there is no video and image processing involved. Thus, it can be used for long-term recordings, allowing people's everyday life to be captured (Manabe and Fukumoto, 2006; Bulling et al., 2011, 2009). Finally, EOG can be adapted to be used in neuroimaging environments such as MEG/MRI. One drawback of EOG is that it requires electrodes to be attached to the skin around the eyes. It is also prone to measurement and environmental noises (Fairclough and Gilleade, 2014; Eggert, 2007).

1.4.2.3 Video-oculography (VOG)

These are recording techniques involving the measurement of features of the eyes under rotation/- translation. These features can be shape of the pupil and the position of the limbus (the iris-sclera boundary) (Duchowski, 2007). Measurement of ocular features provided by these measurement techniques may or may not be made automatically. The limbus eye tracking uses infrared emitters and detectors mounted on head or spectacle frames. VOG eye trackers are reactively cheap and provide a simple measure of eye rotation within the head, but they require effective head restraint.

1.4.2.4 Video-based infrared (IR) pupil-corneal reflection (PCR) eye tracking

These are eye trackers that rely on photography (video). Most video based eye trackers track the first Purkinje image (reflection from the front of the cornea when light is shone) and/or the centre of the pupil. They use advanced image processing methods to the precise location of the necessary landmarks (e.g. pupil and corneal reflection). Video-based tracks use head-mounted or remote visible light video cameras. In the remote eye tracker, the camera records the gaze data and eye features are extracted and analysed on a computer. In the head-mounted system, a scene camera is used to record the visual stimuli simultaneously. To identify the centre of the pupil, a 'dark pupil' tracking approach is mostly used. This technique takes advantage of the fact that under infrared illumination, the pupil appears as a comparatively dark circle compared to the rest of the eye.

Small head movements are differentiated from eye rotation based measurements of the pupil and corneal reflection. Head movements shift both the pupil and corneal

reflection to the same extent, whereas eye rotations shift the pupil and corneal reflection in a differing amount.

The sampling rate of video based eye trackers is determined by the speed of the camera (typically 30–2000 Hz) (Crane, 2018; Klein and Ettinger, 2019). Video-based corneal reflection eye trackers have relatively better data quality in terms of signal to noise ratio compared other eye trackers but their performance may be affected by changes in light conditions. In addition, the accuracy of these video-based eye trackers depends on successful calibration, which does not work well for all individuals (Fairclough and Gilleade, 2014), and can be particularly problematic for individuals with visual impairments: particularly those that affect central vision.

1.5 Some key challenges regarding the use of eye-movements to detect or quantify vision loss

Despite the growing interest in using eye trackers to investigating eye movements with VF loss (glaucoma), techniques to investigate eye movements are underdeveloped. Most studies have been investigating eye movements by quantifying saccades and fixations although eye movements are complex spatio-temporal signals. This thesis investigates natural eye movements collected while subjects watch clips and/or a series of pictures to detect VF loss. Nevertheless, to detect VF loss from natural eye movements with reasonable accuracy, several unique challenges need to be addressed. These include the following:

- Significant individual variability and similarity between subjects in eye movements when watching videos/pictures make it challenging to find robust differences between groups and similarities within groups
- Poor quality data due to inherent technical limitations with eye tracking
- Eye movement analysis methods need to account for cognitive/non-perceptual behaviours, such as the subject's tendency to look at the centre of the screen while watching videos/pictures
- Lack of accurate eye movement data pre-processing tools, especially for dynamic stimuli that can be used to detect eye movement events such as saccades, fixations, and smooth pursuits accurately
- Lack of standard methods and normative datasets for analysing and interpreting naturalistic eye movements of patients with VF loss

All these individual challenges or limitations are subject to detailed research by the

applied vision science community. The focus of this thesis, however, is to develop a reasonably accurate method, using eye movement analysis, to separate patients with glaucoma from healthy controls.

1.6 Objectives

The overall goal of this thesis is to work towards developing methods to detect glaucomatous VF loss from natural eye movements collected while patients watched short video clips and pictures. This thesis also describes an experimental analysis of the eye movements of young, visually healthy participants, whilst they use a gaze-contingent display giving them artificial VF loss, to develop methods that discriminate different levels of VF loss. The specific aims of the individual chapters were as follows:

- **[Chapter 2] To review the literature on eye movements of patients with glaucoma**

  Chapter 2 reviews previous studies examining the impact of glaucomatous vision loss on eye movements. This chapter provides an overview of how eye movement measures are affected due to VF loss while performing different tasks, and identifies current gaps in the literature.
- **[Chapter 3] To investigate whether glaucoma alters eye movements when watching images of natural scenes**

  Chapter 3 reports novel empirical data in which eye movements are compared between the two eyes of glaucoma patients with asymmetric VF loss (i.e., instead of between patients and healthy controls). The 'within-subjects' study design controlled other factors such as cognitive skills, sex, and individual preferences that affect eye movements, measuring the purer effect of VF loss on eye movements. The hypothesis was that patients' eye movements would be altered in their worse eye compared to their better eye when passively viewing a series of images. The work reported in this chapter considers some novel methods for the analysis of the eye movement patterns (Asfaw et al., 2018a).
- **[Chapter 4] To use a simulation study to investigate whether eye movements are clinically useful to detect VF loss**

  Chapter 4 investigates whether natural eye movements can predict the presence of 'artificial' glaucomatous VF loss using gaze-contingent simulated scotoma. VFs of a real patient that were measured at different times, during the course of their condition, were used to simulate VF progression. Young, visually healthy participants then experienced 'artificial' gaze-contingent scotoma while watching different clips and pictures on a computer monitor. This chapter investigates how various eye movement measures are affected due to the onset of simulated

VF loss and whether the measured effect of these altered eye movements would be large enough to be clinically useful for detecting moderate and advanced VF loss.

- **[Chapter 5] To discriminate between patients with glaucoma and age-similar healthy subjects using eye movements**

  Chapter 5 contains two parts. First, it reports the curation of data previously introduced by Crabb et al. (2014), now made freely available online (Asfaw et al., 2018b). Second, it describes a new approach to examining these data in order to discriminate between patients with glaucoma and controls via their natural eye movements. Features extracted from static and sequential eye movements were analysed in a novel fashion using machine-learning classifiers to separate patients with glaucoma from controls.

- **[Chapter 6] Overview of main findings and future work**

  Chapter 6 concludes the thesis with a summary of the key findings and a discussion of potential future work.

- **[Appendix]**

  Supplementary materials for all chapters are included in the appendix.

Chapter 2

Eye movements in glaucoma: A literature review

2.1 Introduction

As described in Chapter 1, glaucoma is an age-related eye condition that can lead to a characteristic visual field (VF) loss. Moreover, VF loss typically goes unnoticed and is only detected by clinical examination. A better method of assessing of VF loss would be useful. As introduced earlier, the work described in this thesis speculates on the idea that changes in eye movement may be characteristic of VF loss in glaucoma. Despite this, understanding how eye movements are affected due to glaucoma remains largely unclear; this question forms the subject of this review.

A recent synthesis of the literature on eye movements of patients with glaucomatous VF loss was recently conducted (Kasneci et al., 2017); however, this was not done systematically. This chapter describes a systematic review of the recent research literature on eye movements in people with glaucoma. In addition, this review surveys the techniques used to analyse the data from eye movement experiments.

I read and screened abstracts and full-text articles for inclusion; uncertainties regarding inclusion were discussed with Pete R. Jones (PJ). I then extracted data from the selected studies and wrote the report, which was reviewed, edited and approved by PJ and David P. Crabb (DC).

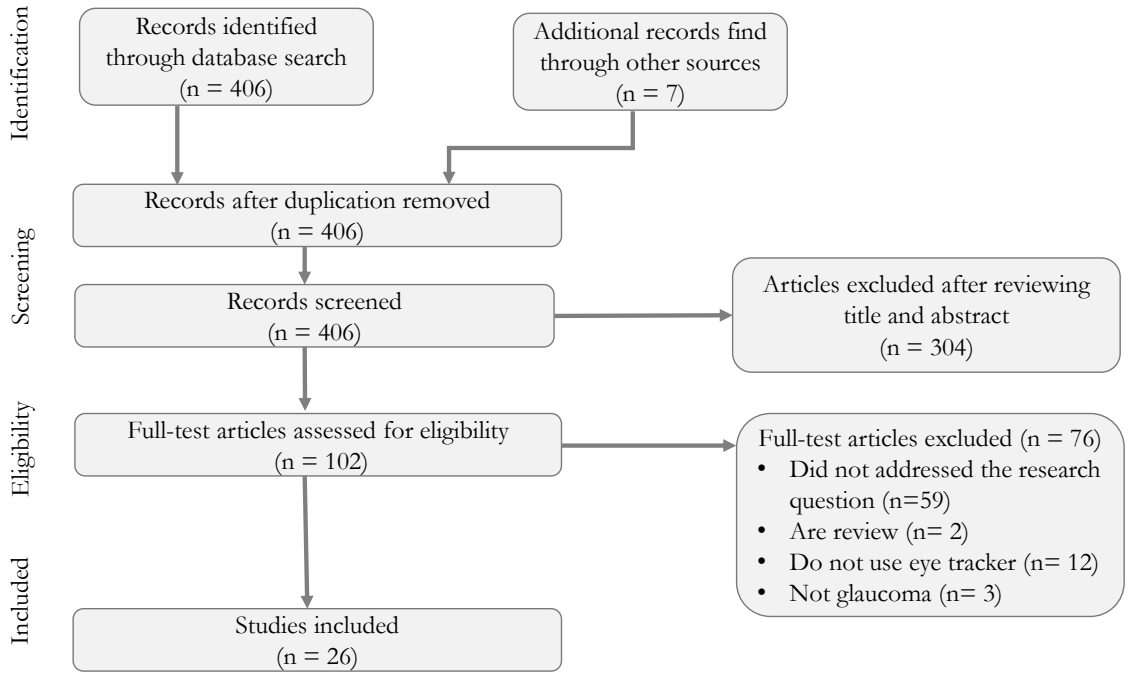

Figure 2.1: Flow of articles selection process in the systematic review.

2.2 Methods

2.2.1 Data Sources and Search Strategies

A single researcher (DA) searched the literature in MEDLINE, EMBASE, CINAHL and PsycINFO using the EBSCOhost searching interface. The searches were not restricted by publication type or study design; however, they were limited to human participants, and English-language papers (no time restriction).

The following string of search terms was used: ('eye movements' OR 'eye tracking' OR 'scanpath' OR 'saccade' OR 'fixation' OR 'gaze') AND ('glaucoma' OR 'peripheral vision' OR 'vision loss'). The results of this search were then restricted to those with mainly elderly participants (>40 years). Search results were recorded and exported into an XML file.

2.2.2 Screening of citations

Search results were imported into Covidence (Covidence systematic review software, Veritas Health Innovation, Melbourne, Australia, available at www.covidence.org). Results were screened first by title and then by abstract initially by a single reviewer (DA) to assess eligibility. Eligible studies were those that used eye tracking to measure task performance, involved people diagnosed with glaucoma, available in English. For this review, conference abstracts or review articles were excluded. The full-text articles

of all potentially relevant sources were obtained and saved as BibTeX files.

In cases where there was uncertainty as to whether a study was appropriate, the full-text copy was obtained and PJ was consulted. Finally, the full texts of the selected papers were reviewed. Information on study design, participant demographics, eye movement outcome measures and main findings were tabulated. A condensed version of this tabulation is shown in Table 2.1.

Table 2.1: Summary of literature reviewed showing sample size, eye movement parameters used for comparison and task involved. The sign (↑) is used when eye movement parameters are larger/more frequent (statistically significant) in patients with glaucoma than in control subjects; conversely, the sign (↓) indicates that eye movement parameters are smaller/less frequent (statistically significant). The sign (-) represents a finding of no difference between patients and control subjects. For completeness, task performance measures used are included.

Source	Population	Task	Outcome measures	Main finding
Sippel et al. (2014)	Glaucoma: 10 Control: 10	Visual search	• Number of correctly collected items • Time to complete the task • Horizontal gaze activity (-) • Glance proportion towards VF defect (↑)	• Patients needed a longer to collect items in a supermarket setting than controls. • Successful task performance of patients is associated with longer and more frequent glancing towards the location of the VF defect.
Coeckelbergh et al. (2002)	Peripheral VF loss (PVFL): 35 Control: 8	Dot counting & visual search	• Search time (↑) • Number of errors (↑) • Saccade amplitude (dot counting task) (-) • Fixation count (dot counting ↑) • Fixation duration (dot counting ↓) • Return saccades (visual search ↑)	• Subjects with PVFL required more fixations and longer search times, made more errors and had shorter fixation durations than control subjects on the dot-counting task. • During the visual-search task, in the PVFL group, there were statistically significant associations between VF extent and search time, and between VF extent and number of fixations.

Smith et al. (2012)	Glaucoma: 40 Control: 40	Visual search	• Saccade rate (↓) • Saccade amplitude (-) • Search duration across trials (-)	• There was an association between an increase in saccade rate and better performance in the search task.
Wiecek et al. (2012)	PVFL: 10 Control: 11	Visual search	• Search duration (-) • Fixation duration (-) • Saccade amplitude (-) • Number of saccades (-) • Direction of saccades	• Patients with PVFL showed a biased directional distribution that was not directly related to the locus of vision loss; patients did not optimally compensate for VF loss during visual search.
Kübler et al. (2015)	Glaucoma: 6 Control: 8	Driving simulator	• Head movement • Fixation duration • Fixations per minute • Saccade directions • Saccade amplitude	• Participants with glaucoma who passed the test showed increased eye-scanning activity (increased fixation rate, head movements and more vertical scanning).
Kasneci et al. (2014)	Homonymous VF defects = 10 Glaucoma = 10 Controls = 20	Driving task on a pre-specified public on-road.	• Direction of saccades (-)	• Patients who passed the test displayed different exploration patterns, focused longer on the central area of the VF and performed more glances towards the area of VF defect.

Crabb et al. (2010)	Glaucoma = 9 Controls = 10	Watching hazard perception test films (HPT)	• Saccade rate (↑) • Fixations rate (↑) • Smooth pursuits rate (↑) • Saccade amplitude (-) • Spread of fixations (-)	• Participants with glaucoma exhibited different eye movements in terms of saccade and fixation rate compared to control subjects.
Vega et al. (2013)	Glaucoma = 23 Controls = 12	Drive in a simulator	• Gaze directed at top (-) • Gaze directed at bottom (-) • Fixation rate (-) • Saccade amplitude (-)	• Glaucoma patients moved their steering wheels more actively, had impaired performance and did not apply visual-compensation mechanisms to compensate for their VF loss.
Gangeddula et al. (2017)	POAG = 20 Controls = 13	Driving in simulator	• Number of correct responses (accuracy) • Response time to the peripheral target • Percentage gaze time on the central fixation target	• Adding cognitive demand to the VF test adversely affected accuracy and response times, affecting functional VF performance in drivers with glaucoma.

Lee et al. (2017)	Glaucoma = 30 Controls = 25	HPT	• Time to first fixation on each hazard • Fixation time on each hazard before the response • Fixation rate (-) • Fixation duration (-) • Saccade amplitude (↓) • Variance in fixation positions (-)	• Participants with glaucoma made smaller saccades and exhibited delays in hazard-response times and first fixations on hazards.
Lee et al. (2018)	Glaucoma = 13 Controls = 10	Driving on a closed-road circuit	• Hazard hit • Lane-crossing time • Saccade amplitude (↑) • Fixation duration (-) • Saccade rate (-) • Horizontal movement variance (↑) • Vertical movement variance (↑) • Yaw head movement variance (-)	• Participants with glaucoma had significantly poorer overall driving scores, exhibited larger saccades and hit more hazards than control subjects. Larger saccades were associated with better driving scores in the glaucoma group.
Burton et al. (2014)	POAG = 54 Controls = 38	Reading	• Reading speed	• The inferior left region of the binocular VF may have relative importance in determining reading speed in people with glaucoma in both eyes.

Smith et al. (2014)	POAG = 32 Controls = 34	Reading	• Reading duration • Saccade rate • Fixation duration	• Patients took longer to read the sentences, made fewer saccades per second with their worse eye than with their better eye. The worse eye with longer reading duration made more backward moving saccades.
Burton et al. (2015)	Glaucoma = 18 Controls = 39	Reading	• Text saturation • Saccade rate	• Some patients with advanced VF loss read more slowly than control subjects, but there was no statistically significant difference between patients and controls in terms of reading speed.
Cerulli et al. (2014)	Glaucoma = 32 Controls = 34	Reading	• Maximum and minimum eye movements along the horizontal and vertical axis (↑) • Saccade speed (-)	• Maximum horizontal and vertical eye movements of the glaucoma group were significantly higher than the values for the control group. • Participants with early and moderate glaucoma made altered eye movements during reading.
Murata et al. (2017)	Glaucoma = 50 Controls = 20	Reading	• Number of fixations per 100 characters • Reading duration • Fixation duration (↑)	• Patients with glaucoma exhibited longer fixation duration than controls. • Monocular VF defects measures were correlated with slower reading.

Smith et al. (2012)	Glaucoma = 30 Controls = 30	Picture viewing	• Saccade amplitude (-) • Number of saccades (↓) • Fixation duration (↑) • BCEA (↓) • Fixation locations (-)	• Glaucoma patients with bilateral VF loss showed altered eye movements (smaller number of saccades, longer fixations and restricted eye movements) when viewing natural images.
Crabb et al. (2014)	Glaucoma = 44 Controls = 32	Watching short films	• Features from saccade direction/amplitude	• Features extracted from eye movements recorded while people freely watched short films can be used to differentiate between glaucoma patients and control subjects.
Geruschat et al. (2006)	Glaucoma = 12 AMD = 9 Controls = 12	Road crossing	• Fixation locations	• Patients and control subjects allocated gaze differently while crossing roads.
Miller et al. (2018)	Glaucoma = 20 Controls = 20	walking	• Walking speed • Fixation locations	• Patients with glaucoma exhibited impaired gaze-foot coordination, resulting in less accurate foot placement.
Lajoie et al. (2018)	Glaucoma = 20 Controls = 20	walking	• Fixation location and duration	• Participants with glaucoma exhibited altered gaze behaviour compared to control subjects when negotiating an array of stationary obstacles and multitasking while walking.

Lamirel et al. (2014)	Glaucoma = 8 Controls = 4	Target tracking	• Saccade latency (↑) • Gain of saccade (↑) • Velocity peak (↓)	• On static targets the saccades were delayed and their accuracy was reduced, compared with those of normal observers. • On a task involving precise motion analysis, the latency and accuracy of the saccades were impaired, compared with those of normal observers.
Najjar et al. (2017)	Glaucoma = 16 Controls = 16	Prosaccade and antisaccade task	• Saccade latency (↑) • Peak velocities (↓) • Gain of prosaccade (↓) • Percentage of errors in antisaccades task (↑)	• POAG patients exhibited a reduced average velocity of saccades compared to controls. • Saccades performed by POAG patients were hypometric, and with reduced amplitude. • POAG patients displayed more antisaccade errors as compared to controls.
Kanjee et al. (2012)	Glaucoma = 16 Controls = 21	Prosaccade and antisaccade task	• Saccade reaction time (↑) • Saccade amplitude (-) • Peak velocity (-)	• Saccadic eye movements are delayed in patients with early, moderate, or advanced glaucoma.
Glen et al. (2013)	Glaucoma = 51 Controls = 39	Face recognition	• Saccade rate (-) • Saccade amplitude (-)	• Patients with bilateral VF defects improved their face recognition performance by making larger saccades.

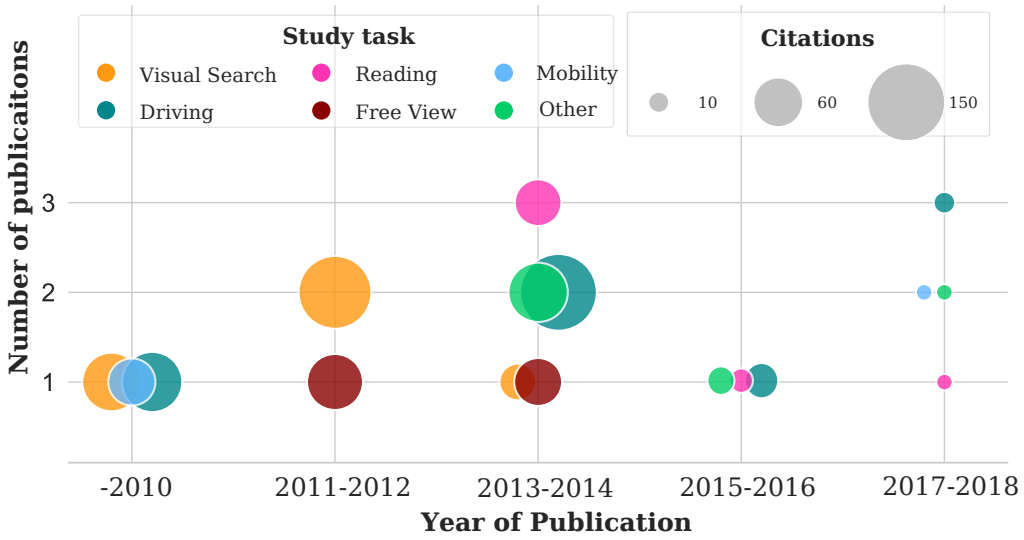

Figure 2.2: The frequency of published papers and the citation received over time grouped by task involved in the study.

2.3 Results

The search, conducted on 8 June 2018, yielded 406 results. After full-text review, a total of 26 studies, involving 624 patients and 514 visually healthy control subjects, were selected for inclusion: seven studies on driving-related tasks, five studies on reading tasks, four studies on visual-search tasks, two studies on free viewing of natural images and videos, three studies on mobility and related tasks and, lastly, five studies on other types of tasks (see Table 2.1). Publication dates, study tasks and frequency of citation are summarised in Figure 2.2 increased (before 2002 no studies had been published on the subject). The number of publications over time has been increasing since 2010. This increase may be attributed to the developments in eye tracking technology.

2.3.1 Driving

Accurate scanning of the visual environment (e.g. traffic lights, road signs, pedestrians and other drivers) is essential in making safe driving decisions and detecting potential hazards (Owsley and McGwin Jr, 2010). People with glaucoma are reported to exhibit delayed reaction times, impaired visual-processing abilities (Tatham et al., 2014) and increased physical frailty compared to peers with healthy vision (Black et al., 2011). These collective declines in visual function and physical status have adverse effects on driving.

Seven papers describing case-control studies related to driving, involving 111 people with glaucoma, were found and assessed. Three of the seven studies used driving simulators to study driving performance and eye movement behaviour of patients with

glaucoma. Vega and colleagues (Vega et al., 2013) compared lane-keeping, letter detection, and obstacle avoidance performance of patients with glaucoma and age-similar controls while driving in a simulated environment. Vega and colleagues reported no difference between patients and controls in terms of eye movements, and patients with glaucoma made no eye movements to compensate for their VF loss. In a similar simulated driving environment, Kübler and colleagues (Kübler et al., 2015) reported that patients with binocular glaucomatous VF loss were able to pass a driving test by increasing their scanning behaviour and head movements. Another study (Gangeddula and colleagues (Gangeddula et al., 2017)) investigated the effect of cognitive demand on functional VF performance. It found that functional VF performance worsened as cognitive demand increased. Cognitively demanding secondary tasks are likely to affect the driving performance of healthy drivers (discussed elsewhere (Engbert et al., 2005; Victor et al., 2005)); however, Gangeddula and colleagues (Gangeddula et al., 2017) showed that reduction in driving performance (such as lane-keeping) is elevated in glaucoma patients.

Two studies assessed driving performance of patients with glaucoma on a real road using portable eye trackers, worn as glasses. Kasneci and colleagues (Kasneci et al., 2014), using an open road driving test task, reported that four out of ten glaucoma patients in their cohort passed a real-road driving assessments despite their binocular VF loss and attributed their results to compensatory eye movements towards the location of VF damage. In addition, there was a significant difference in head and shoulder movements between the glaucoma patients who passed the driving test and those who failed. Another more recent work (Lee and colleagues (Lee et al., 2018)), on a closed-road but familiar to the participants, found that patients who made larger saccades performed well in the driving tasks.

Two studies (involving a total of 39 patients with glaucoma) were identified that investigated the effect of glaucomatous VF loss in computer-based hazard perception tests (HPT). Crabb and colleagues (Crabb et al., 2010) found that glaucoma patients made more altered eye movements compared to age-similar control subjects. Specifically, patients made more saccades/fixations and more smooth pursuits when watching HPT videos, suggesting that the larger number of eye movements made by patients could be due to adaptation to functional deficits. Recently, Lee and colleagues (Lee et al., 2017) investigated the HPT performance of a relatively large group of patients with glaucoma. They reported that patients exhibited delayed hazard-response times and delayed fixations on hazards compared to age-similar controls. Unlike Crabb and colleagues (Crabb et al., 2010), who found no difference between patients and control subjects, Lee and colleagues (Lee et al., 2017) reported that patients made smaller

saccades compared to controls.

2.3.2 Reading

Pre-processing information using the peripheral VF is useful for rapid reading (Ikeda and Saida, 1978). Glaucomatous VF defects, usually associated with peripheral VF loss, have been linked with poor reading performance. Self-reported performance measurements have shown that patients with glaucoma have difficulties with their reading (Freeman et al., 2008; Ramulu, 2009; Crabb et al., 2013). The main advantage of using an eye tracker to evaluate reading performance is the ability to measure eye movements while participants read silently.

A total of five studies using an eye tracker to assess the effects of glaucoma on reading were reviewed. Cerulli and colleagues (Cerulli et al., 2014) investigated eye movements of glaucoma patients who read silently on a Microperimeter Nidek MP1 screen (Nidek Technologies, Padua, Italy). Authors found no significant differences regarding mean reading speed, accuracy and comprehension between patients with glaucoma and the control group; however, the maximum horizontal and vertical eye movement values were significantly increased in patients with glaucoma. Authors speculated that the altered eye movements were due to VF defects since the patients had healthy central 10–2 degree VF (Cerulli et al., 2014).

Four of the five reading studies assessed the performance of glaucoma patients who read texts on a computer screen. Burton and colleagues (Burton et al., 2014) found a significant positive association between perceptual span and reading speed in patients and controls. The patient group exhibited greater average text saturation (average percentage of a line of text covered by the point of regard during reading) than controls; however, no significant difference was found between patients and control subjects in terms of reading speed. Furthermore, Burton and colleagues (Burton et al., 2014) reported that patients with glaucoma made a larger number of saccades compared to control subjects in lexical-decision tasks (i.e., the number of saccades made to read a set of words presented in isolation). Following a similar methodology, Murata and colleagues (Murata et al., 2017) conducted a study on 50 people with glaucoma and 20 age-similar control subjects. They found a longer mean-fixation duration and more prolonged character recognition in people with glaucoma than in controls. Furthermore, they suggested that monocular VF-defect scores are correlated with lower reading performance in both eyes (Murata et al., 2017).

Several studies, including those reviewed here, have demonstrated impaired reading performance in people with glaucoma, especially those with advanced or bilateral field

loss (Fujita et al., 2006; Ramulu, 2009; Ishii et al., 2013). However, reading performance can be affected by a multitude of factors, such as education, cognitive skills and age. To better isolate the effect of VF loss on reading ability, Smith and colleagues (Smith et al., 2014) compared eye movements of the worse (most VF damaged) and better (least VF damage) eyes of 14 people with asymmetric VF loss. Eye movements in the worse eye exhibited a reduced saccade rate and longer reading duration on average, compared to the better eye.

2.3.3 Mobility

Systematic visual scanning is important for navigation and obstacle avoidance since the peripheral VF is utilised to perceive surroundings (Fortenbaugh et al., 2007). Loss of peripheral vision has been linked to difficulties in mobility, and patients with glaucoma have an increased risk of falls (Beurskens and Bock, 2012; Mihailovic et al., 2017). During speed walking, the lower peripheral vision is most important, and loss of the central 20° has been associated with frequent collisions (Turano et al., 2004).

Four papers used portable eye trackers to investigate the eye movement behaviour of patients with peripheral VF loss as they walked. Gang Luo and colleagues (Luo et al., 2008) found that patients and controls exhibited similar distributions of saccade sizes and directions. In a similar study, Geruschat and colleagues (Geruschat et al., 2006) reported that glaucoma patients showed the same fixation allocation as that of healthy control subjects during curb and cross walk tasks. Another study (Miller and colleagues (Miller et al., 2018), however, reported that glaucoma patients developed inefficient gaze-scanning strategies in walking tasks, which could increase their risk of falling, contradicting the results of Geruschat and colleagues(Geruschat et al., 2006). Furthermore, Miller and colleagues (Miller et al., 2018) reported that patients with glaucoma exhibited altered eye movement behaviour (looked sooner at a future step). Kim Lajoie and colleagues (Lajoie et al., 2018) also had similar findings to that of Miller and colleagues (Miller et al., 2018) in their study regarding navigation around an obstacle, patients with glaucoma more likely to direct their gaze to their current position, make a larger proportion of fixations and make more contact with obstacles.

2.3.4 Free viewing

Eye movement behaviour during free viewing in people with glaucoma is a relatively underdeveloped research area. Two works have investigated eye movements during free viewing in patients with glaucoma. Smith and colleagues (Smith et al., 2012) studied eye movements of patients with glaucoma watching natural images passively on a computer screen. The authors reported that fixations made by the patients were

restricted to narrower regions of the image and that patients made fewer saccades compared to control subjects. In an attempt to detect glaucomatous VF loss from eye movements, Crabb and colleagues (Crabb et al., 2014) analysed eye movements of glaucoma patients and age-similar controls watching video clips. They extracted features from saccadic movements and trained a machine-learning classifier. Their results showed reasonable separation between the two groups.

2.3.5 Visual search

Four studies examined the effects of glaucomatous VF loss on eye movements while performing a visual-search task. Sippel and colleagues (Sippel et al., 2014) used head-mounted eye trackers to measure the performance of patients with glaucoma as they searched for items in a supermarket. Their data showed no difference in horizontal-gaze activity between patients and controls. Some patients with glaucoma were able to finish the task (collecting items) as quickly as control subjects by making saccades towards their area of VF defect, suggesting that compensatory eye movements are the source of discrepancies in task-performance results among glaucoma patients. On the other hand, in a study involving 20 patients with peripheral vision loss (age-related macular degeneration, glaucoma, or retinitis pigmentosa), Coeckelbergh and colleagues (Coeckelbergh et al., 2002) found that patients required longer search times, made more fixations and made more errors than control subjects.

Two studies (Wiecek et al., 2012; Smith et al., 2011) investigated eye movements of patients with PVFL while searching for a target in natural images. Wiecek and colleagues (Wiecek et al., 2012) found that search duration, fixation duration, saccade size and the number of saccades per trial were not significantly different between PVFL patients and controls. They also found that patients made fewer eye movements towards the location of scotoma in their VF, suggesting that patients do not optimally compensate for field deficits during visual searches. In contrast, Smith and colleagues (Smith et al., 2011) reported that, in a similar visual-search task, patients exhibited a smaller rate of saccades than controls. They also reported that the saccade rate was more variable in the patient group, and patients who executed a larger number of saccades exhibited improved visual-search performance.

2.3.6 Other tasks

Motion perception is impaired in glaucoma (Shabana et al., 2003). Lamirel and colleagues (Lamirel et al., 2014) studies how impaired visual motion processing in patients with glaucoma could affect ocular motor behaviour, during tasks involving watching a moving target. Glaucoma patients showed delayed and less accurate saccades when

watching static targets than controls, while in tasks that involve precise motion analysis, pre-perimetric glaucoma patients (patients with normal VF) and those with advanced VF defect the latency and accuracy of the saccades were impaired compared to healthy controls. On a similar argument, Kanjee and colleagues (Kanjee et al., 2012) found delayed saccadic eye movements in patients with early, moderate and advanced glaucoma patients in pro-saccade step task compared to age-similar controls. The authors reported that other saccade parameters such as duration, amplitude, and velocity of the saccades were not altered and these parameters showed no significant correlation with VF loss measurements. A similar study to that of Lamirel and colleagues (Lamirel et al., 2014), Najjar and colleagues (Najjar et al., 2017) observed altered saccade velocity and amplitude are reduced in glaucoma patients with no detectable VF loss. The authors suggested that these altered eye movements are possibly due to impairments in cortical and subcortical areas of the brain (Kanjee et al., 2012; Najjar et al., 2017).

Motion perception is impaired in glaucoma (Shabana et al., 2003). Lamirel and colleagues (Lamirel et al., 2014) studied how impaired visual-motion processing could affect ocular motor behaviour as subjects watched a moving target. Glaucoma patients exhibited delayed saccades, compared to controls, when watching static targets, while in tasks involving precise motion analysis, the latency and accuracy of the saccades of patients—both pre-perimetric patients (with normal VF) and those with advanced VF defects were impaired compared to those of healthy controls. Similarly, Kanjee and colleagues (Kanjee et al., 2012) found delayed saccadic eye movements in patients with glaucoma in a pro-saccade task (target detection), compared to age-similar controls. They reported that other saccade parameters, such as duration, amplitude and velocity of saccades, were not altered and showed no statistically significant correlation with VF loss measurements. A similar study by Najjar and colleagues (Najjar et al., 2017) observed altered saccade velocity and amplitude in glaucoma patients with no detectable VF loss. However, in contrast to the findings of both Lamirel and colleagues (Lamirel et al., 2014) and Kanjee and colleagues (Najjar et al., 2017), Najjar and colleagues (Najjar et al., 2017) found no difference in saccade latency between patients and controls.

Glen and colleagues (Glen et al., 2013) investigated the face-recognition performance of people with advanced glaucoma using images on a computer screen. They reported that patients with bilateral central 10° defects made larger saccades, improving their face-recognition performance. In this subgroup of glaucoma patients, there was also a significant association between the frequency of saccades and the percentage of correctly identified faces. A study from Dive and colleagues (Dive et al., 2016) investigated the performance of glaucoma patients in real-world tasks. In the familiar task

of making sandwiches, patients' performance was similar to that of control subjects; however, in an unfamiliar task, involving building a model, patients were slower and made more saccades and longer fixations than healthy control subjects, suggesting that unfamiliar tasks require more peripheral visual input than familiar tasks.

2.4 Discussion

This synthesis of literature reviewed 26 studies on eye movements of patients with glaucoma. All the papers reviewed measured eye movements of patients with glaucomatous VF loss while performing daily tasks. Nearly all these studies suggested that eye movements are altered in patients with glaucoma compared to age-similar, visually healthy controls.

This literature review found that the reported differences between glaucoma patients and controls are not consistent across studies. For instance, Coeckelbergh and colleagues (Coeckelbergh et al., 2002) found that the number of fixations while performing visual-search tasks was higher in the patient group. In contrast, Smith and colleagues (Smith et al., 2011) found smaller saccade rates in glaucoma patients compared to controls, and Wieck and colleagues (Wiecek et al., 2012), in a study on a smaller cohort of patients with PVFL, found no difference between patients and controls in eye movements during a visual-search task. A number of factors could explain these differences. First, the experimental designs were different: for instance, Smith and colleagues (Smith et al., 2011) asked participants to search for a target in photographs, while Coeckelbergh and colleagues (Coeckelbergh et al., 2002) required participants to identify a target (the letter 'O') from an array of distractors.

Second, dissimilarities in patients' ocular pathology—such as the severity of VF loss, visual acuity and contrast sensitivity—may have led to the inconsistent results. Finally, inconsistent pre-processing and data analysis of eye movements might have contributed to the disagreements in results: for instance, Smith and colleagues (Smith et al., 2011) discarded saccades smaller than 0.5° in their analysis, while Coeckelbergh and colleagues (Coeckelbergh et al., 2002) used displacement criteria of 1° to identify saccades. Given that the number of small saccades (less than 3°) is higher than the number of large saccades (Dorr et al., 2010), differences in data pre-processing approaches might have led to inconsistent results.

There are limitations in the literature that affect the interpretability of the findings. First, most of the papers included in this synthesis use simple eye movement parameters, such as saccade count, fixation duration and fixation amplitude, to compare

eye movements. None of these eye movement parameters was able to consistently separate patients with glaucoma from controls across the studies. In other words, these parameters vary widely between studies, regardless of task similarity, indicating that these crude eye movement summary statistics can be unreliable. Second, the low statistical power (because of low sample size) in these studies made them suspectable to inflated effect-size estimates (Button et al., 2013). Only Crabb and colleagues, using relatively large cohorts of patients and healthy controls, demonstrated the potential of natural eye movements to separate patients with glaucoma from controls (Crabb et al., 2014). Further study is warranted to unravel the overlooked information in these data to develop better ways of analysing eye movements.

This review also indicates other gaps in the literature that future research should explore. First, it is unclear which types of static and dynamic stimuli are most useful for distinguishing patients from healthy subjects, e.g. natural eye movements are more coherent (high similarity between subjects) when watching films than when watching natural scenes (Dorr et al., 2010). This thesis in part explores what types of content could be most useful in differentiating between people with VF loss and healthy controls (see Chapter 4). Second, there is limited evidence of how different levels of VF loss affect eye movements. While most of the studies found altered eye movements in glaucoma patients compared to age-similar healthy controls, what is required is a model that can discriminate among the patient group to understand how different VF defects, level of severity and location of scotoma impair patients' visual function and quality of life. This question is partially addressed in Chapter 4.

Some of the reviewed studies suggested that eye trackers could be used for rehabilitation, i.e. to train patients' visual-scanning behaviour to improve their performance in daily tasks (Kasneci et al., 2017). For instance, better task performance in visual-search task in the patient group was associated with frequent glancing towards the location of the VF defect (Smith et al., 2011; Sippel et al., 2014), and better driving performance in people with glaucoma was associated with systematic visual-scanning strategies (Kasneci et al., 2014; Kübler et al., 2015). Nevertheless, no study investigated the effectiveness of compensatory eye movements in clinical rehabilitation of people with glaucomatous VF loss.

Several limitations should be acknowledged in regard to this review. First, only papers published in peer-reviewed journals were included. This is likely to have influenced the results found due to submission bias and/or publication bias. Second, due to lack of translation resources, non-English language papers were excluded. Third, the literature search and data extraction were conducted by a single reviewer (due to

resource and time constraints), and this might have introduced a bias in the review. The PRISMA guidelines (preferred reporting items for systematic reviews and meta-analyses) recommends more than one reviewer to follow through the search process and data extraction.

2.5 Conclusions

- Studies of eye movements in patients with glaucoma are case-control studies mostly limited by small sample size and inconsistent data analysis techniques and findings.
- The cumulative evidence suggests that VF loss alters eye movements during the performance of daily tasks.
- The exact impact of glaucomatous VF loss on eye movements remains unclear since results are inconsistent across studies.
- This review highlights the need for standard tools to pre-process and analyse eye movement data to reconcile inconsistent results.
- Eye movement studies employing free viewing of photographs and videos show promising results in detecting glaucomatous VF loss.
- Some studies have found an association between compensatory eye movements and better task performance, suggesting the potential application of eye trackers in rehabilitation.

Chapter 3

Does glaucoma alter eye movements when viewing images of natural scenes? A between-eye study

3.1 Introduction

As discussed in Chapter 1, visual field (VF) assessments are critical for the detection and management of glaucoma. Current methods of VF assessment (automated perimetry) are demanding for patients to perform, and are often problematic to organize and interpret in busy clinics (Malik et al., 2013; Glen et al., 2014). In short, alternative measures of the visual function in glaucoma are therefore desirable.

As discussed previously, glaucoma patients have been shown to have altered eye movements compared to peers with normal vision when performing everyday tasks, such as reading, (Burton et al., 2014; Ishii et al., 2013) visual search, (Smith et al., 2011) face recognition, (Glen et al., 2013) watching video, (Crabb et al., 2014) driving, (Bowers et al., 2005; Medeiros et al., 2012; Vega et al., 2013; Glen et al., 2015) and viewing images (Smith et al., 2012) (for a review, see Kasneci et al. (2017)). Furthermore, it has been recently reported that people with early-stage glaucoma, with no detectable VFloss, exhibit altered eye movement behaviour (Najjar et al., 2017). More recently, there has even been reports of a possible link between optic nerve head strains induced by eye movements and axonal loss in glaucoma (Wang et al., 2016).

However, as discussed in Chapter 2, existing studies disagree about precisely how eye movements are altered by glaucomatous VF loss. For instance, Crabb et al. (2010)

found glaucoma patients made more saccades, fixations, and smooth pursuit eye movements per second than controls when watching a movie depicting real-world driving. In contrast, Wiecek et al. (2012) reported that peripheral VF loss did not influence saccade amplitude, fixation duration, and number of saccades during visual search tasks. Instead, they observed a significant difference in the direction of saccades between patients and controls. Other studies have variously reported difference in saccade rate but not amplitude (Smith et al., 2011), number of saccades and spread of fixations but not saccade amplitude (Smith et al., 2012), and saccade amplitude but not fixation rate or duration (Lee et al., 2017). Some of these ambiguous results maybe due to differences in task. However, previous studies also suffer from two limitations, both of which I address in the present study.

First, previous studies have exhibited imperfect matching between cases and controls. Most previous studies compared eye movements between independent groups of glaucoma patients and age-similar controls. Individual differences in factors such as cognitive skills, visual acuity (VA), gender, culture, and health status are therefore confounding factors which could have affected eye movements between participants (Smith et al., 2014; Coutrot et al., 2018). Accordingly, in this study, I investigate people with asymmetrical VF loss between eyes. The better (less affected) eye was used as the control for the worse eye. Comparing performance within a patient (i.e., between eyes), instead of comparing across patients and controls, allowed us to control individual differences, resulting in a purer measure of how VF loss affects eye movements.

Second, many previous studies used only a small subset of relatively simple metrics to describe patients' eye movements (e.g., saccade count, fixation count, saccade rate, and fixation duration). These metrics do not capture the spatial or temporal characteristics of the scanpath, and so may be relatively insensitive to the effects of VF loss. Accordingly, in the present work I also quantify the spread of fixations (Crabb et al., 2010) to examine spatial characteristics of eye movements. And I used intersaccadic angle (Amor et al., 2016) (difference in direction between successive saccades) to examine temporal characteristics of saccadic movements.

In short, the current study examined how eye movements are affected by VF loss due to glaucoma. Analyses were performed within-subject (between eyes), using patients with asymmetric VF, in order to isolate the specific impact of VF loss, and novel metrics were used to characterize each eye's spatiotemporal profile. Furthermore, I investigated the relationships between eye movement metrics and common clinical measures (e.g., visual acuity, contrast sensitivity). My main hypothesis was that patients' eye movements would be altered in their worse eye compared to their better eye when

passively viewing a series of images.

This chapter is published in *Investigative Ophthalmology and Visual Science* (Asfaw et al., 2018a). The co-authors of this work are Daniel S. Asfaw (DA), Pete R. Jones (PJ), Nicholas D. Smith (NS), Vera M. Monter (VM), and David P. Crabb (DC). The design of the experiment was conceived by DC. The experiment protocol was designed by DC, NS and VM. Participant recruitment, application for ethical approval and data collection was done by VM. All the data analysis, including the development and conception of novel metrics, was done by DA with support from PJ and DC. The paper was written by DA, and reviewed, edited and approved by all authors. Some of the work presented in this chapter has also been presented as a poster presentation at the Association for Research in Vision and Ophthalmology meeting (Honolulu, Hawaii, USA, 2018).

3.2 Methods

3.2.1 Participants

Fifteen patients with a clinical diagnosis of primary open-angle glaucoma, and no other ocular diseases, were recruited from a database of volunteers (see Table I for patient details). All participants had a distinct asymmetry in their VF loss, as defined by: (1) a between-eyes difference in Mean Deviation (MD) of at least 6 dB or more, and/or (2) a between-eyes difference in glaucoma severity of at least one stage, as measured by the Glaucoma Staging System 2 (Brusini and Filacorda, 2006) (GSS2). All but one of the patients satisfied both criteria, as detailed in Clinical testing. The between eye difference in MD for this patient (patient D, Table 3.1) was 4.7dB. However, when staged using the GSS2 grading, one eye was scored at stage 2, and the fellow eye on stage 4, and so was still included in the study. The study was approved by the Ethics Committee for the School of Health Sciences, City, University of London. The research was carried out in accordance with the Declaration of Helsinki and written informed consent was obtained from all participants.

3.2.2 Clinical testing

Visual Fields (VF): Static threshold perimetry (24-2) was performed monocularly in each eye, using a Humphrey Field Analyzer (HFA; Carl Zeiss Meditec, CA, USA) running the SITA-Standard algorithm. MD values for each eye/test are given in Table I, and were used to determine the 'worse eye' and 'better eye'. HFA greyscales for the 24-2 VF test are shown for each individual in Figure 3.1.

Visual acuity (VA): Recognition acuity was measured monocularly using Early Treatment Diabetic Retinopathy Study (ETDRS) charts. As shown in Table 3.1, all participants (except left eye of patient N) exhibited a VA of 0.18 logMAR or better (Snellen equivalent of 6/9). Severe sight impairment is defined as best-corrected visual acuity of <6/60 in the better-seeing eye (Pezzullo et al., 2018). Thus, the participants did not have severe visual impairment despite severe visual field loss in some participants' worse eye (example, Participant B).

Contrast Sensitivity (CS): Contrast sensitivity was measured monocularly using Pelli-Robson charts.

Table 3.1: Patient information and demographics. Patient IDs colors correspond to marker colors used subsequently in Figures 3.1 and 3.1.

Patient id	Age (years)	Gender	VA (Log)		CS (Log)		24-2 MD (dB)	
			Right	Left	Right	Left	Right	Left
A	70	F	0.10	0.16	1.65	1.35	-14.2	-4.1
B	44	M	-0.08	0.10	1.45	1.80	-31.1	-14.6
C	59	M	-0.04	-0.04	1.90	1.95	1.9	-7.0
D	80	F	0.14	0.14	1.55	1.65	-7.7	-3.0
E	64	M	0.18	-0.06	1.95	1.95	-9.8	-1.2
F	83	M	0.14	0.14	1.45	1.50	-20.7	-4.9
G	65	F	-0.02	0.06	1.95	1.95	-19.5	-6.0
H	56	M	-1.00	-1.50	1.95	1.95	-19.9	-4.8
I	66	M	0.20	0.04	1.95	1.95	-1.2	-7.8
J	74	F	0.18	0.14	1.95	1.95	-9.8	-3.0
K	60	F	0.02	0.06	1.95	1.95	-5.7	-17.9
L	66	M	-0.08	0.16	1.30	1.95	-15.9	-5.9
M	66	M	0.04	0.10	1.65	1.65	-3.3	-12.1
N	84	M	0.16	0.36	1.65	1.35	-0.9	-19.1
O	83	F	0.12	0.08	1.75	1.65	-22.4	-8.4

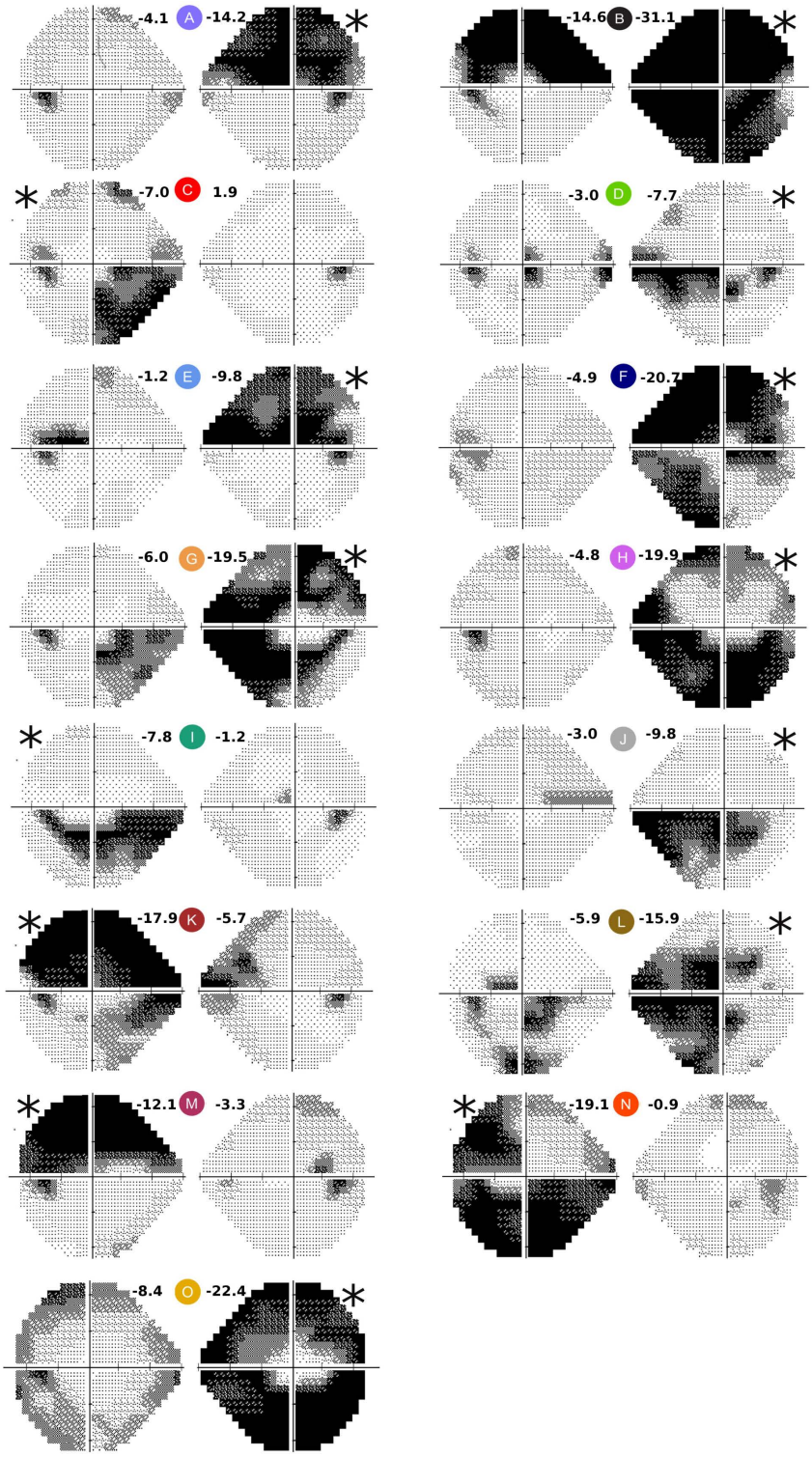

Figure 3.1: HFA Greyscales of monocular visual fields for all 15 participants measured using the 24-2 algorithm (SITA). HFA MD values (dB) are given for each image, and were used to classify the eye as Better or Worse. The worse eye in each image is indicated by asterisk.

3.2.3 Apparatus

The test apparatus is shown in Figure 3.2A. Stimuli were presented on a 56 cm CRT computer monitor (Iiyama Vision Master PRO 514, Iiyama Corporation, Tokyo, Japan) running at 100 Hz with a resolution of 1600 by 1200 pixels. Given the viewing distance of 60 cm, the visual angle of the screen was ±17.0° by ±13.4° (i.e., when fixating centrally). Participants' head position was stabilized using a chin rest, and participants wore the same set of trial frames to ensure that any restriction to the field of view due to spectacle frames was equivalent for each person. Eye movement positions were recorded using the Eyelink 1000 remote eye tracker (SR Research Ltd., Ontario, Canada), which records at 1000 Hz with a spatial precision of $\leq 0.5°$. Before the study commenced, a nine-point grid calibration— the default calibration method of the device — was performed and repeated until the result was rated 'good' by the instrument. Between each trial, a drift check was also performed and recalibration was carried out if substantial drift was detected. Although no keypresses were required during the test trials, participants used a keyboard between trials to indicate when they were ready to continue (see Procedure).

3.2.4 Stimuli

The stimuli consisted of 39 colour images and 81 greyscale images (see Figure A.1 for the complete set of images). The images were taken from a nature documentary (Planet Earth, BBC Television) and depicted natural outdoor scenes, featuring animals, flowers, and underwater images. Images were displayed full screen (1600 by 1200 pixels).

3.2.5 Procedure

Before each trial, participants were asked to fixate on a central cue (Figure 3.2B) and to press the spacebar when ready to continue. The keypress allowed participants to take breaks in between trials, and they were encouraged to do so as required. On each trial, the participant was shown one of 120 images for a mean duration of 4 sec (SD: 0.6 sec; Range: 3—5 sec). During the trial, participants were not required to make an explicit, button-press response, but were instead asked simply to freely view the images as a slideshow. A complete test run consisted of 120 images, presented sequentially in random order (Figure 3.2C). Participants completed two test runs in a single session: once for each eye. The starting eye was randomized among participants. The entire session on average lasted approximately 25 minutes, including breaks.

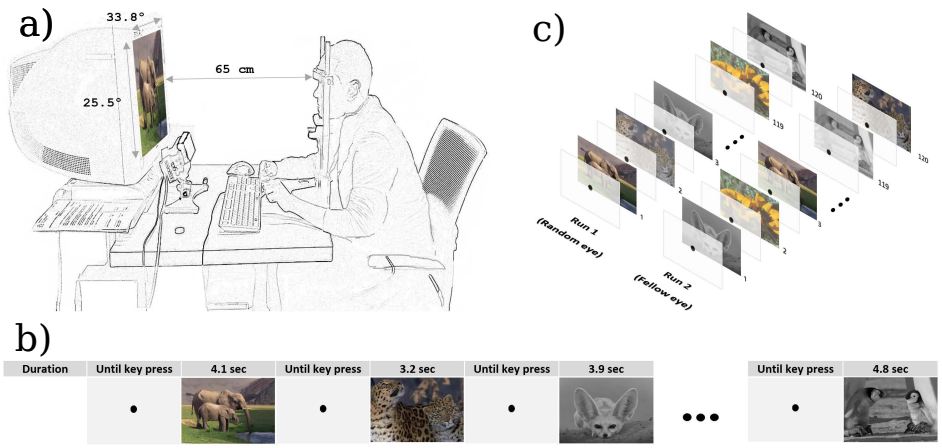

Figure 3.2: Stimuli, Apparatus and Procedures (a) Participants were seated 60 cm from the screen (distance constrained using the chin-/head-rest), and viewed the stimuli monocularly. An eye tracker was mounted below the monitor, and recorded eye movements during test trials. Participants used a computer keyboard to initiate each trial. (b) The stimuli were displayed for a random duration between 3 and 5 seconds. Before each trial a black central fixation point, on a white background, was presented, (c) During each run a patient watched 120 images monocularly, and each patient completed two runs (one per eye).

3.2.6 Eye movement analysis

3.2.6.1 Identifying saccades

An example scanpath for a single trial/participant is shown in Figure 3.3A. Raw gaze samples were recorded at 1000 Hz, and were classified as saccadic if both: (1) velocity > 30°/s, and; (2) acceleration > 8000°/s^2. Following previous similar studies (Smith et al., 2012), small saccades of amplitude < 0.5° were discarded post hoc. This resulted in the exclusion of 5.8% of saccades for the worse eye and 6.0% for the better eye. Eye movement data were analyzed using a bespoke software program written in MATLAB R2017a (MathWorks Inc., Natick, MA, USA).

3.2.6.2 Saccadic reversal rate (SRR)

To understand the temporal dynamics of a scanpath, I derived a novel metric that I term Saccadic Reversal Rate (SRR). This was computed as follows. For each successive pair of saccades, the angular difference in direction, θ_{diff}, was computed (see Figure 3.3B). For example, when two successive saccades moved in the same direction, θ_{diff} was close to 0°. In contrast, if two saccades moved in opposite direction, θ_{diff} was close to 180°. Across a trial, this resulted in a distribution of θ_{diff} values, as shown in Figure 3.3C. In healthy eyes, such reversals are relatively common (5%) and are thought to represent a strategy of revisiting positions "where some information may have been lost or overlooked (Amor et al., 2016)." I therefore hypothesized that such movements would be particularly elevated when vision was impaired. I, therefore, hypothesised

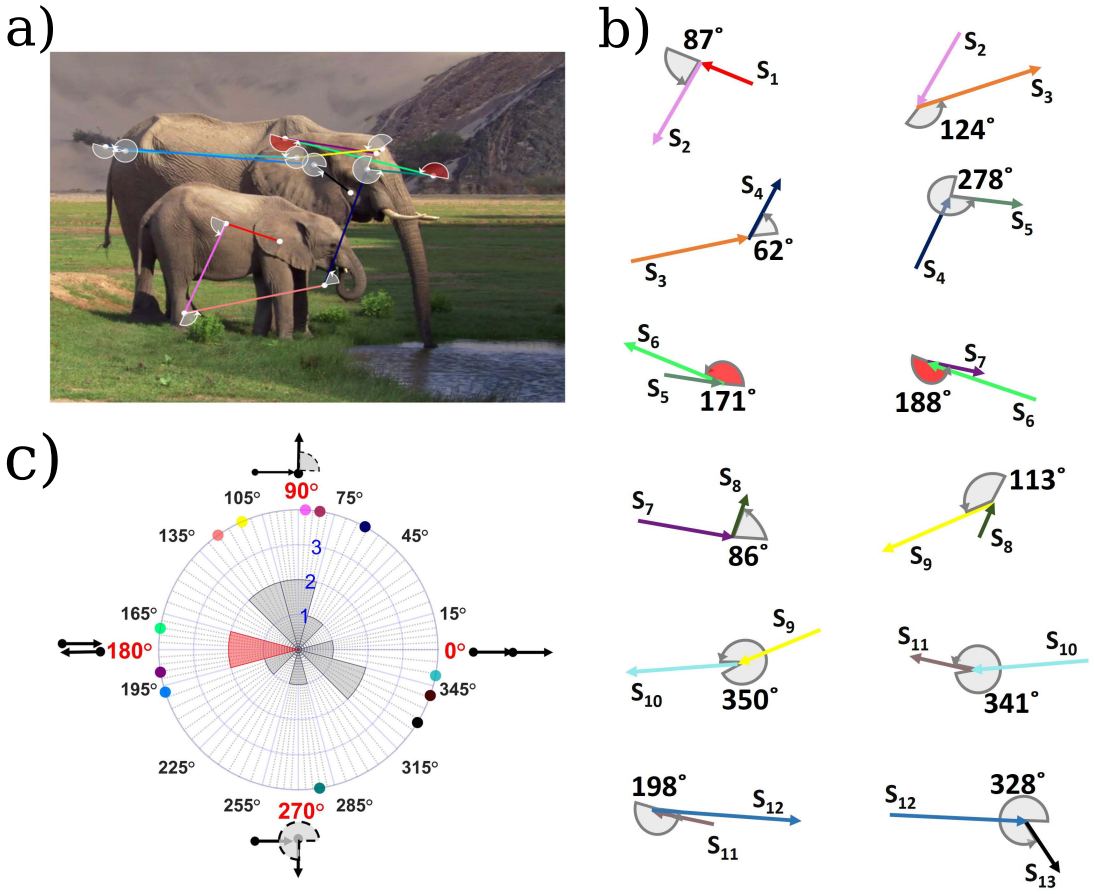

Figure 3.3: Computation of the novel saccadic reversal rate (SRR) (a) Example eye movement data from a single trial. White dots represent fixations, and vectors represent saccades. The arcs represent θ_{diff}: the angular difference between successive pairs of saccades. (b) Illustration of how θ_{diff} values were computed (measured anticlockwise relative to the horizontal) (c) Polar Histogram of θ_{diff} values (same data as panels (a) and (b)). For example, on two occasions θ_{diff} fell within 165°–195°, while on one occasion the angular difference was very small (close to zero). The saccadic reversals are highlighted in red. Coloured dots around the periphery of the histogram show each of the individual θ_{diff} values computed in panel (b). Note that for illustration purposes, the bins shown here are 30° wide, and include data from a single trial only. However, in the final analysis bins of 20° were used, and data were concatenated across all 120 trials.

that such movements would be particularly elevated when vision was impaired.

To quantify SRR formally, I first measured the proportion of θ_{diff} values falling within a 20° bin centred on 180° (red shaded bin in Figure 3.3C). The choice of bin size was arbitrary. However, changing the bin width to 30° or 60° did not affect the overall pattern of results. The angle between saccades (θ_{diff}) was computed as:

$$\theta_{diff} = arctan\left(\frac{S_{i,y}}{S_{i,x}}\right) - arctan\left(\frac{S_{i-1,y}}{S_{i-1,x}}\right) \tag{3.1}$$

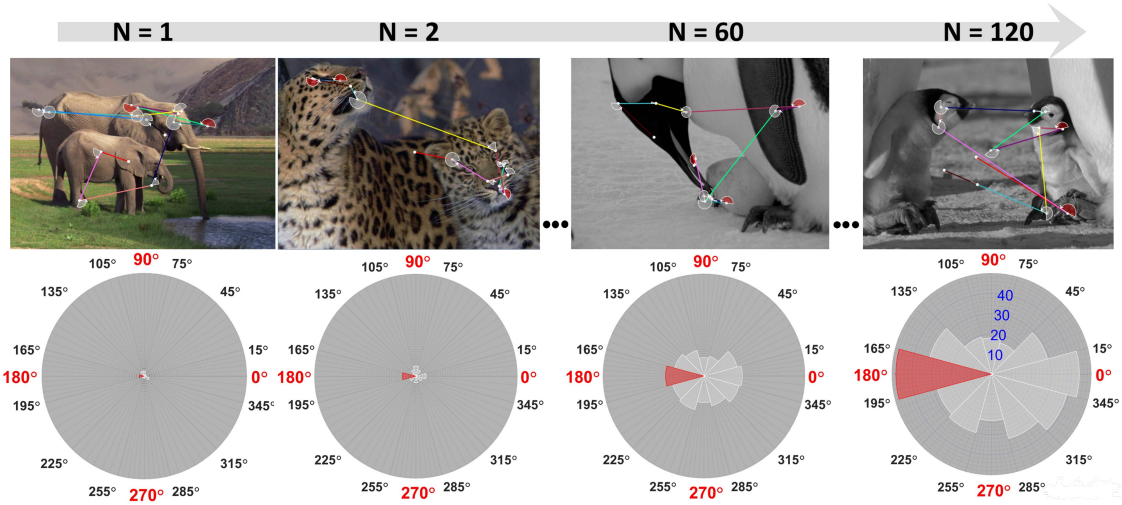

Figure 3.4: SRR analysis (left eye of patient id K). The upper row illustrates the raw scanpaths for individual trials (fixations and saccades represented as points and vectors, respectively). The bottom row shows the corresponding distribution of θ_{diff} values. SRR was computed at the end of a run, and was defined as the proportion of θ_{diff} values that fell in the red bin to the total count of θ_{diff} (Shown here: SRR = 0.13).

where $S_{i,y}$ and $S_{i,x}$ are the y and x components of the i$^{\text{th}}$ saccade, S_i, and S_{i-1} is the preceding saccade. Then, SRR was computed as:

$$SRR = \frac{\text{Proportion of saccadic reversals}}{\text{Total number of } \theta_{diff}} \tag{3.2}$$

SRR was computed at the end of each run (i.e., the rightmost panel in Figure 3.4). This analysis produced one SRR value for each eye, for each participant. It should be noted that SRR is a measure of proportion "saccadic reversals" not the distribution of saccades.

3.2.6.3 Bivariate Contour Ellipse Area (BCEA)

The spread of fixation locations was computed as the Bivariate Contour Ellipse Area (BCEA). The BCEA provides a summary measure of the spread of a participant's gaze over the VF (in degrees visual angle, squared). Previous studies have employed BCEA to study fixation stability in patients with macular degeneration (Bellmann et al., 2004; González et al., 2006) and to analyse eye movement of bilateral glaucomatous participants when viewing driving scenes in a hazard perception test (Crabb et al., 2010) and when viewing everyday scenes (Smith et al., 2012).

To compute BCEA, fixation positions were first transformed into a location in a new plane (see Figure 3.5 first column, N = 1). This was done by aligning fixation positions

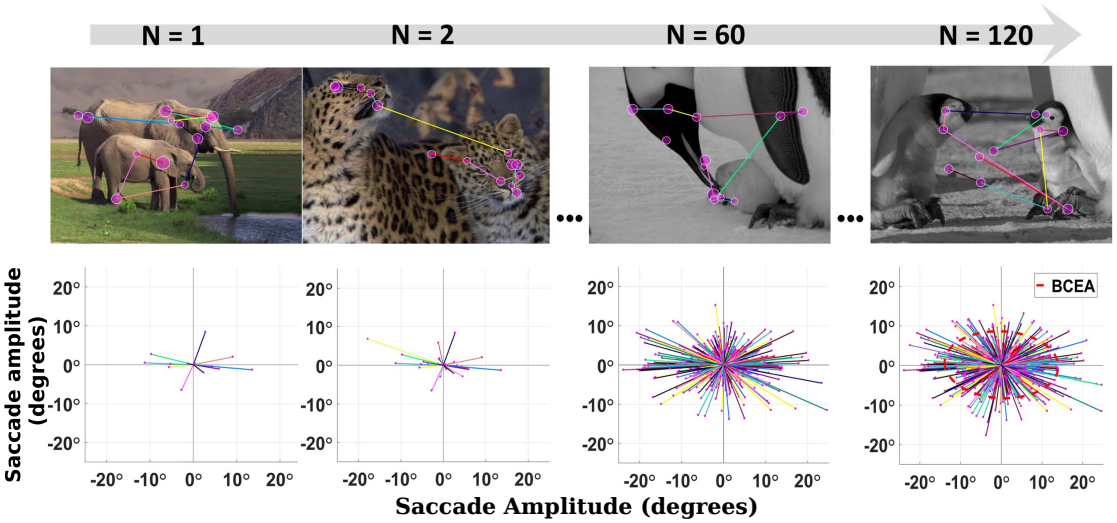

Figure 3.5: BCEA computation across a run (left eye of patient id k). The upper row illustrates the raw scanpaths for individual trials (fixations and saccades represented as points and vectors, respectively). Each saccade is coloured uniquely to match the plots at the bottom. The bottom row shows the aligned saccades/fixations. BCEA was computed at the end of a run Based on the best fitting ellipse (red dashed line).

based on their relative position to the preceding fixation; the preceding fixation position was used as a centre, (0, 0). This transformation maintains the corresponding saccade amplitudes. One BCEA value was computed for each eye at the end of each run (Figure 3.5 last column, N = 120).

3.2.6.4 Additional eye movement metrics

In addition to SRR and BCEA, I also computed other common metrics, widely used in previous similar studies (Smith et al., 2012). These were: (1) number of fixations, (2) fixation duration, (3) saccade amplitude, (4) saccade velocity (speed of saccade), and (5) total scanpath length. The distributions of the parameters were non-Gaussian; therefore, I considered median values for my statistical analysis. In each case, I computed one value for each eye, for each participant.

3.2.7 Statistical analyses

Each metric (SRR, BCEA, additional eye movement metrics) provided a single pair of values for each patient (i.e., one value for the better eye and one value for the worse eye). Pairwise statistical analyses were performed to ascertain any significant differences between the better eye and worse eye. Since the distribution of the data was non-Gaussian, I used non-parametric paired analyses (Wilcoxon's test). Multiple regression analysis was used to explore if any of the parameters, or combination of parameters, were predictive for the between eye differences as measured by between

eye difference in MD. All statistical analyses were conducted using R v3.3.3 (R Core Team, 2017).

3.3 Results

Fifteen patients with glaucoma were recruited (60% men), with a median (interquartile range; IQR) age of 68 (61, 79) years. The median (IQR) HFA MD value was -4.1 (-5.9, -1.7) dB for the better eyes, and -15.9 (-19.8, -9.8) dB for worse eyes. The median between-eye difference in MD value was -10.1 (-14.8, -8.6) dB, reflecting a pronounced asymmetry in VF loss within this group of patients. Between eyes (better versus worse), there were no significant differences in logMAR VA or Pelli-Robson CS values ($p > 0.05$). The right eye was the 'worse eye' in ten of the fifteen participants.

Table 3.2 shows the median (IQR) values for each of the various eye movement parameters. There was no statistically significant difference, between-eyes, in terms of fixation duration, fixation count, saccade velocity, or scanpath length. However, shown in Figure 3.6, better eyes made larger saccades (Wilcoxon signed-rank test;$p = 0.012$), exhibited greater BCEA (Wilcoxon signed-rank test; $p = 0.005$), and lower SRR (Wilcoxon signed-rank test; $p = 0.018$). The median (IQR) between-eye difference (better eye – worse eye) in saccade amplitude was 0.49 degrees (0.0 – 0.9); the median (IQR) difference in SRR and BCEA was -0.014 (-0.003 – -0.023) and 49.0 degrees squared (16.1 - 95.8).

To investigate the presence of possible practice effects, I compared eye movements between the eye tested first versus second (i.e., instead of the better versus the worse eye). There was no significant difference in saccade amplitude ($p = 0.09$), SRR ($p = 0.42$), and BCEA ($p = 0.38$). This indicates that there was no substantial order-effect. Table 3.3 shows the univariate association between each eye movement parameter and various common clinical measures (MD, CS, and VA). I used multiple test correction (Bonferroni correction for four comparisons). There was some indication of a linear relationship between age and saccade amplitude, but it was not statistically significant after correcting for multiple comparisons (Spearman's correlation; $r = 0.62$, $p = 0.02$. There was a statistically significant association between the differences in SRR (between the better and the worse eyes) and differences in logMAR VA ($r = 0.64$, $p = 0.01$) (Figure 3.7A). Furthermore, a statistically significant association was observed between differences in BCEA and differences in MD values ($r = 0.65$, $P = 0.01$) (Figure 3.7B). There was no significant association between any other eye movement parameters and any clinical measures (see Table 3.2).

Table 3.2: Comparison of the difference between worse and the better eyes in different eye movement features. Statistically significant p values are marked with an asterisk and highlighted in bold.

	Better eye (median, IQR)	**Worse eye (median, IQR)**	**Between-eye difference (median, IQR)**	**Wilcoxon's p value**
Fixation duration (sec)	235 (228, 259)	244 (228, 268)	-9 (-16,11)	0.60
Fixation count per trial	12.0 (11.6, 13.8)	12.0 (11.23, 13.0)	0 (-1.4, 1.0)	0.67
Saccade velocity (deg/sec)	230 (182, 258)	215 (169,254)	-14 (-27,7)	0.18
Scanpath length (deg)	60.31 (48.0, 64.8)	55.7 (43.2, 59.3)	-6.4 (-14.9,4.3)	0.15
Saccade amplitude (deg)	3.95 (3.09, 5.42)	3.13 (2.92, 4.66)	0.5 (0.0,0.9)	**0.013***
SRR	0.09 (0.08, 0.12)	0.10 (0.09, 0.12)	-0.014 (-0.021,-0.003)	**0.018***
BCEA (deg squared)	313 (249, 418)	253 (222, 320)	49 (16, 96)	**0.005***

Table 3.3: Spearman's rho correlations comparing between-eye differences in saccade amplitude, BCEA, and SRR with clinical measures and age. Statistically significant associations are marked with an asterisk and highlighted in bold. (Following Bonferroni correction for four comparisons, the criterion for significance was $p < 0.013$.)

		Clinical Measures			
Eye movement		**MD**	**VA**	**CS**	**Age**
Saccade amplitude	r	0.23	0.13	0.30	0.62
	p value	0.42	0.66	0.28	0.02
SRR	r	-0.36	**0.64**	-0.30	0.15
	p value	0.18	**0.01***	0.28	0.59
BCEA	r	**0.65**	0.03	-0.08	0.10
	p value	**0.01***	0.93	0.78	0.73

Stepwise multiple regression analysis (Backward elimination) showed that between-eye differences in BCEA alone were a statistically significant predictor of between-eye differences in MD values (F=7.37, $R^2 = 0.36$, $p = 0.01$): for every 1 dB difference in MD, BCEA decreased by an average of 6.2% (95 confidence interval 1.6% to 10.3%) between-eyes. This indicates that as the VF worsens the spatial extent of eye movements reduces.

3.4 Discussion

This study assessed the effect of glaucomatous VF damage on eye movements. In patients with between-eye asymmetric VF loss, median saccade amplitudes were smaller in the worse eye, and the total spread of fixations (BCEA) was reduced. In addition, I computed the SRR: a novel eye movement parameter that considers the geometric-relationship between temporal sequences of saccades. SRR was significantly greater

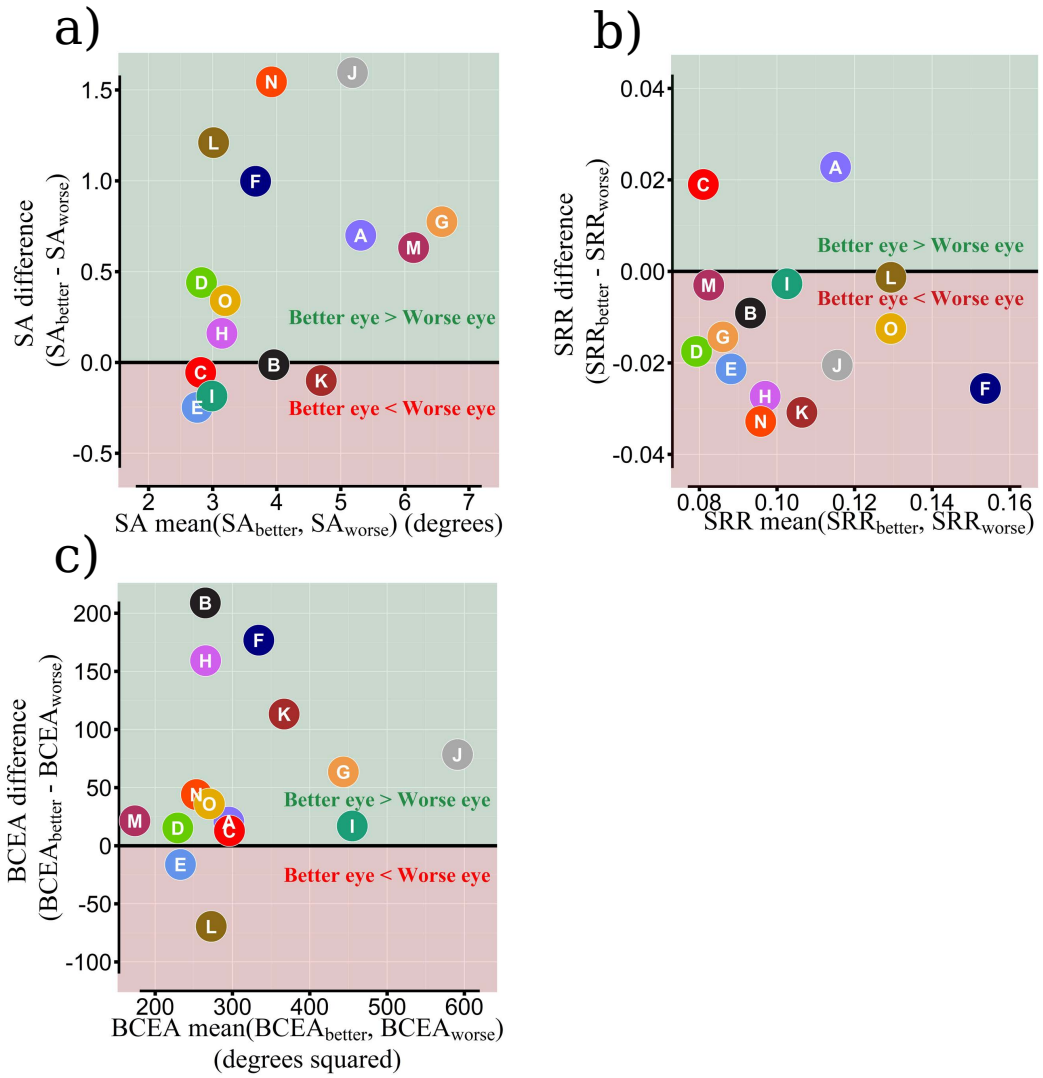

Figure 3.6: Plots of difference between the better and worse eye in (a) median value of a saccade amplitude (b) SRR (c) BCEA. The black solid line in each plot marks the null hypothesis ('no difference between the eyes').

in the worse eye, indicating that the worse eye exhibited more back-and-forth saccadic movements compared to the fellow, better eye. There were also significant relationships between eye movement parameters and clinical measures. Specifically, between-eye differences in BCEA were correlated with MD, while SRR was correlated with visual acuity. In terms of more basic eye movement metrics, such as saccade count, fixation count, fixation duration, and scanpath length, this study did not find a significant difference between worse and the better eyes.

3.4.1 Comparison with previous findings

My findings of smaller saccades and reduced spread of fixations are consistent with previous reports. Thus, BCEA has been reported to be smaller in glaucoma patient

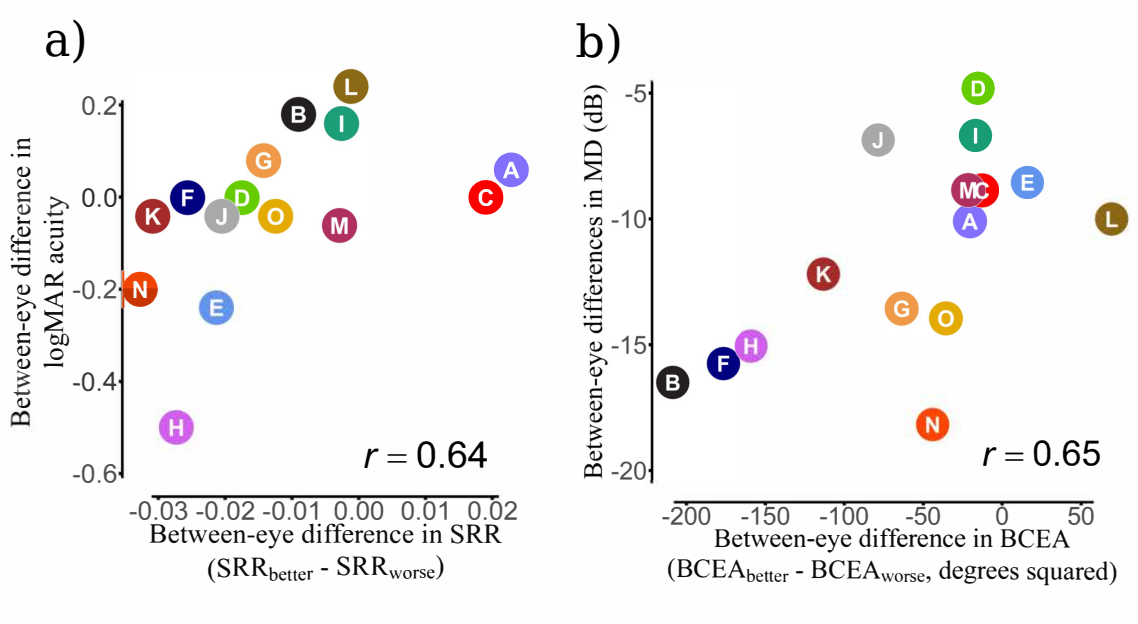

Figure 3.7: Scatter plots depicting relationships between (a) between-eye differences in SRR and VA, $p = 0.01$ (b) between-eye differences in BCEA and 24-2 MD values, $p = 0.01$.

than age-similar healthy controls (Cheong et al., 2008; Smith et al., 2012). Similarly, saccade amplitudes in glaucoma patients have been reported to be smaller compared to controls in some (Lee et al., 2017; Najjar et al., 2017), though not all (Smith et al., 2012; Wiecek et al., 2012), previous studies. To the best of my knowledge, this is the first study that analysed the angle between saccades to evaluate eye movements of patients with VF loss. Taken together, these results provide novel and compelling evidence that eye movements are altered following VF damage.

I did not find statistically significant differences between the worse and better eye in terms of more basic parameters, such as saccade count, fixation count, saccade rate, and fixation duration. In contrast, some (though not all (Wiecek et al., 2012; Vega et al., 2013) previous studies reported significant differences between glaucoma patients and controls in terms of number of saccades, (Smith et al., 2012) fixation rate, fixation duration, (Crabb et al., 2010) and saccade rate (Smith et al., 2011). One possible reason for this disparity may be due to differences in task. For instance, in Smith and colleagues (Smith et al., 2011) participants were asked to search for targets in photographs. However, in this study participants were asked to view photographs freely. Another possible reason is that the effects of these parameters are very small, and I lacked the statistical power in the present study to detect them reliably. Finally, it may be that these simple eye movement metrics are more susceptible to individual differences and do not always occur reliably.

3.4.2 Relationship between eye movements and common clinical measures

When using their worse eye, patients made more spatially restricted eye movements (i.e., saccade amplitude and BCEA of the worse eye were smaller). Since other possible factors that affect eye movements (such as cognitive skills, age, personal preference) were controlled for, these differences in eye movements are likely due to their visual impairment. For example, since the worse eye typically exhibited substantial VF loss (see Figure 3.1), the spatial narrowing of eye movements might be explained by an absence of exogenous cueing at more peripheral locations (Thorpe et al., 2001; Larson and Loschky, 2009; Kwon and Legge, 2012). If this were the case, one would expect a relationship between measurements of VF loss and the spread of fixations. Consistent with this, my data showed that decreases in VF MD values were positively correlated with reductions in the spread of fixations (BCEA).

When viewing a scene, it is normal for normally sighted observers to make a number of saccadic reversals (Amor et al., 2016). However, my data showed that saccadic reversal rates were increased on average in glaucomatous eyes, and this was statistically significant. As with the other eye movement parameters (BCEA, saccade amplitude), this may be primarily a consequence of their restricted VF, with patients opting to revisit parts of the image in the absence of any peripheral cues to attract their attention. If this is the case, one could similarly predict a normal eye to exhibit greater SRRs when viewing a visual stimulus where all salient information is confined to a narrow spatial region. Alternatively (or in addition), it may be that increased SRRs represent an adaptive strategy to cope with reductions in acuity, with patients 'revisiting' parts of the image in order to gain more information ('re-sampling'). Consistent with this, increases in SRR (between the eyes) were correlated with decreases in VA (Figure 3.7B).

Between-eyes, there was a positive association between BCEA (spread of fixations) and MD values, and also between SRR and VA. This is encouraging, as it suggests that natural eye movements could in future provide complementary biomarkers to traditional clinical measurements. This would have substantial practical advantages, due to the ease at which it would be possible to collect large amounts of data with minimal burden or discomfort to patients (Crabb et al., 2014).

3.4.3 Implications and future work

The present work could be developed in a number of ways. First, this study has shown eye movement parameters (saccade amplitude, SRR, and BCEA) are altered by worsening VF loss, but I cannot say the measures can be used to diagnose VF loss. To answer this, one would have to build a model that can detect patients from healthy

subjects and evaluate its diagnostic sensitivity and specificity in an appropriately designed study (Bossuyt et al., 2003; Eusebi, 2013). Second, the present work showed a relationship between eye movements and summary metrics of visual impairment, such as VA and MD. However, the small sample size prevents any investigation into the relationship between eye movement and different patterns or location of VF loss.

3.5 Conclusions

When viewing images monocularly, patients with asymmetric VF loss exhibited systematically different eye movements in their worse eye. Specifically, the worse eyes were shown to be restricted in spatial extent, and to exhibit more frequent back-and-forth ('reversal') saccades. These differences in eye movements were shown to correlate with common clinical measures, with differences in BCEA and SRR associated with changes in MD and VA, respectively. This work introduces a novel eye movement summary statistic, SRR, which could be applied to analyse eye movements of patients with other ophthalmic or neurodegenerative conditions.

Chapter 4

Using eye movements to detect visual field loss: a pragmatic assessment using simulated scotoma

4.1 Introduction

As discussed in the opening chapter, glaucoma is a chronic eye disease affecting 1 in 28 people aged 40-80 years (Weinreb et al., 2016). It is characterised by progressive VF (VF) loss, and this vision loss is irreversible. Early detection is therefore crucial (Pizzi et al., 2018). At present,successful detection of glaucoma requires a detailed assessment by a specialist clinician, including measurements of intraocular pressure (IOP), VF loss by standard automated perimetry, and inspection of the optic nerve head. Unfortunately, many adults do not attend routine eye-checks due to associated costs (real and perceived), lack of awareness, aversion to the methods used, and lack of understanding about their purpose (Biddyr and Jones, 2015; Cook and Foster, 2012).

As outlined in Chapter 1, screening for glaucoma might start to become viable if an inexpensive, automated screening tool could be developed to identify high-risk individuals. Central to this thesis has been the idea that modern eye tracking technologies may be able to provide such a tool. Studies have shown that eye movements are altered in instances of glaucomatous VF loss (Chapter 2). For example, glaucoma patients have been shown to exhibit differences in saccade frequency and spread of

gaze when free-viewing images, relative to normally sighted controls (Smith et al., 2008). While, more recently, as reported in Chapter 3, I demonstrated differences in eye movements between the two eyes of glaucoma patients with asymmetric VF loss, when free-viewing pictures monocularly (Asfaw et al., 2018a). Several other studies have also confirmed a link between simulated VF loss and altered eye movements (Parkhurst et al., 2000; Bertera and Rayner, 2000; Cornelissen et al., 2005; Foulsham et al., 2011; Geringswald and Pollmann, 2015; Cajar et al., 2016; Nuthmann, 2014).

As discussed in Chapter 1, the idea of using natural eye movements for disease detection is exciting, as eye movements can be recorded easily and cheaply using ordinary commercial technologies (hardware that is already becoming increasingly ubiquitous in people's homes, via computer screens, TVs, and smartphones) (Krafka et al., 2016; Wood and Bulling, 2014). Furthermore, unlike conventional VF assessments, which require sustained concentration during a protracted test that many patients find demanding, (Jampel et al., 2011; Glen et al., 2014; Malik et al., 2013) natural eye movements require no explicit task, and could even be monitored while individuals go about their everyday activities (e.g., watching TV). In short, and central to the idea of this thesis, natural eye movements appear attractive as a cheap and easy way of screening for glaucoma (Asfaw et al., 2018a; Crabb et al., 2014; Grillini et al., 2018).

However, despite existing evidence that VF loss alters eye movements, it remains unclear whether these changes are sufficiently great to be clinically useful. Exactly what level of sensitivity and specificity a test requires to be clinically useful is difficult to define. However, standard automated perimetry, a well-established tool for detecting VF loss, is able to discriminate between healthy vision and moderate-or-advanced (not early) VF loss with almost 100% accuracy. For example, Cello et al. (2000) reported that an automated perimeter (FDT C-20) displayed 100% sensitivity and 100% specificity for detecting advanced VF loss (mean defect (MD) between –12 and –22 dB), and 96% sensitivity and 96% specificity for moderate VF loss (MD between –6 and –12 dB). Similarly, Budenz et al. (2002) reported 100% sensitivity and 96% specificity for detecting moderate or advanced defects using the Humphrey VF analyzer (Swedish interactive threshold algorithm (SITA) and SITA fast algorithms) (Budenz et al., 2002).

In the present study, I used simulated VF loss to explore the power of natural eye movements to detect eye disease. The simulation is central to the idea of this study. Simulation of VF loss allowed systematic manipulation of key VF loss characteristics, such as location and size, to quickly collect large sets of data in a relatively short period of time, and to control individual variability by recruiting a relatively homogenous cohort of healthy, young adults (Cornelissen et al., 2005).

Several techniques have been developed previously to simulate VF loss. One approach is to use contact lenses with a region of opacity (Foley-Fisher and Murphy, 1987; Murphy and Foley-Fisher, 1989; Almutleb et al., 2018). However, this method results in a poorly localised VF loss and causes an unrealistic dimming across the retina (Butt et al., 2015). Recent studies have therefore focused instead on utilising eye trackers to control the position of an artificial VF loss on a computer, relative to the current point of fixation (gaze-contingent presentation) (Cajar et al., 2016; Cornelissen et al., 2005). One such gaze-contingent VF loss simulator ('GazeSS'), capable of applying real patient's VF defects (measured by standard automated perimetry) onto dynamic film content has been previously developed (Glen et al., 2015, 2016).

The purpose of the present work was to consider whether natural eye movements can provide a clinically useful biomarker for glaucomatous VF loss. I contended that, to be clinically useful, eye movements should be at least be robust enough to identify substantial VF loss consistently when all of the key confounding variables are strictly controlled (e.g., the environment, exact form of VF loss, and participants' age and general health). To assess this, I asked normally sighted young adults to watch videos and images with or without a gaze-contingent simulated VF loss (based on clinical data from a single glaucoma patient). Unlike most previous studies, my primary interest was not to establish whether any changes in eye movements were statistically significant. Instead, I used the receiver operating characteristic (ROC) to examine the diagnostic accuracy (i.e., sensitivity, specificity) of natural eye movements in discriminating healthy eyes from those with surrogates of glaucomatous VF loss. I investigated individual eye movement features and their combinations, including saccade amplitude, proportion of saccades landing on the pre-VF loss (SLV) location, spread of saccade endpoints (measured using bivariate contour ellipse area; BCEA), and consistency of fixation locations in time between participants (using kernel density estimation; KDE). Further details on how these variables were computed are given in the Methods section.

The study described in this chapter is published in journal of *Nature Scientfic Reports*. The co-authors of this work are Pete R. Jones (PJ), Nick D. Smith (NS), Laura A. Edwards (LE), and David P. Crabb (DC). The original design of the experiment was conceived by DA, PJ, and DC. Some original pilot work (not included in the chapter) and a draft for the ethical approval was done by LE. The gaze-contingent VF loss simulator ('GazeSS') was programmed and developed by NS. Refinement of the experiment and further programming was done by DA. Participant recruitment, testing, data collection was all conducted by DA. All of the data analysis was done by DA with support from PJ and DC. The paper was written by DA, and reviewed, edited and approved by all authors.

4.2 Methods

4.2.1 Task overview

The previously described GazeSS software (Glen et al., 2015) was used to simulate two binocular VF conditions (Asaoka et al., 2011; Crabb and Viswanathan, 2005) ('moderate loss', and 'advanced loss'). Both conditions were based on perimetric data from a single patient with an established diagnosis of glaucoma (measurements taken longitudinally, using standard automated perimetry). Young adults with healthy vision were asked to watch short video clips and images, either with no simulated VF loss, or under one of the two simulated field loss conditions (between-subjects design). I analysed eye movements using common eye movement parameters as well as using a novel measure designed to index the extent to which the observers with simulated VF loss looked at the same screen locations as the no VF loss (control) group.

4.2.2 Participants

Fifty-five young adults (mean age: 24, SD: 5 years) with normal vision were recruited via advertisements placed in the vicinity of the City, University of London. Normal vision was defined as having no history of eye disease and was confirmed by good performance on the functional vision tests described below. Three potential participants failed the vision screening and were excluded from the study. The study was approved by the Ethics Committee of the School of Health Sciences, City, University of London (#SHS025). The research was carried out in accordance with the Declaration of Helsinki and written informed consent was obtained from all participants.

4.2.2.1 Clinical screening for normal vision

Visual Fields (VF): Static threshold perimetry (24-2) was performed monocularly in both eyes using a Humphrey Field Analyser (HFA; Carl Zeiss Meditec, CA, USA) running the SITA-Standard algorithm. One participant failed due to a VF defect in one eye and was subsequently excluded from the study. For all of remaining 55 participants, the glaucoma hemifield test on the HFA was 'within normal limits'.

Visual acuity: Recognition acuity was measured monocularly in both eyes using Early Treatment Diabetic Retinopathy Study (ETDRS) charts. All 55 participants exhibited a corrected visual acuity of 0.18 logMAR or better (Snellen equivalent of 6/9).

Colour deficiency: Colour vision testing was carried out (binocularly) using the 38-plate Ishihara pseudoisochromatic test, 2011 edition (Handaya, Tokyo, Japan). All 55 participants correctly recognised all of the letters and patterns in the test.

4.2.2.2 Apparatus

The experiment apparatus (Figure 4.1a) consisted of an LCD monitor (51 × 25.5 cm; 1920 × 1080 pixels; 60 Hz) and the Tobii TX300 eye tracker (Tobii, Danderyd, Sweden) configured to record eye gaze at 60 Hz. My reasoning for using 60 Hz was partly pragmatic. Affordable eye trackers with similar sampling rate capabilities are available, and could be used for home monitoring (e.g., screening for VF loss while watching TV) if found to be effective (Jones et al., 2019). This sampling rate was also matched to the refresh rate of the screen, and helped to minimize the computational overhead of generating the artificial scotoma (i.e., a higher sampling rate may have added addition delay or imprecision into to the overall system). However, there was a small amount of lag before any changes in gaze could be registered. The manufacturer claims that the overall latency of its eye tracker system is < 10 msec. If I further factor in the refresh rate of the screen (60 Hz) and 3D rendering time, the total expected lag was approximately 35–45 msec. Studies have shown that system delays of up to 60 msec have an insignificant effect in disrupting perceptual processing (Loschky et al., 2007). Moreover, the effect of system latency of gaze-contingent setups on large scotomas is low when compared with small central scotomas (Saunders and Woods, 2014).

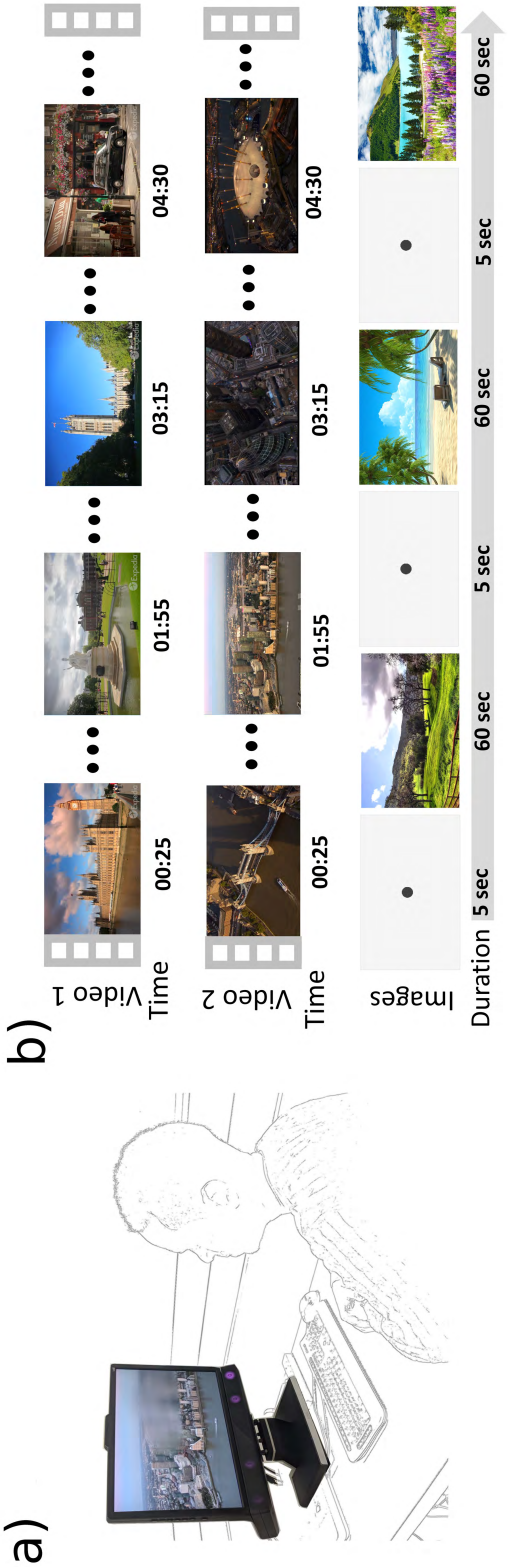

Figure 4.1: Apparatus, stimuli, and procedure. (a) The experiment apparatus consisted of an LCD monitor (51 x 25.5 cm; 1,920 x 1,080 pixels; 60 Hz) with an integrated eye tracker. Participants viewed the screen binocularly and were seated at approximately 60 cm away from the eye tracker without a head/chin rest, meaning that the screen subtended at a visual angle of 46° x 24°. Study participants were only required to look at the screen during test trials (no explicit response) and a keyboard was provided between trials on which to indicate their readiness to continue. Changes in viewing distance were monitored using the eye tracker and the size of the artificial VF loss was dynamically adjusted. (b) The stimuli consisted of two video clips and three static images, the latter of which were displayed for 60 seconds each. The two videos were presented for their full duration of 301 seconds and 307 seconds, respectively. The resolution of video and the images were presented at a resolution of 1,280 x 720 pixels and the frame rate of the two videos were 30 frames/second. All stimuli were displayed in a full-screen mode (resolution of 1,920 x 1,080 pixels). Stimulus order was randomised between participants.

4.2.3 Stimuli and Study design

The stimuli consisted of two videos and three static images (see Figure 4.1b for all images and selected frames from both videos). The videos were arbitrarily selected from (YouTube, San Bruno, California, United States), and I had no prior hypothesis of the eye movements the stimulus would elicit. VIDEO 1 was an aerial film of London (301 seconds) and VIDEO 2 was an advert showing attractions in London (373 seconds, from the London Vacation Travel Guide; Expedia, Bellevue, Washington, USA). The three images used were outdoor scenes, with two depicting landscapes and one depicting a beach. Unlike previous studiesAsfaw et al. (2018a); Smith et al. (2008) that involved a large number of images, this study investigated the feasibility of using just a few numbers of images to detect VF loss.

GazeSS (Glen et al., 2015) was used to simulate gaze-contingent VF loss, mimicking the expected binocular VF loss based on (monocular) perimetric data from a real patient. In this implementation, blur was used since patients with early or intermediate loss often perceive VF loss as a region of a blur (Crabb et al., 2013; Hu et al., 2014). GazeSS was a custom-written application (in C# using Microsoft XNA Game Studio) that generates a 'simulated' VF loss based on current gaze position. For each frame in the video or image, locations of the scene that correspond to regions of VF loss ($\sim< 25dB$) are degraded systematically. The application applies layers of Gaussian 'blur' coded using High-Level Shader Language, whereby the blur intensity increases depending on the severity of VF loss. When the sensitivity value at a particular location in VF was $\sim< 20dB$, the corresponding location in the scene was obscured by the blur. The blur effect was produced by applying a 2D Gaussian smoothing kernel (9X9) iteratively (four times). The current study used two integrated VFs (IVFs) generated from a real glaucomatous patient's monocular VF assessments carried out twice during the course of the condition (Figure 4.2). The patient was arbitrarily selected from our database of patients with a clinically established diagnosis of open-angle glaucoma. Glaucoma was defined as VF defects in both eyes (binocular defect) with corresponding damage to the optic nerve head and an open iridocorneal drainage angle on gonioscopy. Here, I simulated superior binocular visual field loss, which is representative of a clinical population of patients with binocular visual field loss (Hu et al., 2015).

As described in Chapter 1, IVF estimates the binocular VF from the two monocular (left and right eye) VFs in such a way that sensitivity values for each point in the IVF were computed by taking the maximum sensitivity from corresponding points in the left and right eye VFs (Asaoka et al., 2011; Crabb and Viswanathan, 2005). Based on the VF of the worse eye, the results of the two visits were classified as moderate (-12 ≤ MD ≤ -6 dB) and advanced VF loss (MD < -12 dB) (Iester and Zingirian, 2002).

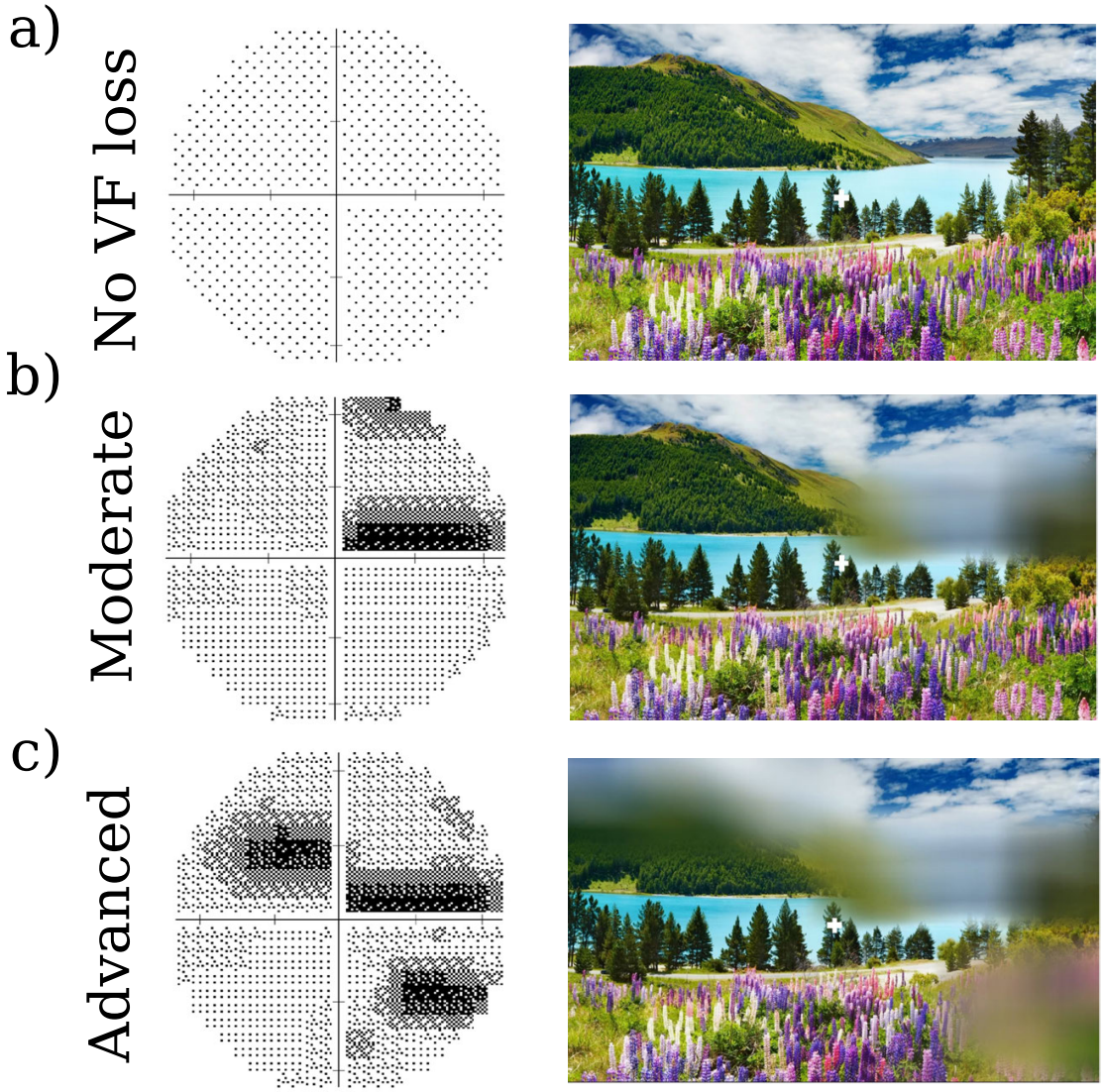

Figure 4.2: IVFs and example screenshots from the three simulated-VF loss conditions: (a) no VF loss. (b) moderate VF loss. (c) advanced VF loss. The impairments were constructed on monocular field data from a single real patient. The IVF was estimated by taking the maximum sensitivity from corresponding points in the left- and right-eye VFs. Note that the simulated VF loss moved depending upon the observer's current point of gaze (white cross), and so remained approximately static in retinal coordinates.

4.2.4 Procedure

The first 45 participants were assigned randomly using a lottery to one of the three groups (i.e., no VF loss, moderate VF loss, and advanced VF loss). An additional 10 participants were subsequently recruited to the no VF loss group. These additional 10 participants were recruited as part of a related project, and were included in the present work to maximise statistical power (a posthoc power calculation (Lewallen and Courtright, 1998), considering an Cohen's effect size of 0.5, indicated that these additional 10 controls increased statistical power by 7%). However, the present results were qualitatively unchanged if these additional 10 observers were not included. Re-

gardless of impairment type, all the participants watched the same set of five stimuli (i.e., VIDEO 1, VIDEO 2, and IMAGES), presented in a randomised order that varied among the participants. The static images were presented for 60 seconds each, and the two videos were presented for their full duration (301 seconds and 307 seconds). Prior to the presentation of each stimulus, participants were asked to fixate on a target presented in the centre of the screen. However, during the stimulus presentation interval, participants were free to move their eyes, and were encouraged to take short breaks between trials as required. They completed the study in a single session lasting approximately 35 minutes.

Before testing, a five-point eye tracker calibration was carried out, using the procedure provided by the manufacturer. The results of calibration were represented in a schematic representation, marking calibration points that were successfully calibrated with error lines (i.e., the differences between the position-of-gaze calculated by the eye tracker and the actual location of the calibration point) and leaving the calibration blank if there was no reading. The accuracy of the calibration was assessed by manual inspection and was repeated until "good" level was a precision was obtained (i.e., when error lines were within the circle drawn by the system).

As part of the consent procedure, participants were given an information sheet explaining the general objective of the study, which was to understand the effects of sight loss on eye movements while watching videos and images on a computer. During the study they were instructed simply to relax and look at the screen normally, as though they were watching television at home.

4.2.5 Eye movement analysis

4.2.5.1 Preprocessing

Eye gaze was recorded binocularly at 60 Hz. The eye tracker produces raw gaze position (horizontal and vertical positioning in pixels) and distance of the participant from the tracker (in mm). All of the raw gaze data were converted to degrees using the distance information for each raw gaze positions. Saccade and fixation identification routines were adapted from PyGaze (Dalmaijer et al., 2014). Movements were classified as saccadic if both: the velocity > 30°/s, and the acceleration > 8000°/s^2. To exclude microsaccades or minor artefacts of the eye tracker, similarly to in previous studies, Smith et al. (2012) small saccades of amplitude < 0.5° were discarded post-hoc. Fixations > 500 msec were discarded to avoid long smooth pursuit movements. Eye movement data were analysed using a custom software program written in MATLAB R2017a (MathWorks Inc., Natick, MA, USA). I examined four eye movement features

as described below.

4.2.5.2 Saccade amplitude

Saccadic amplitude describes the magnitude (in degrees) of the rapid eye movements that met the 'saccadic' criteria (see data preprocessing) (Figure 4.3a). Since the distribution of saccadic amplitudes is often non-Gaussian, I considered median values of saccade amplitude as the summary measures for statistical analyses (Figure 4.3b). One median saccade amplitude value was computed per participant, per stimulus.

4.2.5.3 Bivariate contour ellipse area (BCEA)

BCEA was computed to measure the spread of saccadic endpoints. Following a previously described analysis approach, 55 saccade endpoints were first mapped into a location in a new plane (Figure 4.3c) by first translating the saccade start position to the centre (0, 0) and then by applying the same translation to saccade endpoints. The BCEA was computed with a probability area of 95%. This produced one BCEA value per participant per stimulus.

4.2.5.4 Proportion of saccades landing on the pre-VF loss (SLV) location

SLV was computed as the proportion of saccades (aligned) landing on the VF loss locations to the total number of saccades (Figure 4.3d). For each participant in the VF loss groups (moderate and advanced), one SLV value was computed per stimulus, while for each participant in the no VF loss group, two separate SLV values were computed (based on the scotoma locations of the moderate and advanced scotoma groups) for comparison with the moderate and advanced VF loss groups.

4.2.5.5 Kernel density estimate (KDE) of gaze fixations

The three metrics described above have been used extensively to characterise eye movement data in the past (McIlreavy et al., 2012; Smith et al., 2012), and it is possible that these 'simple' metrics are sufficient for indexing VF loss. However, an alternative and in some ways, a more direct way of classifying an observer as healthy or abnormal is to quantify the likelihood that a given set of eye movements belongs to somebody with/without VF loss.

To do this, I developed the following 'KDE' procedure. In this procedure, gaze positions belonging to saccades were excluded, meaning that only available gaze positions of fixations and pursuits were considered. For each frame in every clip, the average gaze positions $(x_i, y_i), i = 1, ..., n$ of the no VF loss group participants $i = 1, ..., n$

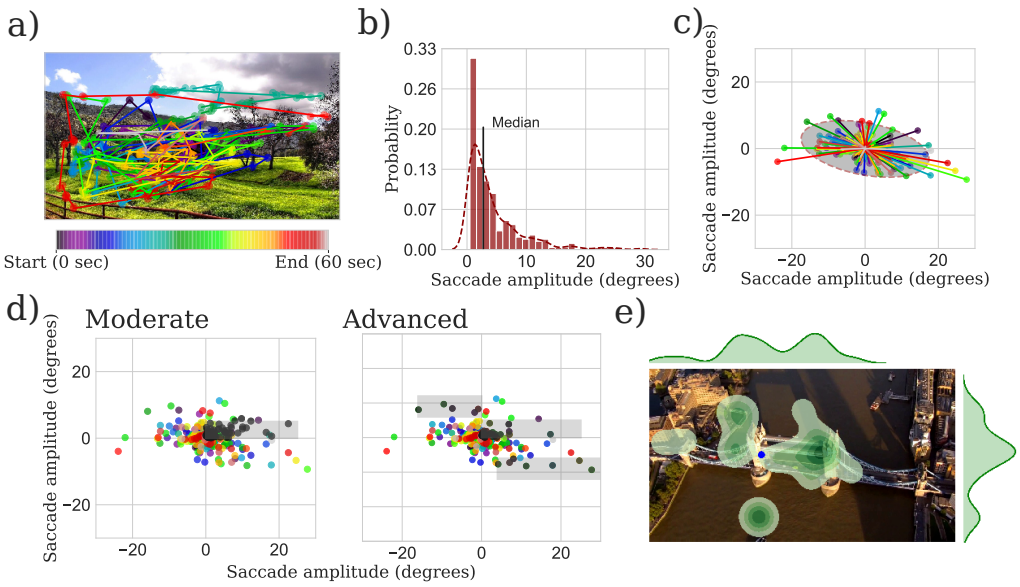

Figure 4.3: Four methods of eye movement analysis. (a) Example eye movements obtained from a single participant, during free-viewing of one of the static images. The colour of the scanpath codes time. (b) Histogram of the saccades, computed from (a). The median amplitude was used as the summary measure. (c) Aligned plots of the saccades in the VF. The BCEA is the area of the ellipse (grey shaded region). (d) Saccadic movements in the direction of/landed on the pre-saccade VF loss location (black dots falling in the grey shaded region) for the moderate and advanced group. (e) An illustration of KDE analysis of gaze data for the frames of the videos. The KDE model was used to compute the probability score of a test point (average gaze position in a frame for a given participant, shown in blue dot).

were used to compute a model (probability mass function) based on KDE. The two gaze positions available per frames were averaged (based on 60 Hz eye tracker and 30 frames/sec video). The KDE was computed by adding Gaussians (subsequently normalised to unity), each centred at one fixation location of the participants in the no VF loss group.

$$f(x,y) = \frac{1}{n}\sum_{i=0}^{n} K_{h_x}(x-x_i)K_{h_y}(y-y_i) \tag{4.1}$$

where K_{h_x} and K_{h_y} are kernel function, in this case Gaussian kernel, given by:

$$K_{h_x}(x-x_i) = \frac{1}{\sqrt{2\pi h}} exp(-\frac{x-x_i}{2h}) \text{ and } K_{h_y}(y-y_i) = \frac{1}{\sqrt{2\pi h}} exp(-\frac{y-y_i}{2h})$$

where the subscript h is the standard deviation of the Gaussian kernel.

A Gaussian kernel function with a standard deviation of h = 1.5° was chosen based on the assumption that each gaze represents a foveal vision from a participant. Fixations

in proximity sum up to a higher value, whereas fixations at a distant space contribute to the density function to a small degree. A similar method has been proposed previously to compute the coincidence between the gaze points of multiple subjects (Dorr et al., 2010, 2012).

Before computing the KDE, outliers at each frame from the available gaze data of the no VF loss group were excluded using isolation forest method (Liu et al., 2008). For each video and every frame, the KDE function (f(x,y)) was used to compute the probability of the average gaze positions of participants in the VF loss group. To compute the probability of gaze among participants in the no VF loss group, I used a standard 'leave-one-out' method from machine learning (Wong, 2015). This produced one probability value for every frame of each video, for every participant (see the Figure 4.3. in Results section for illustration). This magnitude of the probability value explains how far the spatial distance of a given participant's gaze in a given frame is from the gaze positions of participants in the no VF loss group. The probability of a gaze from a test participant would be higher if located at a closer proximity to the gaze positions of the participants in the no VF loss group, and vice versa. For statistical analysis, the mean of the probability scores of all frames in a video was computed (single value per participant per video). The KDE analysis was performed using the SCIKIT-LEARN package in Python (Pedregosa et al., 2011).

4.2.6 Statistical analyses

Kruskal–Wallis one-way analysis of variance was used to test whether there was a statistically significant difference between the three VF groups. Whenever a significant difference was found, post-hoc analyses were conducted using a Mann–Whitney U test (two-tailed) with Bonferroni corrections for multiple comparisons. The alpha level was set to 0.05.

4.2.7 Further analysis to improve separation performance

To assess the ability of individual eye movements parameters to separate between VF loss groups (no vs. moderate VF loss; no vs. advanced VF loss), receiver operating characteristics (ROCs) were computed using individual eye movement parameters (e.g., saccade amplitude, BCEA, and KDE). To try to improve the separation between the groups, multiple eye movement features were extracted and analysed using machine learning techniques. Eighty-four additional features were extracted from the saccadic movements, following similar procedure introduced by Crabb et al. (2014). These features were extracted by analysing the saccades (centralised) using polar histograms (see Figure B.2). In total, 87 features were analysed for each video (86 features

for the IMAGES).

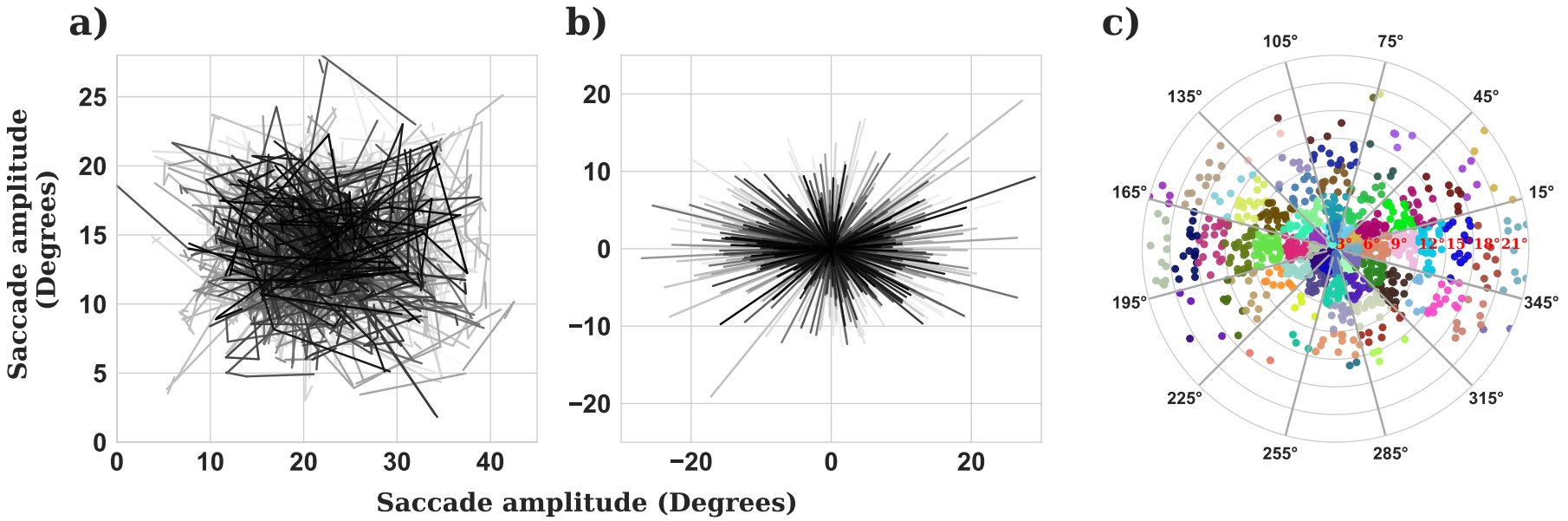

Figure 4.4: Method of extracting features from saccadic movements. (a) Example of a scanpath from a participant who watched VIDEO 2. (b) Each saccade is mapped to a new planned by setting their starting position to as (0,0). (c) Scatter plot, showing the end location of each saccade in polar coordinates. Saccades that landed in the same bin are shown using the same color. Each bin measures 3° (radial) and by 30° (angular). In total, there were 84 bins (resolution of seven in the radial direction and 12 in the angular direction). The extracted features represent the number of saccades that landed in each bin. For example, the first bin represents the saccades that were greater than 0° and less than 3° in amplitude and executed in a direction between 345° and 15°.

The features were serialized into a vector and were transformed into a new space using kernel principal component analysis (KPCA). The KPCA analysis extracted principal components (or features) from a high-dimensional feature space that are nonlinearly related to the input variables (i.e., features from each participant). The feature space, also known as the kernel matrix, contains distances between the features of each participant and was of size (NXN), where N is the number of participants. The distance K_{ij} between feature vectors of two participants, i and j is computed using the following Gaussian kernel:

$$K_{ij} = \gamma |X_i - X_j|^2 \tag{4.2}$$

where γ is the variance of the Gaussian kernel and its value was determined using cross-validation. The resulting kernel matrix was normalized and decomposed to its principal components (eigenvector). The dimension of the feature vector was reduced by selecting eigenvectors with the corresponding highest eigenvalues. The resulting features were classified using AdaBoost classifier (Freund and Schapire, 1995; Hastie et al., 2009). The AdaBoost algorithm recursively generates classifier that learns from the previous weak classifier by focusing on the hard to classify instances. The final prediction was the weighted sum of the weak classifiers. I used a Decision tree classifier as a weak learner. Best performing parameters (variance of the Gaussian in KPCA, the depth of decision trees, the learning rate) were selected using cross-validation.

4.2.8 Receiver operating characteristics (ROCs) analysis

Predictive machine learning model (a test) predict the probability of a subject being positive or negative with a probability score (range 0 - 1). A cutoff value, indicating whether an individual can be classified as positive or negative, and the known status of the subject (i.e., ground truth) values are used to divide the cohort under study into one the following 4 subgroups: true positive (TP), false positive (FP), true negative (TN), and false negative (FN). TP are subjects with the condition and predicted to have the condition by the test based on the cutoff value used. FP are subjects predicted to have the condition when they have not. TN are subject without the condition and predicted to be without the condition. FN are subjects predicted not to have the condition when they have (Zweig and Campbell, 1993; Altman and Bland, 1994).

Sensitivity is the proportion of TP subjects with the condition in a total group of subjects with the condition: TP/(TP + FN). It describes the ability of the test in detecting the positive subjects. On the other hand, specificity defines the proportion of subjects

predicted to be negative by the test from all the subjects without the condition: TN/(TN + FP). It relates to the ability of a test in detecting the negative subjects (healthy) (Akobeng, 2007; Greiner et al., 2000).

The ROC curve assesses the discriminative ability of a given test between those with and without the condition (Zweig and Campbell, 1993; Altman and Bland, 1994). It graphically depicts the trade-off between the sensitivity and the specificity of a test at various cut-offs values; a pair of diagnostic sensitivity and specificity values are computed for every single cut-off. To construct the ROC curve, these pairs of values are plotted on ROC space with 1 – specificity on the x-axis and sensitivity on the y-axis. The AUC summarizes the discriminative ability of a test in a single value. The AUC can have any value between 0 and 1. The shape of the ROC curve and the AUC value are commonly used to estimate the performance of the test. The curve that closer to upper-left corner and with larger the AUC values indicates a better test. A perfect diagnostic test has an AUC of 1.0, whereas a nondiscriminating test has an area of 0.5 (chance level performance).

To assess the ability of individual eye movements parameters to separate between VF loss groups (no vs. moderate VF loss; no vs. advanced VF loss), receiver operating characteristics (ROCs) were computed using individual eye movement parameters (e.g., saccade amplitude, BCEA, and KDE).

4.3 Results

4.3.1 Statistical analysis results

Figure 4.5 shows the median ($\pm$95% confidence interval; CI) values for each of four eye movement parameters (saccade amplitude, bivariate contour ellipse area, saccades landing on the pre-VF loss locations, and kernel density estimation probability), measured across three visual impairment conditions (no VF loss, moderate VF loss, and advanced VF loss). See Methods for definitions of each of these four measures and details of how they were computed.

The specific results from each measurement are described in detail below. However, the overall pattern revealed several statistically significant differences, but indicated that no single parameter provided a consistent, unambiguous biomarker for detecting VF loss. See Table for the statistical analysis. Note that for the analyses reported here and in Table , eye movement data from the three images were combined (concatenated) into a single stream, for ease of analysis and reporting. Analysis of individual eye movements

from each image showed that there was no statistically significant difference on eye movements within each group (for example in terms of saccade amplitude: F(2, 48) = 2.5, p = 0.92 for no VF loss group; F(2, 28) = 3.22, p = 0.05 for moderate VF loss group and F(2, 28) = 0.75, p = 0.45 for advanced VF loss group).

4.3.1.1 Saccade Amplitude

In terms of saccade amplitude (Figure 4.5a), the Kruskal-Wallis H test showed that there was a statistically significant main effect of visual impairment condition across all the stimuli (for VIDEO 1: $\chi^2(2) = 8.67$, p = 0.013; for VIDEO 2: $\chi^2(2) = 7.87$, p = 0.019; and for IMAGES: $\chi^2(2) = 10.2$, p = 0.006). Pairwise comparisons using the Mann–Whitney U test (Bonferroni corrected for three comparisons) revealed that the median saccade amplitude in the no VF loss group was significantly reduced in VIDEO 1 (U = 79, p = 0.003, η^2 = 0.23), VIDEO 2 (U = 76, p = 0.003, η^2 = 0.24), and IMAGES (U = 68, p = 0.001, η^2 = 0.28), compared to the advanced VF loss group. However, there were no statistically significant differences between no VF loss and moderate VF loss, or between moderate and advanced VF loss (both $p > 0.05$).

A follow-up analysis of saccade amplitudes as a function of time (using linear regression) indicated that average saccade amplitude decrease over time when viewing IMAGES (example in image 1 (Figure B.2), t(57) = -2.36, p = 0.02 for No VF loss group; t(57) = -2.63, p = 0.01 for moderate VF loss group; and t(57) = -2.76, p = 0.008 for advanced VF loss group) but not when watching VIDEO 1 ($p > 0.05$) AND VIDEO 2 ($p > 0.05$). There was no statistically significant difference for changes with time in the average saccade amplitude between no VF loss and the VF loss groups ($p > 0.05$).

4.3.1.2 Bivariate Contour Ellipse Area (BCEA)

In terms of BCEA (Figure 4.5b; distribution of saccade endpoints), a Kruskal-Wallis H test showed a statistically significant main effect of visual impairment condition for all stimuli (for VIDEO 1: $\chi^2(2) = 16.1$, $p < 0.001$; for VIDEO 2: $\chi^2(2) = 18.9$, $p < 0.001$; and for IMAGES: $\chi^2(2) = 6.6$, p = 0.03). Pairwise comparisons using the Mann–Whitney U test (Bonferroni corrected for three comparisons) revealed that the average BCEA for no VF loss group was significantly reduced compared in VIDEO 1 (U = 94, p = 0.010, η^2 = 0.17) and VIDEO 2 (U = 100, p = 0.020, η^2 = 0.15), compared to the advanced VF loss group. However, there were no statistically significant differences between no and moderate VF loss, or between moderate and advanced VF loss (both $p > 0.05$). With the three images, Mann–Whitney U tests (Bonferroni corrected for three comparisons) found no statistically significant difference between the no and moderate VF loss (U = 193, p = 0.99, η^2 = 0.004) or between the no and advanced VF loss groups (U = 143, p =

0.330, $\eta^2 = 0.04$).

4.3.1.3 Saccades Landing on the pre-VF loss locations (SLV)

The proportion of saccade endpoints landing on pre-saccade VF loss locations of the moderate VF loss group in VIDEO 1 (U = 81, $p = 0.002$, $\eta^2 = 0.22$) and VIDEO 2 (U = 52, $p < 0.001$, $\eta^2 = 0.36$) was higher compared to the no VF loss group (Figure 4.5c). However, there was no statistically significant difference between no VF loss and advanced VF loss ($p > 0.05$).

4.3.1.4 Kernel Density Estimate (KDE) probability

Kruskal-Wallis H tests found a statistically significant difference in the mean KDE scores (Figure 4.5d) when viewing VIDEO 1 ($\chi^2(2) = 11.4$, $p = 0.003$) and VIDEO 2 ($\chi^2(2) = 9.1$, $p = 0.010$). Mann–Whitney U tests (Bonferroni corrected for three comparisons) revealed that the average KDE probability score of the moderate VF loss group in VIDEO 1 (U = 72, $p = 0.002$, $\eta^2 = 0.26$) and VIDEO 2 (U = 91, $p = 0.010$, $\eta^2 = 0.18$) was significantly reduced compared to the no VF loss group.

Analysis of eye movements from each individual image found no statistically significant difference on eye movements within each group (for example in terms of saccade amplitude: F(2, 48) = 2.5, $p = 0.92$ for no VF loss group; F(2, 28) = 3.22, $p = 0.05$ for moderate VF loss group and F(2, 28) = 0.75, $p = 0.45$ for advanced VF loss group).

4.3.2 Receiver operating characteristic (ROC) analysis results

The results from the preceding analyses revealed multiple statistically significant differences between no VF loss and moderate VF loss in terms of KDE probability, and between no VF loss and advanced VF loss in terms of saccade amplitude and BCEA. To assess whether these statistical differences are sufficient to robustly discriminate between individuals with/without VF loss, I computed the Receiver Operator Characteristics (ROCs) shown in Figure 4.6.

There was a modest separation between the moderate and no VF loss groups in terms of BCEA for VIDEO 2 (area under the curve (AUC) = 0.72) and KDE probability for VIDEO 1 (AUC = 0.76), and likewise between the no and advanced VF loss groups in terms of saccade amplitude for VIDEO 1 (AUC = 0.78), and VIDEO 2 (AUC = 0.79), and IMAGES (AUC = 0.83). Overall, the results indicate that modest separation between the no VF loss and moderate groups could be achieved using KDE probability (76% sensitivity and 80% specificity). Similarly, modest separation could be achieved

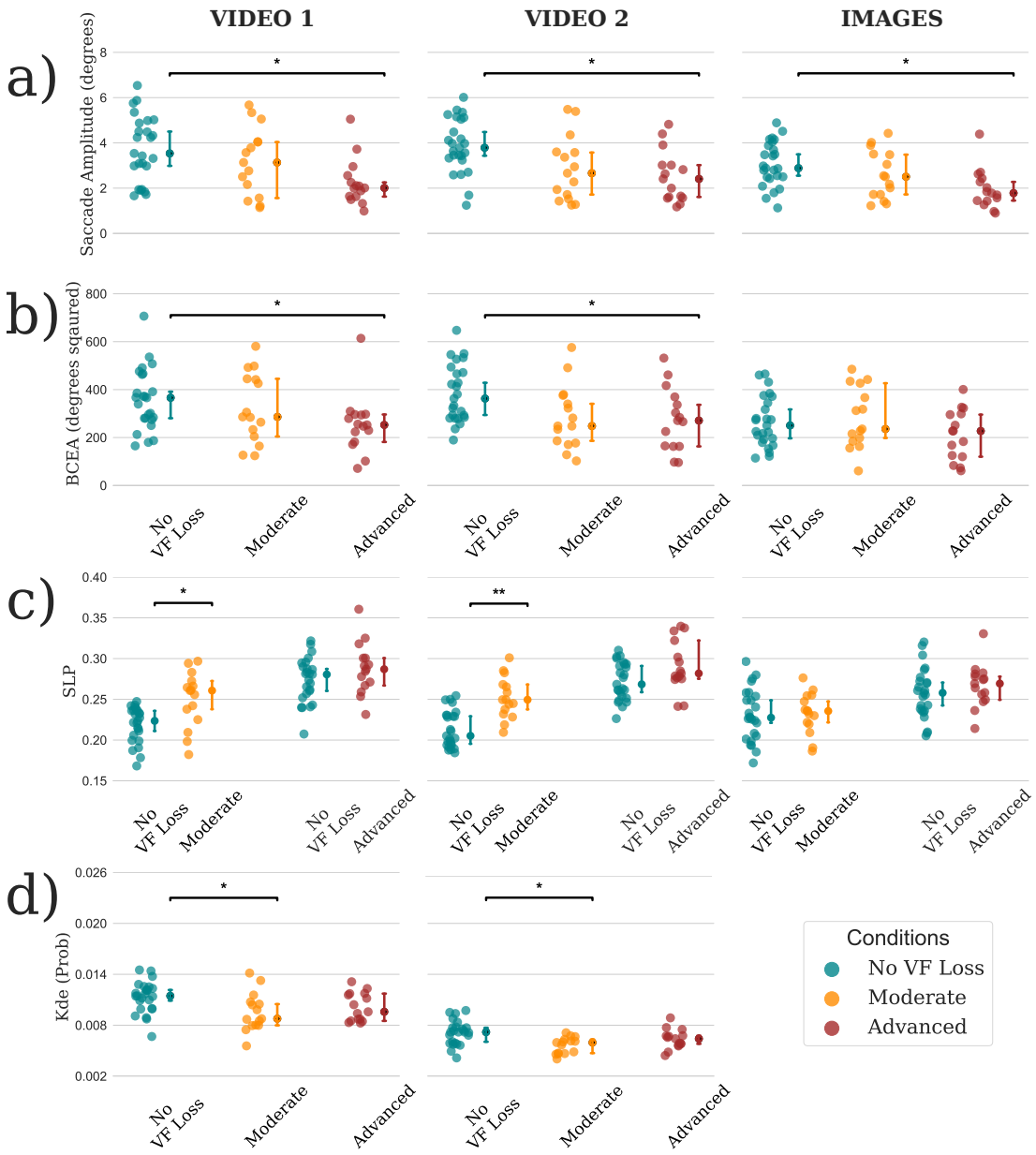

Figure 4.5: Median values (±95% confidence intervals) for (a) median saccade amplitude, (b) bivariate contour ellipse area (BCEA), (c) proportion of saccades landing on the pre-scotoma locations (SLV), and (d) kernel density estimation (KDE) probabilities, split into experimental conditions (no VF loss, moderate, and advanced) and stimulus type (VIDEO 1, VIDEO 2, and IMAGES). Statistically significant differences are denoted with an asterisk (* for $p < 0.05$ and ** for $p < 0.001$).

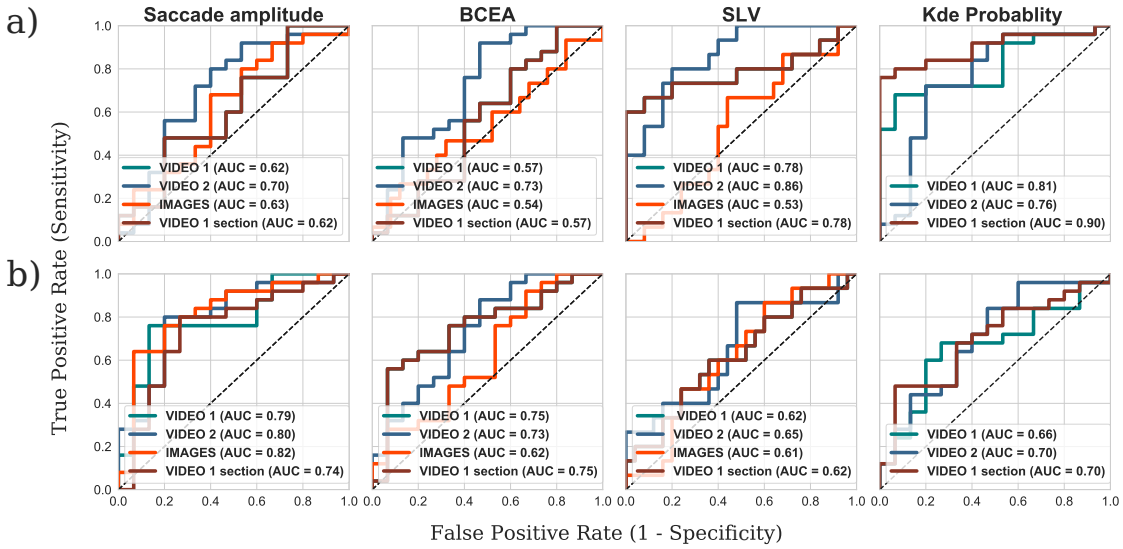

Figure 4.6: ROC curves and the AUC scores showing the separation between (a) the no VF loss and moderate (b) the no VF loss and advanced simulated VF losses for the measures described in Figure 4.5. The separation was best between no and moderate VF loss in terms of the SLV and KDE probability score, and between no and advanced VF loss in terms of saccade amplitude and BCEA.

between no and advanced VF loss using saccade amplitude (80% sensitivity and 80% specificity).

4.3.3 Improving separation performance

To see whether I could further improve separation between groups I performed two additional analyses. First, I examined the temporal trace from KDE probability analysis (Figure 4.7), and identified two sections of VIDEO 1 (totalling 120 sec) where the separation between the no and moderate VF loss groups appeared most pronounced(grey shaded regions in Figure 4.7). These regions were selected based on visual inspection of the temporal trace in Figure 4.7 (minimal overlap between the two medians ± IQR values), and the results reported below did not qualitatively differ if the periods were made slightly longer or shorter. In terms of content, these sections of the VIDEO appeared particularly monotonous, with no highly salient objects, e.g. moving vehicles or important landmarks. During these periods participants in no VF loss group tended to 'rest' at the centre of the screen, whereas participants with moderate VF loss exhibited more active 'search' strategies. Using data from only these 'cherry picked' subsections improved discrimination performance from AUC_{all} = 0.81 to $AUC_{subsection}$ = 0.90. Pairwise comparison between the groups showed the difference between the moderate and no VF loss group was statistically significant (Mann-Whitney U test; U = 65, p = 0.002, Bonferroni adjusted for three comparisons) in the grey shaded region of VIDEO 1 (Figure 4.7).

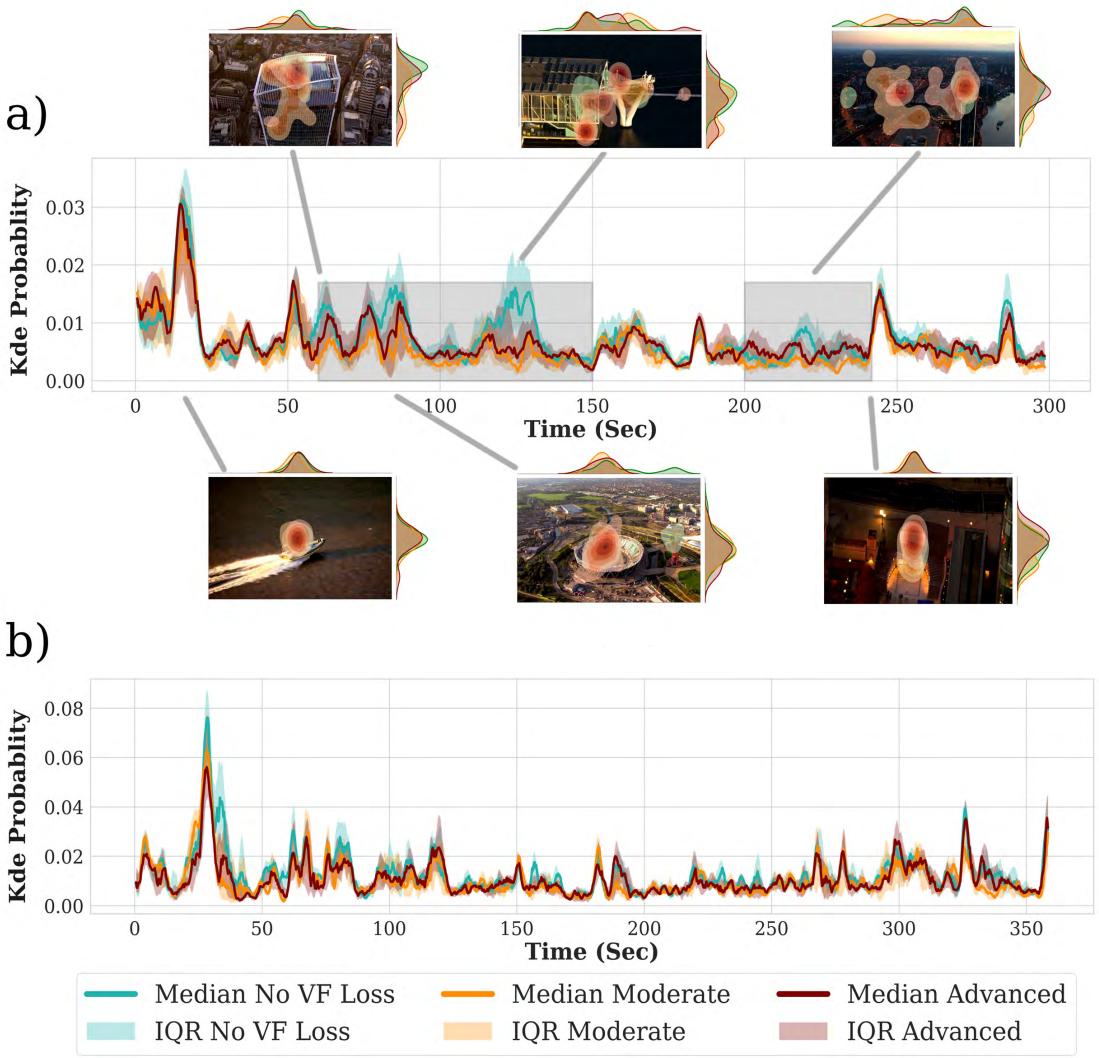

Figure 4.7: KDE analysis of fixation data, including KDE probability scores as a function of time for (a) VIDEO 1 and (b) VIDEO 2. The solid lines show the median values for each group. The shaded regions indicate the interquartile ranges. The average (median) probability score for the participants in the moderate group was smaller than for the no VF loss group ($p < 0.05$). This difference was more substantial in the grey shaded region of VIDEO 1.

In a second attempt to improve performance, I extracted multiple saccadic features and analysed using a machine learning technique (see Further analysis to improve separation performance). A leave-one-out technique was used to estimate the CI of classification sensitivity and specificity. Using these features improved the separation between no VF loss and moderate VF loss to AUC = 0.85 for VIDEO 1, 0.85 for VIDEO 2, and 0.87 for IMAGES (Figure 4.8a). Similarly, the separation between no VF loss and advanced VF loss increased to AUC = 0.91 for VIDEO 1, 0.89 for VIDEO 2 and 0.89 for IMAGES (Figure 4.8b). Average sensitivity for correctly identifying a moderate VF loss at a fixed specificity of 90% was 80% for VIDEO 1; 60% for VIDEO 2 and 60% for IMAGES. Similarly, the average sensitivity for correctly identifying advanced VF

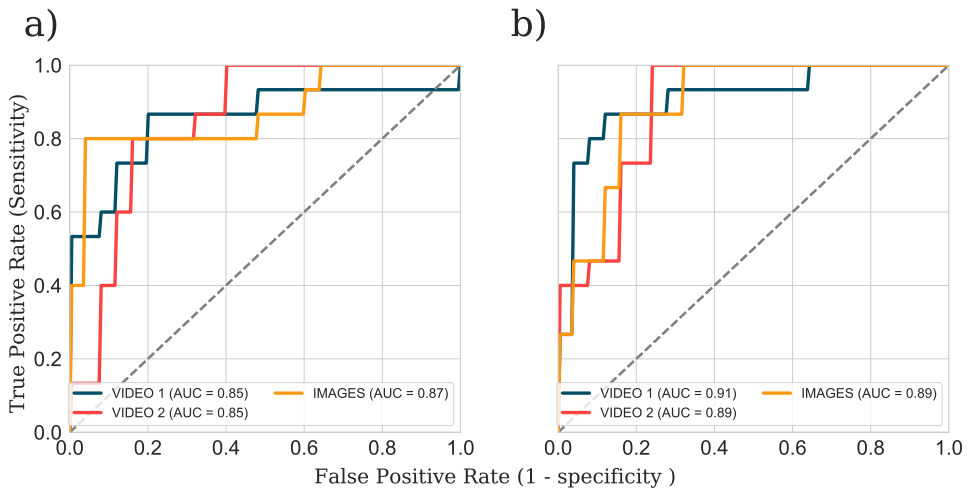

Figure 4.8: ROC after analysing multiple eye movement parameters to separate (a) no VF loss and moderate VF loss group, (b) no VF loss and advanced VF loss.

loss at a fixed specificity of 90% was 88% for VIDEO 1; 48% for VIDEO 2 and 48%. The individual ROCs from three stimuli exhibited very similar AUC scores. In short, these results indicated that using multiple eye movement parameters can improve VF loss detection. However, the performance was still modest relative to the current 'gold standard' ophthalmic measures (see *Introduction* section 4.1).

4.4 Discussion

This study assessed the sensitivity and specificity of natural eye movements as biomarkers for glaucomatous VF loss. Consistent with previous studies (Smith et al., 2012; Asfaw et al., 2018a), the data showed that natural eye movements are altered due to VF loss when looking at videos and images, and the observed 'group' differences were statistically significant, especially due to advanced VF loss. Participants with simulated advanced VF loss exhibited smaller saccade sizes and a reduction in the spread of saccade endpoints (Bivariate Contour Ellipse Area; BCEA) as compared with participants with no VF loss. A novel measure based on kernel density estimation (KDE) also differed significantly between conditions. However, ROC analysis revealed that the effects were relatively small, despite simulating substantial VF loss. Using any single measure, the data showed a modest separation between the no and moderate VF loss groups (AUC = 0.81), and between the no and advanced VF loss groups (AUC = 0.82).

To improve separation, I further attempted examining eye movements only in the most informative parts of the videos, and tried combining eye movement metrics to make an ensemble discrimination. These approaches resulted in encouraging performance gains (AUC $\approx$ 0.9), and indicate that with further development (i.e., better hardware and

data analysis techniques), natural eye movements may have the potential to provide a useful biomarker for gross screening of VF loss. However, a discriminative ability of 0.9 still remains relatively poor by clinical standards, given that even the smallest VF defects that I simulated would be detected by automated perimetry with nearly 100% sensitivity and specificity.

Part of the reason for this low discrimination may be due to the fact that eye movements were recorded binocularly. Detecting VF loss from a binocular assessment will always be limited by the fact that binocular vision is often better preserved than vision in either eye alone (even when considering the better seeing eye (Asaoka et al., 2011)). It is likely that greater accuracy could be achieved by making the assessment more similar to traditional perimetry: with the use of monocular viewing (patching), head-restraints, fixations targets, and simple stimuli. This, however, I feel would be a mistake. The principle attraction of using natural eye movements is the ease and accessibility by which data can be acquired. These characteristics would be lost if participants were forced to comply with a rigorous testing protocol. It may be that this in turn places a hard limit on the sensitivity and specificity of the approach. However, this may be acceptable if natural eye movements are viewed as complementary to traditional diagnostic tools, such as perimetry and structural examinations, and not as a like-for-like replacement. Furthermore, even at this stage natural eye movements could potentially be useful for assessing hard to reach patient groups, such as those who lack the physical or cognitive capacity to undergo conventional perimetry.

The data from this experiment are in general agreement with existing findings. Previous studies have shown that gaze-contingent peripheral VF loss leads to shorter saccade amplitudes when observers perform visual search tasks (Bertera and Rayner, 2000; Cornelissen et al., 2005; Nuthmann, 2014) or view pictures freely (David et al., 2018). Real glaucoma patients have likewise been found to exhibit reduced saccade amplitudes when watching hazard perception videos (Lee et al., 2017) or freely viewing pictures (Asfaw et al., 2018a), although conflicting results have also been reported in this regard (Smith et al., 2012; Lee et al., 2018). Glaucoma patients also exhibit a smaller spread of fixations (measured using BCEA) (Smith et al., 2012; Najjar et al., 2017) and smaller saccade amplitudes (Smith et al., 2012; Asfaw et al., 2018a) when viewing pictures freely.

Several study limitations should also be acknowledged when interpreting the results. First, the system used to simulate the peripheral VF loss (GazeSS) (Glen et al., 2015) operates by applying gaze-contingent blur to regions of the VF. Real patients, however, often report additional symptoms, such as glare and spatial distortions (Crabb et al.,

2013; Hu et al., 2014). Thus, the simulation does not entirely accurately mimic the effects of binocular VF perfectly, and it would be instructive to replicate the results with real patients in future. Furthermore, the simulated VF loss was based on data from a single patient with a VF defect near the fovea. Since VF loss can be highly heterogeneous across patients, different forms of VF loss (in terms of severity and location) may alter eye movements differently. Therefore, it would be instructive to systematically assess how eye movements differ as a function of VF loss distribution or location and this could be the subject of future work. It is also important to note that participants in the present study experienced an extremely acute onset of simulated vision loss. This is in contrast to real visual impairment, which often progresses gradually over many years (Leske et al., 2003).

In terms of improving the discriminative power of eye movements, future work should focus on determining the principles that make a stimulus more or less informative by investigating a variety of video clips that can elicit different eye movements. For example, my pilot study involving 10 people indicated that short clips of sports scenes (football, gymnastics and cycling) were less discriminatory. Future studies should also investigate methods of combining eye movement metrics with other easily obtainable data sources (e.g., interocular pressure, demographics, family history), and focus on obtaining larger datasets that could be used to train 'deep learning' networks that may be capable of identifying more subtle signs of eye disease (Rahimy, 2018; De Fauw et al., 2018). Furthermore, better approaches that consider the effect of centre bias on natural eye movements could be explored to help provide better separation between the study groups. For example, using techniques proposed by Marsman et al. (2016) to identify scenes with high viewing priorities prior to computing the KDE. Future work could also consider other techniques that have described characteristics of attention and eye movement changes during the viewing of pictures.

In summary, the present study demonstrated that participants with simulated glaucomatous VF loss exhibited smaller saccades, explored the screen less, and fixated at different locations than the participants with no visual impairment. However, despite these differences being statistically significant, sensitivity and specificity analyses showed that eye movements alone were only able to provide modest separation between participants with/without substantial VF loss. At this stage it is only possible to conclude that further development is required before eye movements can provide a clinically useful biomarker for eye-disease in practice.

Chapter 5

Detecting glaucomatous visual field loss using a novel spatiotemporal analysis of eye movements

5.1 Introduction

As described in Chapter 1, Crabb et al. (2014) described a study using scanpaths of eye movements recorded whilst people freely watched films to test the feasibility of separating patients with glaucoma from healthy peers. The average sensitivity for correctly identifying a glaucoma patient at a fixed specificity of 90% was 79% (95% CI: 58 to 86%). The area under the receiver operating characteristic (ROC) curve was 0.84 (95% CI: 0.82 to 0.87). This chapter first describes the work done to comprehensively curate the dataset used in Crabb et al. (2014) to make it publicly available for other researchers to use. Next, I develop novel methods of analysis of this dataset with the aim of improving, or matching, the diagnostic accuracy reported in the original paper. In part this was motivated by the results from the study described in the previous chapter. That is an attempt to think of better ways of extracting information from the data that may be contained within the natural eye movements to afford better diagnostic performance.

The newly organised and curated data set was reported in a published paper in the journal *Data in Brief* (Asfaw et al., 2018b). The co-authors of this work are Pete R. Jones (PJ), Nick D. Smith (NS), and David P. Crabb (DC). All of the data was reorganised and aligned with all of the clinical measures by DA working with an archive of data prepared in part by NS. The paper was written by DA, and reviewed, edited and

approved by all authors. I conceived, developed and tested all of the work in the second half of this chapter under the supervision of PJ and DC, and this work is under preparation for submission to a scientific journal.

PART I: Data on eye movements in people with glaucoma and peers with normal vision

What follows is a description of the curated dataset. Eye movement data were originally collected to test the hypothesis that age-related neurodegenerative eye disease can be detected in a person's spontaneous eye movements while watching video clips (Crabb et al., 2014). Gaze was recorded in 44 glaucoma patients, and 32 age-similar people with healthy vision. All patients had an established clinical diagnosis of chronic open-angle glaucoma (COAG): In short, each participant watched three video clips, for approximately 16 minutes in total, and completed standard clinical tests of visual function (visual acuity, contrast sensitivity, VF examination). The dataset contains raw gaze data, processed eye movement data, clinical vision test results, and basic demographic information (age, sex). Importantly, the dataset is now made freely available for any academic, educational, and research purposes (at https://doi.org/10.5281/zenodo.1156863).

5.1.1 Participants

Forty-four people with glaucoma were recruited from clinics at Moorfields Eye Hospital NHS Foundation Trust, London in 2012/13. All patients had an established clinical diagnosis of COAG for at least two years and were between 50 and 80 years of age. COAG was defined, following clinical guidelines, by the presence of reproducible VF defects in at least one eye with corresponding damage to the optic nerve head and an open iridocorneal drainage angle on gonioscopy. The diagnosis was made by a glaucoma specialist. A deliberate attempt was made to recruit a sample of patients with a range of disease severity according to VF loss. Patients were purposely not recruited if they had any ocular disease other than glaucoma (except for an uncomplicated lens replacement cataract surgery). In addition, at the point of recruitment, patients had slit lamp biomicroscopy performed by an ophthalmologist to further exclude any other concomitant macular pathology, ocular surface disease or any significant problems with dry eye.

Thirty-two healthy people (controls), of a similar age to the patients, were recruited from the City University London Optometry Clinic; this is a primary care centre where people routinely receive a full eye examination, which includes measurement of visual acuity, refraction, binocular vision assessment, pupil reactions, slit-lamp assessment of the anterior eye, measurement of intraocular pressure, VF assessment and indirect

ophthalmoscopy of the macula, optic nerve head, and peripheral retina.

5.1.2 Clinical Vision Tests

All participants underwent an examination of visual function by a qualified optometrist on the day of testing. Corrected binocular visual acuity (VA) was measured using an Early Treatment Diabetic Retinopathy Study (ETDRS) letter chart. Since the study was designed to recorded binocular eye movements, binocular clinical vision tests (VA and CS) were performed. All participants had binocular VA of at least 0.18 logMAR (Snellen equivalent of 6/9). Binocular Contrast Sensitivity (CS) was measured with a Pelli-Robson chart. VFs were measured monocularly in both eyes using automated static threshold perimetry. This was performed using a Humphrey Field Analyzer (HFA; Carl Zeiss Meditec, CA, USA), with a standard 24-2 grid and the Swedish Interactive Testing Algorithm (SITA). HFA mean deviation (MD) is a standard measure of overall VF loss, relative to healthy age-matched observers, with more negative values indicating a greater loss. The Oculus C-Quant straylight meter (Oculus GmbH, Wetzlar, Germany) was used to measure abnormal light scattering in the eye media, to exclude participants with media opacity and other lens type artifacts. Participants were required to be within 'normal limits' for this test. Furthermore, all participants were examined with a modified version of the Middlesex Elderly Assessment of Mental State (MEAMS, Pearson, London, UK), a psychometric test designed to detect gross impairment of specific cognitive skills such as memory and object recognition in an elderly population. All participants passed the MEAMS test. The light scattering and MEAMS tests results are not included in the hosted data; however, VA, CS, and VF data are included.

Summary measures of these vision tests, such as HFA MD in decibels (dB), visual acuity (VA) in logMAR, and contrast sensitivity (CS) in log units are provided in a single comma-separated file, along with basic demographic information. A sample of these data is shown in Table 5.1. These data allow investigating the relationship between different eye movement parameters (such as saccade amplitudes and rates) and common clinical measures of vision.

Individual Differential Light Sensitivity values for each of the 54 test points in the 24-2 VF test are provided for every participant/eye. These values are stored in a single row, as shown in Table 5.2 and can be visualized in VF map as shown in Figure 5.1 (see Figure C.1 IVF of all the patients with glaucoma).

Table 5.1: Sample clinical information of participants. The complete tables for both patients and controls are uploaded in a spreadsheet file. The tables have eight fields: participants' ID, the eye used for the study, age, sex, MD measurements (for both left and right eyes), binocular VA, and CS measurements. Participants were assigned a unique ID, G001–G044 for patients and C001–C032 for controls. Shown here are the data from the first five patients.

Participant ID	**Study eye**	**Age**	**Sex**	**Right MD**	**Left MD**	**VA (log)**	**CS (log)**
G001	L	63	Female	-20.84	-6.1	-0.02	1.95
G002	L	69	Female	-8.17	-12.05	0.04	1.95
G003	L	77	Female	-3.61	-2.24	0.16	1.95
G004	L	74	Male	-10.42	-4.66	0.14	1.95
G005	L	64	Male	-3.56	-6.45	0.02	1.65

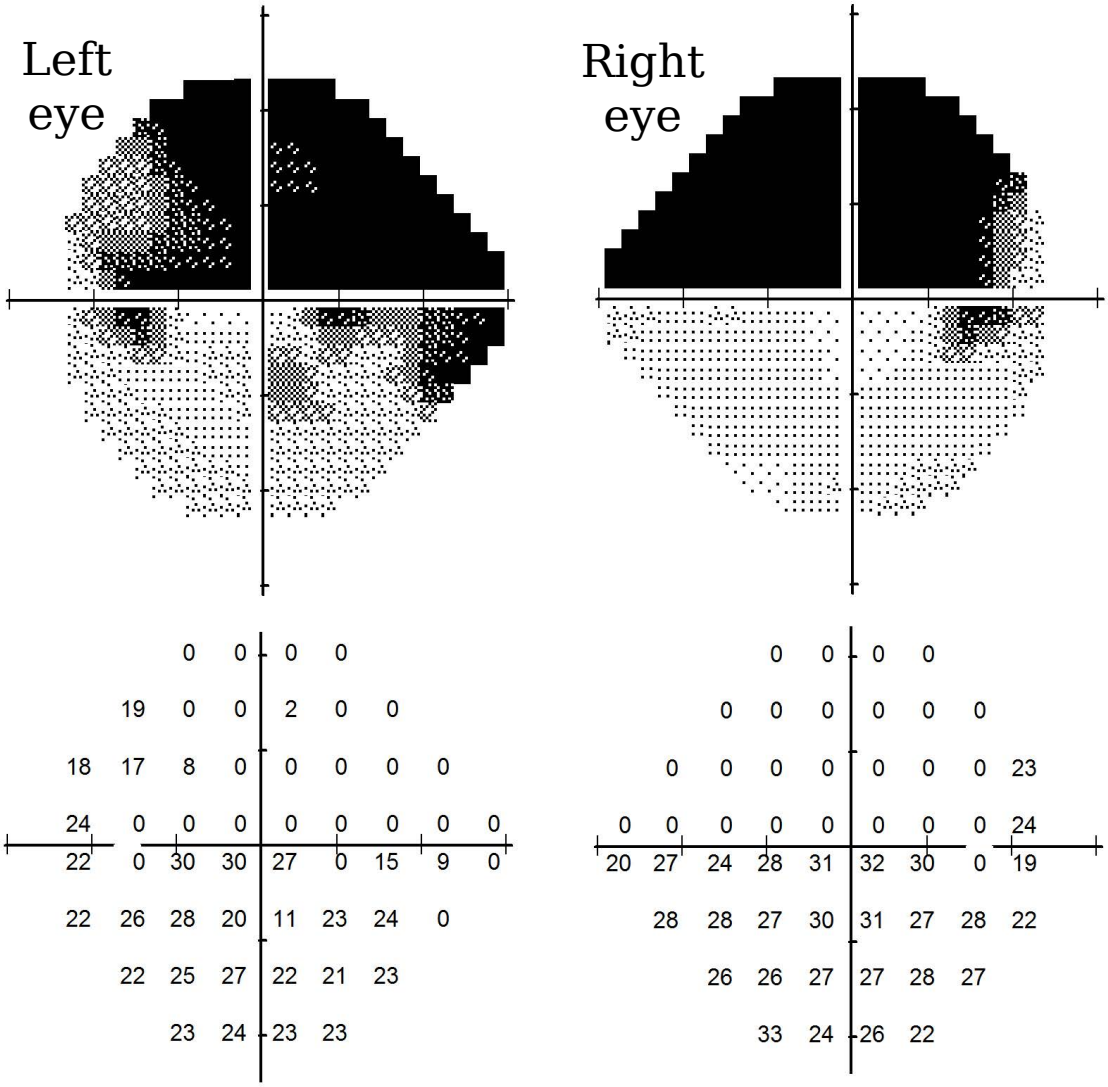

Figure 5.1: Sample 24-2 VF greyscale plots and the corresponding numeric VF map (for participant G007). The 54 sensitivity values in the VF map are vectorized and stored in a comma separated file (see Table 5.1). The vectorization was performed by concatenating sensitivity values starting from first row (top) to the last row (bottom). The same vectorization procedure was applied to the sensitivity values of both eyes.

Table 5.2: Sample sensitivity values for each of the 54 test points in the 24-2 VF test. The results provided are for every participant/eye. The data for G007 is also shown graphically in Figure 5.1.

Participant ID	Eye										
G001	L	27	22	28	23	29	···	29	29	28	21
G001	R	11	10	7	0	6	···	10	23	25	23
⋮	⋮										
G007	L	0	0	0	0	19	···	23	24	23	23
G007	R	0	0	0	0	0	···	33	24	26	22
⋮	⋮										
G044	L	26	26	25	19	25	···	31	31	28	27
G044	R	28	28	19	23	28	···	27	28	28	26

5.1.3 Raw gaze data

Gaze was measured using an Eyelink 1000 eye tracker (SR Research Ltd., Ontario, Canada). Participants were positioned, using a chin rest, at a viewing distance of 60 cm. The eye tracker outputs data in a proprietary EDF file format (.EDF; Eyelink Data File). For ease of use, these EDF files were converted into ASC file using a translator program (EDF2ASC) that was supplied by SR-Research. The ASC files contain the entire recorded eye tracking events, including the start and end time of all the eye movement events such as fixations, saccades, and blinks. During fixations and saccades, the eye position (in screen coordinate) was recorded. Other eye tracking information such as calibration and synchronization information were also stored in the ASC files. The gaze data for each participant were stored in individual ASC files (i.e., 44 and 32 ASC files for glaucoma and controls, respectively). A detailed description of the ASC file's format and structure are provided by the manufacturer (SR Research; https://www.sr-research.com).

5.1.4 Processed eye movement data

The raw ASC file was processed to extract fixations and saccades using a bespoke C++ program. The program searches for flags that indicate the end of a fixation ('EFIX') or a saccade ('ESACC') in the ASC file. Each fixation end flag contains its start and end time, duration, mean position, and mean pupil size during the fixation. Similarly, a saccade end flag contains its amplitude, velocity, duration, start and end time, and start and end position. The extracted fixation and saccade events have eight and eleven fields, respectively (Table 5.3). These processed eye movement data were stored in CSV file format. Thus, the dataset contains 44 and 32 CSV files for glaucoma and controls, respectively. It should be noted that due to poor tracking and technical errors, the data

Table 5.3: Description of fixation and saccade fields contained within the 'processed eye movement data' CSV files. Five events (trial name, eye, start time, end time, and duration) are similar for both fixation and saccade events. Saccade and fixation positions are expressed using four (Start X, Start Y, End X, and End Y) and two (X and Y) fields, respectively. In addition, each saccade has two additional fields that describe the size and speed of the saccade.

Field	Description
Trial name	Name of video (one of 'DadsArmy' (VIDEO A), 'HistoryBoys' (VIDEO B), and 'SkiCross' (VIDEO C); see Figure 5.2)
Eye	The study eye (left or right)
Start time	Start time of the event (e.g., saccade start, saccade end; in millisecond)
End time	End time of the event (in millisecond)
Duration	Difference between the start and end of the event in millisecond
X	The x position of fixation in screen coordinate in pixels (range from 1 to 1600)
Y	The y position of fixation in screen coordinate in pixels (range from 1 to 1200)
Pupil area	Pupil area of the eye during fixation
Start X	The x coordinate of saccade's starting position in pixels (range from 1 to 1600)
Start Y	The y coordinate of saccade's starting position in pixels (range from 1 to 1200)
End X	The x coordinate of saccade's end position in pixels (range from 1 to 1600)
End Y	The y coordinate of saccade's end position in pixels (range from 1 to 1200)
Amplitude	Size of the saccade in degrees visual angle
Peak Velocity	Speed of the saccade in degrees/second

from five controls (C019 - C023) and one patient (G010) are incomplete. Their data, however, are included in the dataset for purpose of completeness.

Within the data archive, a Minimal Working Example MATLAB script ('SaccadeAmplitudePlot.m') was included to demonstrate how this processed data can be used (in this case, to plot the distribution of saccade amplitude of each participant). This program can be extended easily to compute other eye movement metrics such as fixation duration and saccade rates.

5.2 Experimental design, materials and methods

5.2.1 Apparatus

Participants viewed (with both eyes open) three separate unmodified TV and film clips (including audio) on a 22-inch monitor (Iiyama Vision Master PRO 514, Iiyama Corporation, Tokyo, Japan) at a resolution of 1600 by 1200 pixels (refresh rate 100 Hz). Monocular eye movements were recorded using an Eyelink 1000 eye tracker (SR Research, Ontario, Canada), while participants were watching three separate video clips monocularly. The eye tracker was configured to detect saccades using velocity and acceleration thresholds of 30°/s and 8000°/s^2, respectively. The eye giving the best quality pupil detection and corneal reflection was chosen for tracking. The EyeLink proprietary algorithm (nine-point calibration) was used to calibrate the eye tracker and was repeated, as required, until the accuracy flagged by the system to be of a 'good'.

Figure 5.2: Sample frames excerpted at a specific time from the three video clips used in the experiment.

Table 5.4: Details of the stimuli (three video clips) used in the experiment.

Clip	Subtending angle (half-angle)	Length (minutes: seconds)	Frame width (pixels)	Frame height (pixels)	Frame rate (frames/second)
Dads Army (VIDEO A)	20.4° X 14.9°	05:09	1280	720	29
History Boys (VIDEO B)	ang17.3 X 10.6°	03:20	720	576	25
Ski cross (VIDEO C)	ang17.3 X 10.6°	07:18	720	576	25

Drift correction was also performed before each of the three films was displayed, and in the case where a large drift (greater than 5°) was detected, a recalibration was performed.

5.2.2 Stimuli

One clip VIDEO A, top row in Figure 5.2) was an excerpt from an entertainment program (309 sec; Dads Army, BBC Television) which covered the full screen (subtending a half-angle of 20.3° by 14.9°). The other two clips (VIDEO B and VIDEO C middle and bottom rows respectively in Figure 5.2) were taken from a feature film (200 sec; The History Boys, 20th Century Fox) and a sport program (436 sec; 2010 Vancouver Winter Olympics Men's Ski Cross, BBC Television); both of these clips were recorded at a 16:9 ratio, therefore they contained black rectangles at the top and bottom of the screen (subtended a half-angle of 17.3° by 10.6°). I summarized the characteristics of the three stimuli in Table 5.4.

PART II: Novel spatiotemporal analysis of eye movements using Machine Learning

Crabb et al. (2014) demonstrated how scanpaths of eye movements recorded whilst people freely watch TV films can be processed into maps that contain a signature of VF loss. In the proof of principle study, they demonstrated that a group of patients with glaucoma can be reasonably well separated from a group of healthy peers by considering these eye movement signatures alone. In short, saccade density maps extracted from the scanpaths were analysed to train a machine learning classifier. A similar analysis approach was used to detect moderate and advanced simulated VF loss, as presented in Chapter 4.

Other studies have analysed eye movements using machine learning classifiers to detect simulated VF loss (David et al., 2019; Grillini et al., 2018). For example, Grillini et al. (2018) classified simulated central and peripheral VF loss using a decision tree classifiers trained using features extracted based on the latency of eye movements to randomly moving visual stimulus. More recently, David et al. (2019) used the hidden Markov model (HMM) and recurrent neural networks to detect simulated central and peripheral VF loss from eye movements recorded while participants watched images.

Outside of ophthalmology, machine learning classifiers have also been applied to eye movements to detect neurodegenerative conditions. For example, Lagun et al. (2011) used a machine learning classifier to separate three groups—patients with Alzheimer's disease, patients with mild cognitive impairment, and age-similar healthy controls—by extracting eye movement features such as saccadic orientation, fixation duration and re-fixations to train the classifier. Tseng et al. (2013) used eye movement features, such as fixation duration and saccade amplitude to detect Parkinson's disease, attention deficit hyperactivity disorder and foetal alcohol spectrum disorder. The main limitation in these studies was that they relied on simple and/or static (average of eye movement measures over time) eye movement summary statistics. Eye movements, however, are temporal signals and there is a wealth of information in this temporal dimension. I hoped to exploit this idea in the work presented in this chapter. In the literature, a few other researchers, for different applications, have attempted to model sequential information in eye movements using the HMM (Chuk et al., 2017; Coutrot et al., 2016, 2018). This model, however, is not suitable for working with video stimuli since the regions of interest in videos change with time.

In this section, the approach discussed in Chapter 4 is further developed, in a novel fashion, by considering temporal sequences of successive saccadic movements to im-

prove classification accuracy. My aim was to match, or improve, the diagnostic performance of the proof of principle results presented in Crabb et al. (2014) study. Two reference standards, against which my novel method was to be compared, were used. The main reference standard was the performance of the previously proposed classification method described in Crabb et al. (2014), and for this, I reproduced the analysis. For compatibility with the results in Chapter 4, I also considered a reference standard based on the diagnostic performance simply based on a range of eye movement summary statistics used in isolation (saccade amplitude, saccade rate, fixation duration, saccadic reversal rate, and spread of fixations). The Index method, which I compared with these reference standards, was my newly proposed analysis which for these purposes is named the 'Novel Spatiotemporal Analysis' (Index). The performance of each method was quantified in terms of its ability to separate patients from controls, specifically using ROC analysis.

5.3 Methods

5.3.1 Pre-processing of the eye movements data

Following a similar procedure in Crabb et al. (2014) a sliding window was used to count the number of saccades made per second. The percentage of 1-second regions containing one or more saccades was delineated per video clip per person. Eye movements that do not contain a saccade in more than a quarter (25%) of the 1-second regions of each clip were excluded (see supplementary Figure C.2 and Figure C.3 for excluded data). Appendix C also summarises the definition and calculation of the standard eye movement summary statistics.

5.3.2 Reference methods

The approach proposed in Crabb et al. (2014) was reproduced to use it as the reference method. In short, for each video and for each participant, a feature vector of length 116 was extracted based on saccadic movements. All features extracted from the three video clips were subjected to Kernel principal component analysis (KPCA). For this, the authors computed the difference measure between every pair of participants' feature vectors. The resulting features were classified using Naïve Bayes classifier. The performance of the classifier was evaluated using 10-fold cross-validation which was repeated 100 times to estimate the confidence interval (CI) of classification sensitivity and specificity. Crabb et al. (2014) applied KPCA before performing cross-validation. That is the dimensionality reduction was applied before splitting the data into training and validation sets. This flaw was corrected in my implementation of this.

For consistency with Chapter 4, I also calculated amplitude, saccade rate, and fixation duration, spread of fixations measured using KDE, spread of saccade endpoints measure, and SRR to see how well they could separate the patients and controls in the present data set (A recap of the calculations is given in Appendix C).

5.3.3 Novel spatiotemporal analysis (Index method)

5.3.3.1 Analysis of the sequential data

One idea behind the novel method of analysis was to base it on some methods used in *information retrieval*, which is a collection of established computer science techniques for searching for information in documents (Manning et al., 2008). In short, information retrieval is a process that responds to a user query by examining a collection of documents and returning a sorted document list that should be relevant to the user requirements as expressed in the query. For example, internet search using textual web search query.

Within information retrieval, the so called Term frequency-inverse document frequency (TF-IDF) is a well established and specific approach for text analysis (Jones, 1972; Beel et al., 2016; Wu et al., 2008). TF-IDF assigns a score (weight) to terms (a word, or group of words) in a document based on the importance of a given term within the given document (Robertson, 2004). The intuition of this approach is that if a term is frequent in a corpus (collection of documents), then it is not informative, and should be given less weight than one which occurs in few documents. The TF-IDF has two components: TF and IDF. TF captures the importance of the term in the document, whereas IDF attempts to measure how informative a term is in the corpus. For example, in document classification task words, such as 'the', 'this', and 'of' are less informative and will be assigned small TF-TDF weights since they are likely to appear in every document.

TF-IDF assigns a weight to a term in each document using the TF-IDF formulation:

$$W_{i,j} = TF_{ij} * IDF_i \tag{5.1}$$

$$W_{i,j} = TF_{ij} * log(\frac{N}{DF_i}) \tag{5.2}$$

where W_{ij} is the weight for term i in document j, N is the number of documents in the

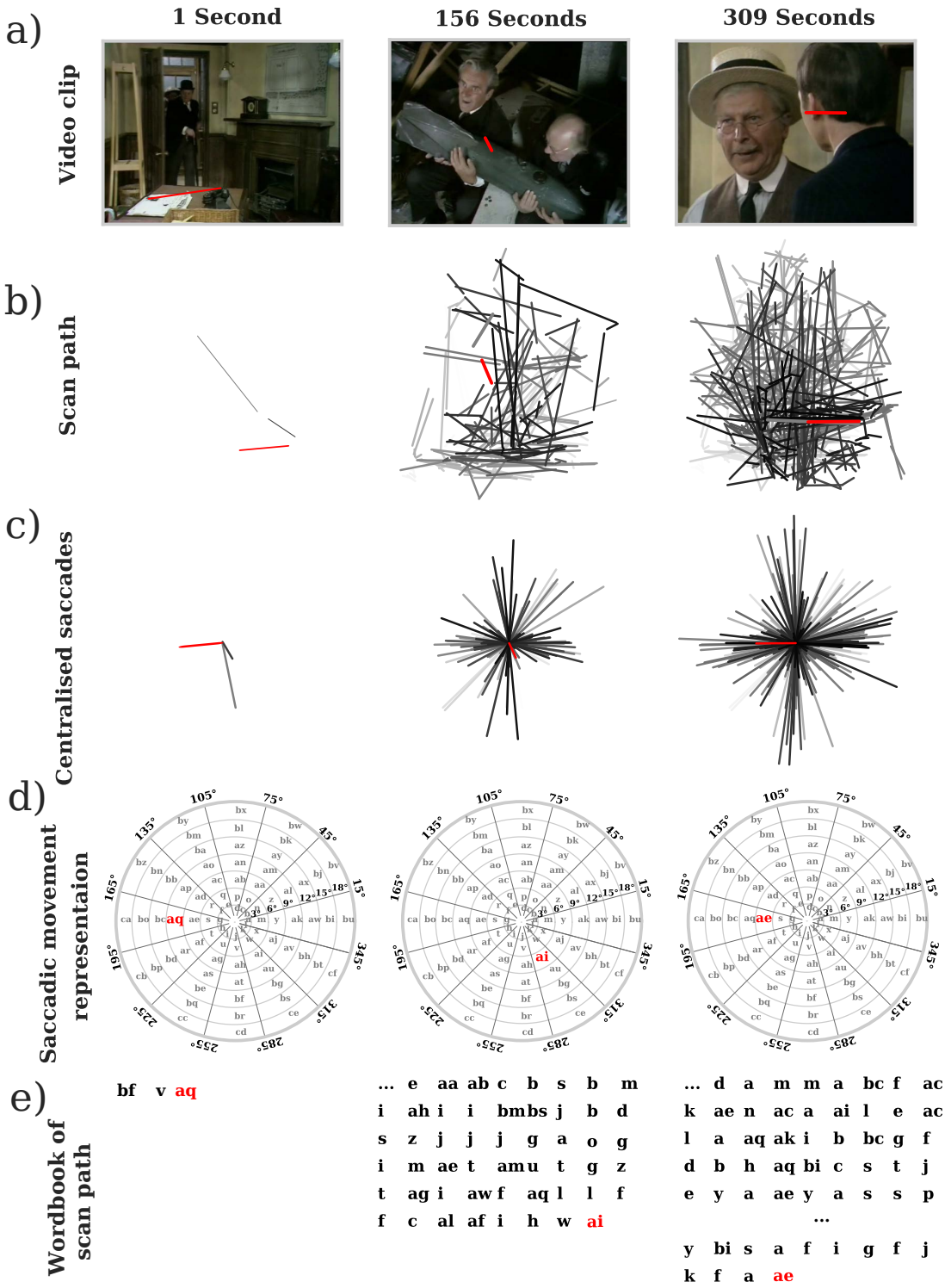

Figure 5.3: Saccadic-movement representation using tokens. The underlying scanpath is from a single participant in the control group watching VIDEO A. (a) Frames from the clip and raw saccades made at a given time while watching the clip. (b) Scanpath of saccades made until the given time in the video. (c) Centralised saccades plotted by setting the start of all saccades to the centre (0,0). (d) Tokens (letters and their combination) used to encode saccadic movements based on the direction and size of the saccade. For illustration, the size of each bin in the polar grid is of size 3° in the radial and 30° in the angular coordinate. The token highlighted in red corresponds to the saccade (e.g., the first column represents a saccade of 10° in size and executed at an angle of 190°) highlighted in the same colour as in (c). (e) Example of a wordbook that stores each term that encodes a series of saccades.

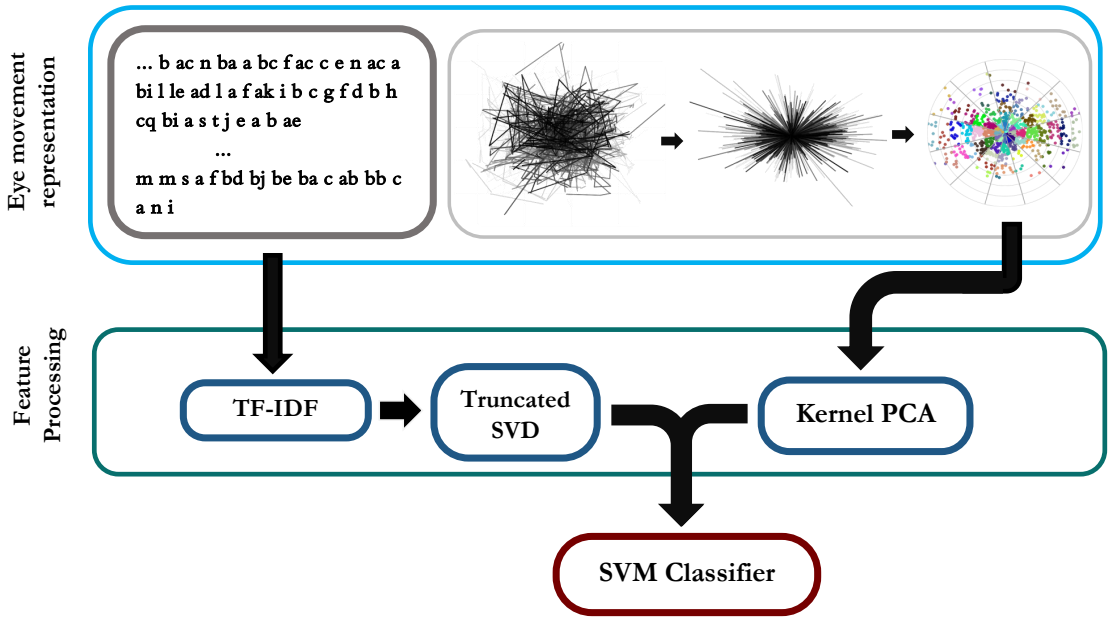

Figure 5.4: Architecture for the Novel Spatiotemporal Analysis (Index method). The workbook from each participant, sequential eye movement representation as illustrated in Figure 5.1 were encoded using TF-IDF, with the first and resulting matrix reduced using principal component analysis (PCA). The extracted static features include counts of saccades that land on each bin in the polar histogram, and other common eye movement metrics, such as saccade amplitude, were serialised. Kernel PCA (KPCA) was used to reduce the dimension of the extracted static features. The resulting features from static and sequential features were serialised and fed into a support vector machine (SVM) classifier.

Corpus, $TF_{i,j}$ is the term frequency of term i in document j and DF_i is the document frequency of term i in the corpus.

To efficiently analyse sequential saccadic movements, each saccade was represented using tokens $('a','b','c',\cdots 'ce','cf')$ based on the size and direction of the saccade. For this saccades were centralised—saccades are treated as a vector starting at the origin (0, 0) on a polar grid. Each bin in the polar grid is of size 2° in the radial and 30° in the angular coordinate, making a total of 156 bins (12 X 13). For example, a saccade of length 1°, travelling at an angle of 10° is assigned token $'a'$. A saccade with the same length but travelling at an angle of 20° is assigned token $'b'$. A saccade of length 4° travelling at an angle of 0° is assigned token $'m'$ (Figure 5.3).

Sequential saccadic features were extracted using a so-called n-gram model. An n-gram is a contiguous sequence of n tokens from a given sample of text (Brown et al., 1992; Peng and Schuurmans, 2003). In the usual text analysis, an n-gram is simply a sequence of N words: a 2-gram (or bigram) is a two-word sequence of words like 'This is', 'is a', 'a great', or 'great thesis' and a 3-gram (or trigram) is a three-word sequence of words like 'is a great', or 'a great thesis'. An n-gram model computes

the frequency of such series of words of length n in a given document. Here, the n-gram was used to count the occurrence of distinct successive saccadic movements of length n in a scanpath. For example, n = 2 (bigram) represents two successive saccadic movements $(e.g.,'a, b','ac, k','d, f')$. Based on the 156 token representation used here, there were 24,336 (156 x 156) possible bigram movement permutations. That means, using the bigram analysis, for each participant and each video, a vector of length 24,336 was extracted. In practice, a smaller number of features is extracted since participants do not make all forms of possible successive saccades. The best value(s) of n (between 1 and 4) was selected using cross-validation. Each extracted feature was assigned a weight using the TF-IDF. This process produces a large sparse matrix. The dimension of this matrix was reduced using truncated singular value decomposition (SVD) (Halko et al., 2011). SVD decomposes a given matrix X into the product of three matrices USV^T, where U and V are in column orthonormal form (i.e., the columns are orthogonal and have unit length, $U^T U = V^T V = \mathrm{I}$) and S is a diagonal matrix of singular values. A truncated SVD approximates the matrix X as

$$X \approx X_k = U_k S_k V_k^T \tag{5.3}$$

where $U_k = [U_1, U_2, ..., U_k]$, $V_k = [V_1, V_2, ..., V_k]$ and $S_k = diag[S_1, S_2, ..., S_k]$ are the first k columns of U, V and S. This gives the best rank k approximation to the original matrix. In other words, the matrix X is very sparse (mostly zeros), but the truncated X_k is dense.

5.3.3.2 Analysis of the static eye movement features

Since the TF-IDF gives a score based on the occurrence of saccadic movements, non-sequential saccadic movements (n = 1 in the n-gram model) have a low score (low importance) in the sequence analysis. Therefore, these features were analysed separately as static features. These non-sequential saccadic movements have been shown to be useful in analysing eye movements (Crabb et al., 2014). To extract static features, first saccades are centralised (i.e., the start of each saccade is translated to the [0,0] position), following the feature extraction approach proposed in Chapter 4 (see also Figure 5.3). Then a polar histogram was computed to count the number of saccades that land in each bin. Each bin measures 2° in the radial and 30° in the angular coordinate. In total, there were 156 bins. That means that for each participant and each video, a static feature of length 156 was extracted.

In addition to the 156 features from the polar histogram of saccades, six additional

features (saccade amplitude, saccade rate, BCEA, SRR, kde, and fixation duration) were extracted from the saccadic movements following a similar procedure to that presented in Chapter 4. The dimension of the static features was reduced using kernel principal component analysis (KPCA) (Schölkopf et al., 1998), a nonlinear generalisation of PCA.

Note that the feature extraction technique of the Reference method and the Index method (specifically the static features) are similar, but they do differ in two key ways. First, the Reference method considers only saccades of size between 2° and 12°, but the Index method considers all saccades except those greater than 25°. Second, the Reference method used all data from the three video clips to build a kernel matrix (a matrix that holds the distance among the participants' feature vector), whilst in the new Index method each trail video are analysed separately.

5.3.3.3 Training a machine learning classifier

Features extracted from static and sequential eye movements were serialised and fed to a support vector machine (SVM) (Cortes and Vapnik, 1995), a well-established and widely used classifier (Figure 5.4). SVM algorithm computes a decision boundary that classifies the data points by maximizing the distances between nearest data point (either class) and the decision boundary. Here, an SVM with a radial basis kernel was used to transform the input feature values, allowing for non-linear discriminations (Buhmann, 2003). Three SVM models were built, one for each clip.

The performance of the classifier in separating glaucomatous patients from the peers with normal vision (controls) was evaluated using ROC (discussed/defined in 4.2.8), which calculates the trade-off between the sensitivity (true-positive rate) and 1 minus the specificity (false-positive rate), with the area under the ROC curve (AUC) used as a summary statistic of diagnostic accuracy. An AUC of 1.0 represents perfect discrimination, whereas an area of 0.5 represents baseline (chance) discrimination.

During the training procedure, I had no *apriori* hypothesis concerning which parameters (n-grams of features, size of the bins in the polar histogram, and KPCA and SVM classifier parameters) would be useful; therefore, an automatic cross-validation procedure was used to optimise the parameters using SCIKIT-LEARN's GridSearchCV function in Python (Pedregosa et al., 2011). Grid search requires setting values for each hyperparameter and assembling every possible combination of values to form a set of trials (Bergstra and Bengio, 2012). The set that provides the best ROC value was selected to generate the final result. Stratified cross-validation was performed to ensure that all the training and validation sets share the same number of positive and negative instances (Parker et al., 2007). The sensitivity and specificity of the classifier

were evaluated using 10-fold cross-validation. The cross-validation was repeated 100 times; for each iteration, the data were shuffled to ensure different combinations of training and validation samples.

All eye movement analyses (both static and sequential feature extraction and feature transformation and classification) were performed and written using the SCIKIT-LEARN package in Python (Pedregosa et al., 2011).

5.4 Results

Figure 5.5 shows the median value (and 95% confidence intervals [CI]) for each of the six 'simple' eye movement parameters (saccade amplitude, saccade rate, fixation duration, BCEA, SRR, and KDE probability) measured across each of the two VF conditions (controls and glaucoma). This figure is revealing because it illustrates the huge overlap between the patients and controls for all measures. In short, without further analyses, it clearly suggests that none of these measures, used in isolation, will be a good classifier or predictor for glaucomatous VF loss.

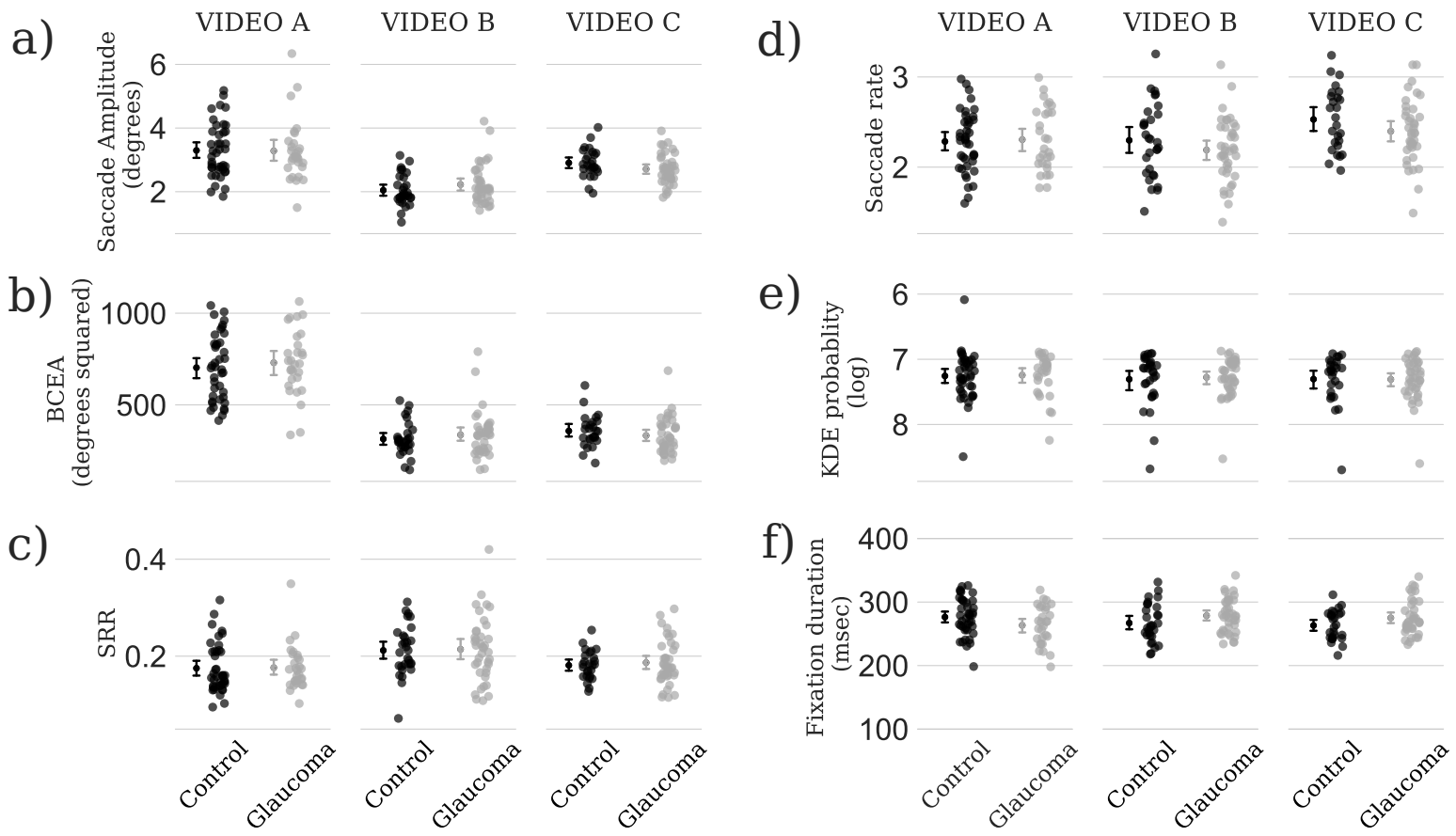

Figure 5.5: Median values (95% confidence interval) for (a) saccade amplitude, (b) saccade rate, (c) spread of fixations as measured using BCEA, (d) fixation duration, (e) KDE probabilities and (f) fixation duration split into experimental conditions (glaucoma and controls) and video type (VIDEO A, VIDEO B, and VIDEO C).

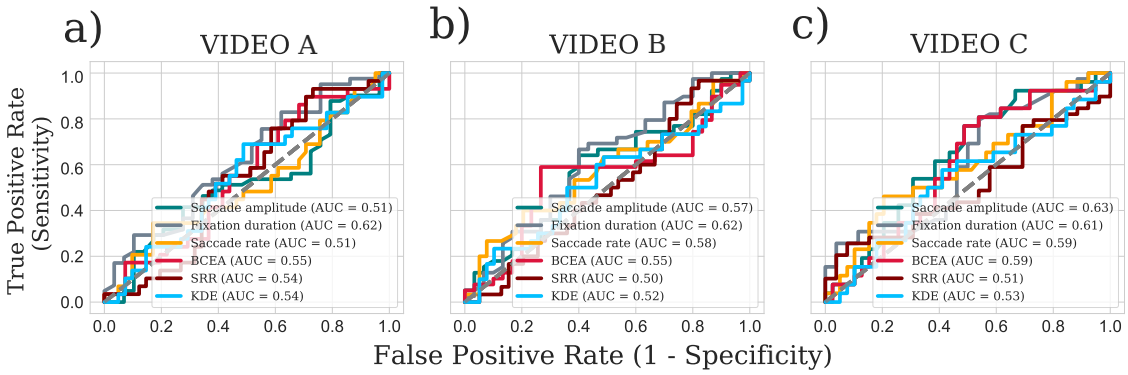

Figure 5.6: ROC curves based on the proposed analysis of sequential and static features and their combination for (a) VIDEO A (b) VIDEO B and (c) VIDEO C.

For completeness, ROC analyses were performed to evaluate the performance of individual eye movement parameters, as shown in Figure 5.6. This supports the finding illustrated in Figure 5.5 because the discrimination using these parameters offered nothing better than chance.

For the novel spatiotemporal analysis (Index method) I first present results from the static and sequential Index features separately (Figure 5.7). The performance of the static and sequential features was comparable in terms of VIDEO A and VIDEO B, yet for VIDEO C (there was some gain using the sequential features AUC of 0.75 [95% CI 0.79–0.71] versus 0.64 [95% CI 0.60–0.68]. Overall, combining the two features improved the separation slightly in terms of AUC between the two groups: the AUC improved by 4% for VIDEO A, 6% for VIDEO B, and 4% for VIDEO C.

The main result of this chapter is illustrated in Figure 5.8. Using the Index method, the separation between the groups was relatively consistent across the three video clips

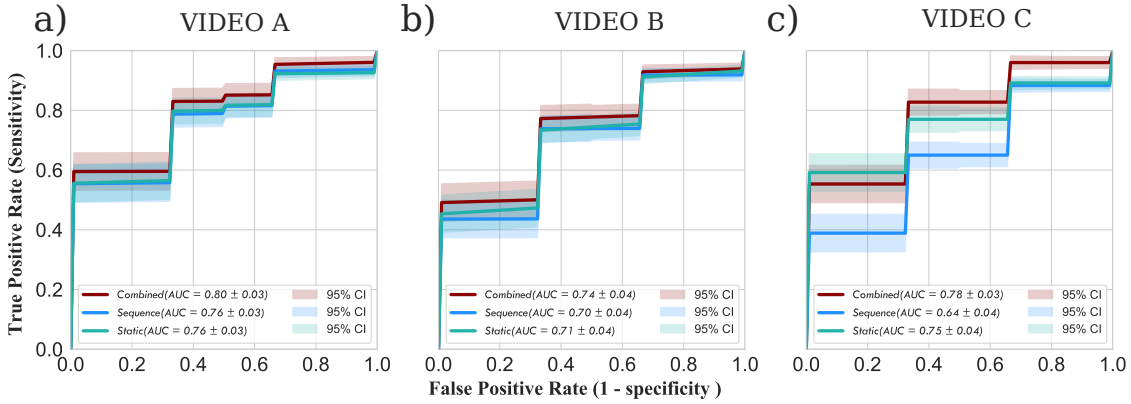

Figure 5.7: ROC curves and the AUC scores showing the separation between glaucoma and control groups for the measures described in Fig 5.5 for (a) VIDEO A (b) VIDEO B and (c) VIDEO C.

(Figure 5.8). The sensitivity and specificity of the classifier were evaluated using 10-fold cross-validation. The cross-validation was repeated 100 times; for each iteration, the data were shuffled to ensure different combinations of training and validation samples. Moreover, the AUCs were all slightly greater than that generated by the main Reference Method. In the worst case, the performance of the Reference method (based on the amended implementation and using an SVM classifier) was comparable to that of the Index method.

Although not the main subject of this work, I investigated the performance of the Index method as the size of the data increased. In other words data from two or more videos were combined (serialised). However, the results showed that the separation between the groups did not improve. For example, when combining data from VIDEO A and VIDEO B, the AUC was 0.76 (95% CI 0.72–0.80). This suggests that the extracted eye movement features can achieve only limited separation performance and adding more data does not improve the separation.

It is also worth highlighting that the AUC for the main Reference method was 0.65 (95% CI 0.61–0.69) using Naïve Bayes classifier and 0.70 (95% CI 0.66–0.74) using an SVM classifier. Both values are smaller than the result reported in Crabb et al. (2014) (AUC of 0.85 (95% CI 0.82–0.87)). The difference in the results was likely due to differences in the KPCA analysis, as discussed in the *Methods* section 5.3.2.

5.5 Discussion

5.5.1 Significance of results

I have proposed a novel approach to analyse eye movements that uses the spatiotemporal characteristics of saccadic eye movements. Specifically, to analyse sequential saccadic movements, saccades were represented using tokens based on the size and direction of the saccades and were analysed using TF-IDF. This is a novel application of computational technique commonly used for searching for information in documents. Additional static features, based on the counts of saccadic eye movements and common eye movement features, such as mean saccade amplitude and mean fixation duration, were incorporated to train an SVM classifier. The classification results, based on repeated cross-validation, demonstrated reasonable separation between patients with glaucoma and healthy controls (AUC 0.78), compared to AUC = 0.63 using simple summary statistics (e.g., saccade amplitude) and AUC = 0.71 using a previous classification technique (Crabb et al., 2014). The results indicate that eye movements recorded with minimal input from patients whilst freely watching short (5 min) video

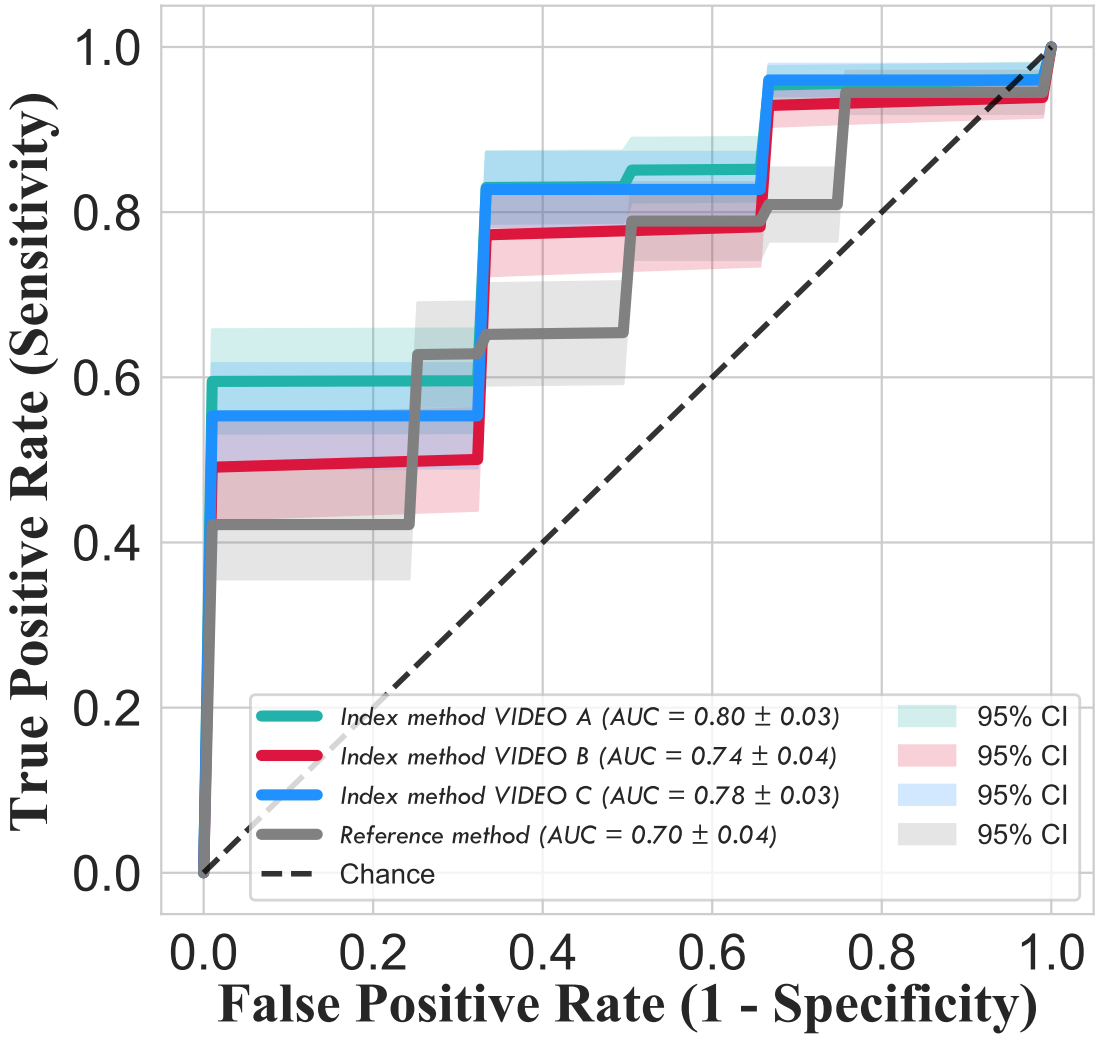

Figure 5.8: Evaluation of the proposed method (a) ROC curves for separation between controls and glaucoma patients for three video clips. For each video stimulus, 10-fold cross-validation was performed to evaluate the classifier, and this was repeated 100 times to estimate the mean and 95% CI of the sensitivity and the specificity of the classifier. The coloured ROCs represent results based on the Index method, while the grey ROC is based on the Reference method.

clips can provide some useful information regarding VF loss and support the original findings from Crabb et al. (2014).

The proposed method provides an easy means to combine sequential and static eye movements. The results of this method are promising and should be explored with eye movements of patients with other ophthalmic or neurodegenerative conditions. The proposed approach can also be used to analyse eye movements in behavioural studies Hoppe et al. (2018).

5.5.2 Prior work on using machine learning classifiers to analyse eye movements

Features analysed from natural eye movements coupled with saliency features of a video stimulus have been shown to separate patients with Parkinson's disease from healthy controls (Tseng et al., 2013). Other studies have shown that eye movements could be analysed using machine learning classifiers to separate patients with Alzheimer's disease from age-similar healthy controls. In a different application, Coutrot et al. (2018) analysed fixations using HMM to classify the task at hand and the presence/absence of soundtrack video stimuli, while another study by similar authors (Coutrot et al., 2016) used them to classify the gender of the participants (i.e., female and male). However, HMM is only effective when there is a distinct region of interest in the stimuli, such as in static images, so it would be challenging to apply HMM to classify eye movements from watching videos where regions of interest move across time. Furthermore, unlike my method, the proposed HMM approach in Coutrot et al. (2018) was based only on fixation features and did not account for saccadic movements. Furthermore, HMM cannot model gaze information past previous fixations, whereas the proposed approach can account long temporal periods of saccadic movements by varying the length of n-gram features, as well as by considering a selected number of saccadic sequences. For example, it is possible to analyse two or three successive saccadic movements.

In terms of eye movement data analysis, my proposed approach is similar to methods proposed by Hoppe et al. (2018) and Bulling et al. (2010) that used scanpaths to classify personality traits and activities, respectively. The authors extracted features based on common eye movement features and sequences of saccadic movements. However, the features extracted were based on a coarse representation of saccadic movements (from 24 possible saccadic movements) and count statistics were used to extract sequential movements; in contrast, in this study, a dense representation of saccadic movements (156 possible movements) was used, and the sequential movements were analysed using a TF-IDF to identify the most discriminative sequential movements.

5.5.3 Effect of video content

When inspecting the raw eye tracking data, it was notable that multiple participants often exhibited similar eye movements when watching the same video and the same participants exhibited dissimilar eye movements when watching different videos. This was borne out both by conventional and more advanced summary statistics, as has been reported previously, including in Chapter 4 of this thesis. Dorr et al. (2010) also reported that eye movement parameters, such as saccade amplitude and fixation

duration, vary depending on the video content. This indicates the strong effect of the content (bottom-up factor) on eye movements in free-viewing tasks. One possible factor that elicits similar eye movements while watching videos is the motion cue, causing people to look at the same location at the same time (Dorr et al., 2010; Wang et al., 2012). Other evidence showed that certain features of Hollywood-style films, described as the 'tyranny of film', contribute largely to where people fixate (Carmi and Itti, 2006b; Mital et al., 2011; Loschky et al., 2015). Furthermore, socially relevant cues such as faces, especially talking faces, and body movement also serve as powerful predictors of eye movements (Birmingham et al., 2008; Coutrot and Guyader, 2014).

5.5.4 Potential limitations and future work

The novel spatiotemporal analysis did not consistently perform well across the videos. Using only the sequential features, the separation between the two groups was better when participants viewed VIDEO A and VIDEO B when compared to VIDEO C. In addition, whilst my approach separated the two groups well, the analysis suffers from a lack of interpretability, that is, the analysis did not reveal which static or sequential eye movement features were crucial in discriminating between groups. Finally, the proposed approach was evaluated on a limited number of patients with glaucoma and controls, thus it might not have covered the entire extent of the VF profile. Furthermore, the present work has focused on the method of analysis, but future studies need to think carefully about the type of video content.

Other improvements could be afforded by considering the effect of centre biases when watching videos. Future studies could develop methods that exclude saccadic movements caused by centre biases, perhaps by detecting temporal locations of scene cuts in clips. Future studies could develop methods that exclude saccadic movements caused by centre biases, perhaps by detecting temporal locations of scene cuts on the clips. Another alternative would be to analyse eye movements using deep learning techniques (Rahimy, 2018; De Fauw et al., 2018), possibly by first representing saccadic movements in the Cartesian plane and analysing them using 2D-convolutional neural networks or by analysing sequences of saccades and/or fixations using 1D-convolutional neural networks or recurrent neural networks.

In conclusion, I have demonstrated the potential and feasibility of properly designed eye movement feature analysis and machine learning classification methods to separate patients with glaucomatous VF loss from age-similar healthy controls.

Chapter 6

Overview and future work

At present, standard automated perimetry (SAP) is the gold standard measure of VF loss for the diagnosis and monitoring of glaucoma. Simply put, SAP requires patients to press a button in response to a small flashing light presented at different locations across their field of view. Throughout the test — which typically last around 5—10 minutes per eye — the patient must fixate on a central target and keep their perfectly head still. This test is challenging to perform and expensive to administer. Furthermore, it is only available in eye clinics, and one of the key problems with glaucoma is that people are often unaware in the early stages that they have it. Ideally a simpler, cheaper way of detecting VF loss is needed, which could potentially be used at home or in community settings.

My thesis is that glaucomotous VF loss can be detected from natural eye movements, recorded while an individual watched movies or looked at a picture. What follows is a short overview of the main findings of the four chapters, followed by a summary of the novel contributions described in this thesis and a brief discussion on ideas for future research.

Chapter 2 reviewed the literature on the eye movements of patients with glaucoma. The aim was to summarise the literature and to explore how eye movements were analysed. Peer-reviewed studies on this subject were systemically searched and screened. Results from the 26 reviewed studies indicated that eye movements were altered due to VF loss while performing daily tasks, such as reading, driving, doing a visual search, watching videos and looking at pictures. However, the extent to which eye movements were altered in the presence of glaucoma is unclear due to inconsistent results across different studies. The incompatible results may have arisen due to differences in the design of the experiments, or inconsistent data analysis techniques. The review

indicated that there is likely a need for standard tools to pre-process and analyse eye movement data.

The purpose of chapter 3 was to measure the pure, perceptual effect of VF loss on eye movements by comparing eye-movements within subject, in individuals with asymmetric sight loss (thereby controlling for cognitive factors). Patients viewed 120 pictures in the form of a slide show, with each picture displayed for an average of three seconds. The results of this study showed that eye movements were altered by worsening of VF loss. Specifically, compared to the eye movements of the better eye, the worse eye exhibited shorter saccade size, a smaller spread of fixations and a higher rate of saccade reversals – the latter being a novel parameter. Furthermore, there was a correlation between the between-eye differences in the BCEA and the differences in the MD, while the differences in SRR were correlated with differences in visual acuity. These results suggest that the natural eye movements of patients with glaucoma could be related to the associated functional deficits. The results from this study supported my thesis that the monitoring of natural eye movements could be developed as a cheap and easy-to-obtain biomarker of VF loss.

The study in Chapter 4 assessed the effect of simulated (artificial) glaucomatous VF loss on natural eye movements. The study aimed to explore further whether altered eye movements due to VF loss are sufficiently robust to be clinically practical. For this, a gaze-contingent simulated VF loss paradigm was used, in which participants experienced a variable magnitude of simulated VF loss (moderate and advanced glaucoma), based on longitudinal data from a real glaucoma patient. I investigated measures of eye-movement, including saccade amplitude, the spread of saccade endpoints (measured using the bivariate contour ellipse area), the location of saccade landing positions and the similarity between fixation locations among participants (quantified using kernel density estimation). The data showed that eye movements are altered following the onset of simulated VF loss, but these measures—alone or in combination—had only limited sensitivity and specificity. This suggests that these measures of natural eye-movements alone are insufficient to be of clinical utility. To better detect VF loss from natural eye movements, future studies are warranted to develop more precise measures, or to consider how eye-movement metrics may be combined with other sources of information (e.g., demographic data, or other clinical data).

Chapter 5 curated and analysed a previously collected dataset of the eye movements from 46 glaucomatous patients and 32 age-similar visually healthy controls (data originally introduced in Crabb et al. (2014)). Importantly this makes the data freely available for others to use. Eye movements were recorded while participants passively

viewed three separate video clips. I aimed to improve previously reported results by developing a more advanced approach to analyse spatiotemporal saccadic sequences. Static and sequential eye movement features were extracted to train a support vector machine classifier. The proposed eye movement analysis approach separated glaucoma patients from age-similar healthy controls with better accuracy than the approach proposed previously by Crabb et al. (2014). It also out-performed more simple methods based on conventional eye-movement metrics. The results suggested that more powerful classification techniques such as the Index method introduced here could be used to further improve the passive detection of glaucomatous VF loss.

6.1 Update to systematic review

The original review literature search was conducted in June 2018. In order to identify any new and relevant work appearing since then, the search was replicated on 22nd May 2020. An additional two studies meeting inclusion criteria described in Chapter 2 were identified. The first study Lee et al. (2019) investigated eye movement behaviour of thirty-one drivers with glaucoma and twenty-five age-matched controls while performing DriveSafe test (reporting objects in real world driving scene images). Drivers with glaucoma made significantly more errors in identifying items in the scene, fixated on road users for shorter durations, and exhibited smaller saccades compared with controls. The authors concluded that patients with glaucoma have difficulty identifying objects in their visual scene. The second paper described a study of spatial allocation of eye movements in a panoramic driving simulator in eight drivers with glaucoma and five with suspected glaucoma (Anderson et al., 2019). Their results showed that drivers with larger binocular VF loss showed more restricted, spatially biased eye movements and this bias was more increased by increase in task load. They speculated that these differences reflect compensatory behaviours in drivers with glaucomatous visual fields.

6.2 Thesis contributions

The main contributions of the work in this thesis can be summarised as follows:

- A review of the literature regarding the eye movements of patients with glaucoma, with particular emphasis on highlighting current gaps in understanding (Chapter 2).
- The development and application of a novel summary statistic, based on the geometric relationship between temporal sequences of saccades (SRR). SRR was

able to separate the worse eye from the better eye, and this was correlated with differences in visual acuity between the two eyes (Chapter 3).

- Confirmatory evidence that saccade amplitude and the spread of fixations are reduced by worsening in VF loss. The change in the measure of the spread of fixation was correlated with worsening in VF mean deviation (Chapter 3).
- Empirical evidence that worsening in artificial (simulated)VF loss can be detected from natural eye movements and whether these changes can be used as clinical biomarkers for VF loss (Chapter 4).
- The development and application of a novel measure of consistency in eye movements between subjects when watching videos using KDE analysis. This novel measure revealed the similarity in fixational eye movements when watching videos regardless of the VF loss condition (Chapter 4).
- The development and application of a novel analysis of eye movements based on spatiotemporal saccadic movements to detect glaucoma from natural eye movements. The proposed method was able to detect glaucoma consistently across three videos and showed better separation performance than previously proposed approaches (Chapter 5).

6.3 Limitations and future work

Specific ideas to develop the findings in each chapter are discussed in the respective chapters. In contrast, the following ideas arise from the body of work as a whole.

Chapter 3 demonstrated that individuals with asymmetric glaucomatous VF loss made altered eye movements in their worse eye compared to their better eye whilst they viewed pictures. However, as discussed in Section 1.3.2, eye movements are can be affected by several other, non-perceptual factors such as age, cognitive skill, gender, and individual interests. It may be that in practice these non-perceptual factors occlude the eye-health 'fingerprint' that we primarily wish to measure. Future studies, therefore, should focus to detect VF loss from eye movements recorded while looking at pictures by comparing between subjects.

In Chapters 4 and 5, eye movements were recorded binocularly. Although measuring binocular eye movements is simple, quick, and provides the 'real-life' experience, detecting mild and moderate VF loss from binocular measurement may be challenging, since glaucomatous VF loss is often asymmetric. Furthermore, it is less clear how the visual system adapts to functional loss in glaucoma to compensate for the missing visual information when viewing binocularly. Therefore, future studies could further assess monocular natural eye movements.

The results in Chapter 5 showed that eye movements recorded for as little as three minutes can detect glaucoma with some accuracy. However, the average person in the UK spends several hours a day watching TV (and even longer looking at screens in general (Scholes et al., 2013)). To improve the reliability of detection accuracy, future studies should therefore consider larger datasets, including extended period of at-home viewing. One might also consider looking at additional eye movement metrics based on simple tasks such as visual search.

In this thesis, the aim was to separate patients with glaucoma from controls using eye movements. For many clinical purposes, however, one would ideally want to know the location and severity of the VF loss, and this should be a subject of future studies, for example, comparing natural eye movements between eyes with moderate and mild VF loss.

In Chapter 3 and 5, patients with preserved, corrected binocular visual acuity of at least 0.18 logMAR (Snellen equivalent of 6/9) were recruited. However, it is not uncommon for peripheral loss to be accompanied with central visual impairments (Chan et al., 2015). Future work, therefore, should investigate the generalisability of these results on those patients who have poor VA.

Similarly, the performance of BCEA was relatively limited for the dataset presented in Chapter 5 compared to the dataset in Chapter 4. This discrepancy could be attributed to experimental design differences. Specifically, the eye movements in Chapter 4 were based on artificial scotoma, while the data in Chapter 5 was from real patients. Overall, the results of analysing eye movements using SRR and BCEA can at least be described as encouraging, if not inconsistent in their effect; theyshould be validated on other cohorts of patients with glaucoma or other ophthalmic conditions.

The methods proposed in this thesis have the potential, after further refinement, to be developed into a device that assesses VF loss, particularly one that is portable, inexpensive and user-friendly. It is worth speculating more on this point. For example, such a tool would enable assessment of people who are hard-to-reach (because of their physical or mental conditions) or who are geographically distant (such as patients in developing counties). However, due to the low prevalence of glaucoma, targeting only for glaucoma during screening is likely not cost-effective (Momont and Mills, 2013). The proposed approach, therefore, ought to be extended to target other eye conditions such as age-related macular degeneration (AMD). This is the subject of future study. To start test this hypothesis, Figure 6.1 shows that eye movement data of 29 patients with dry AMD whose eye movements were recorded and analysed following the same

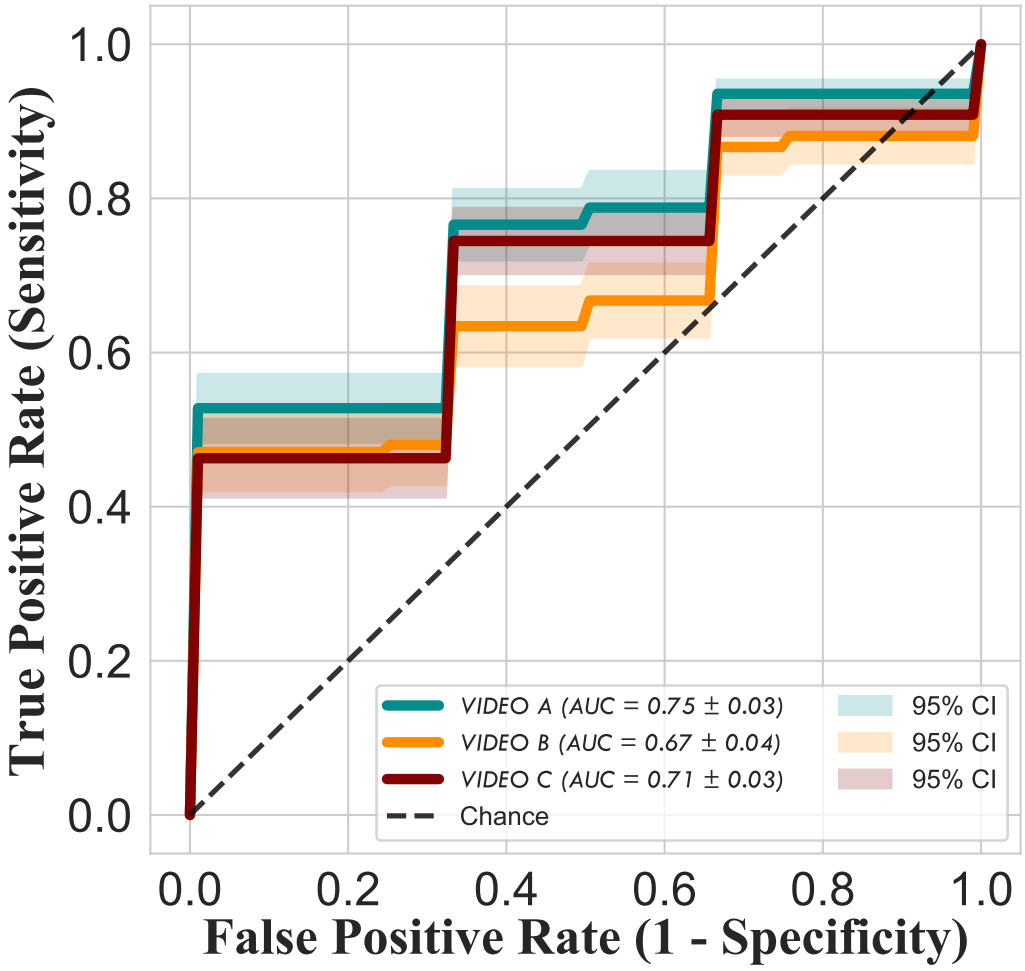

Figure 6.1: ROC curves and the AUC scores showing the separation between glaucoma and AMD combined vs. control groups using the proposed Index method for the three videos described in Chapter 5.

procedure described in Chapter 5.

The results showed that the method proposed in Chapter 5 could separate patients with AMD from the controls with reasonable accuracy (Figure 6.1). Although only preliminary work, this is encouraging as it suggests that the methods that I have developed in this thesis for detecting glaucoma may by generalisable to other eye conditions.

In terms of analysis, to improve the accuracy of the separation between patients and controls, future studies could explore methods based on deep learning. Eye movements can be represented as two-dimensional data using centralised saccade representation (Chapter 5) and can be trained using convolutional neural networks. To mitigate overfitting, transfer learning methods ought to be explored.

Finally, the concept of using natural eye movements to detect and assess eye conditions is an appealing one. I hope this might provide a starting point for future studies that could realise the potential of this concept.

Appendix A

Images used for the experiment in Chapter 3

Figure A.1: All the 120 images used in the experiment. Images were presented sequentially in random order.

Appendix B

Supplemental material for Chapter 4

Figure B.1: Rank sum tests comparison results (statistics, p-value) between no VF loss and moderate and no VF loss and advanced in SA, BCEA, SLV and KDE probability scores. Statistically significant associations are marked with an asterisk and highlighted in bold.

		Saccade Amplitude (U ,P-value, η^2)	*BCEA (U, P-value, η^2)*	*SLV (U, P-value, η^2)*	*KDE Probability (U, P-value, η^2)*
No VF loss Vs Moderate	VIDEO **1**	**(144,0.33,0.03)**	**(163, 0.75, 0.01)**	**(81, 0.002, 0.22)**	**(72,0.002,0.26)**
	VIDEO **2**	**(112, 0.05, 0.11)**	**(103,0.03, 0.14)**	**(52,<0.001, 0.36)**	**(91, 0.01,0.18)**
	IMAGES	**(140, 0.28, 0.04)**	**(173,0.99,.004)**	**(175,0.37,0.003)**	**N/A**
No VF loss Vs Advanced	VIDEO **1**	**(79,0.003, 0.23)**	**(94,0.014, 0.17)**	**(141, 0.1, 0.04)**	**(111,0.05,.11)**
	VIDEO **2**	**(76, 0.003, 0.24)**	**(100,0.02, 0.15)**	**(130, 0.06, 0.07)**	**(120,0.09,.089)**
	IMAGES	**(68,0.001, 0.28)**	**(143, 0.33,0.04)**	**(145,0.12, 0.04)**	**N/A**

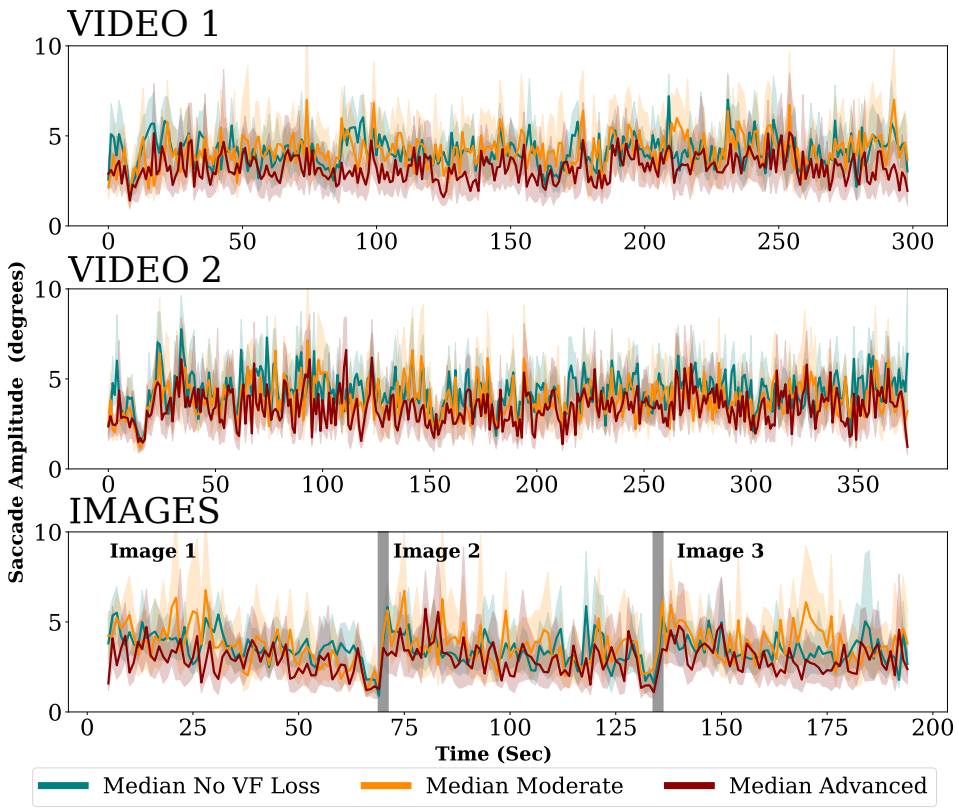

Figure B.2: Saccade amplitude function of time for VIDEO 1 and VIDEO 2 and IMAGES. For each participant in each group, the median saccade amplitude in every second was computed. The solid lines show the median values for each group. The shaded regions indicate the interquartile ranges.

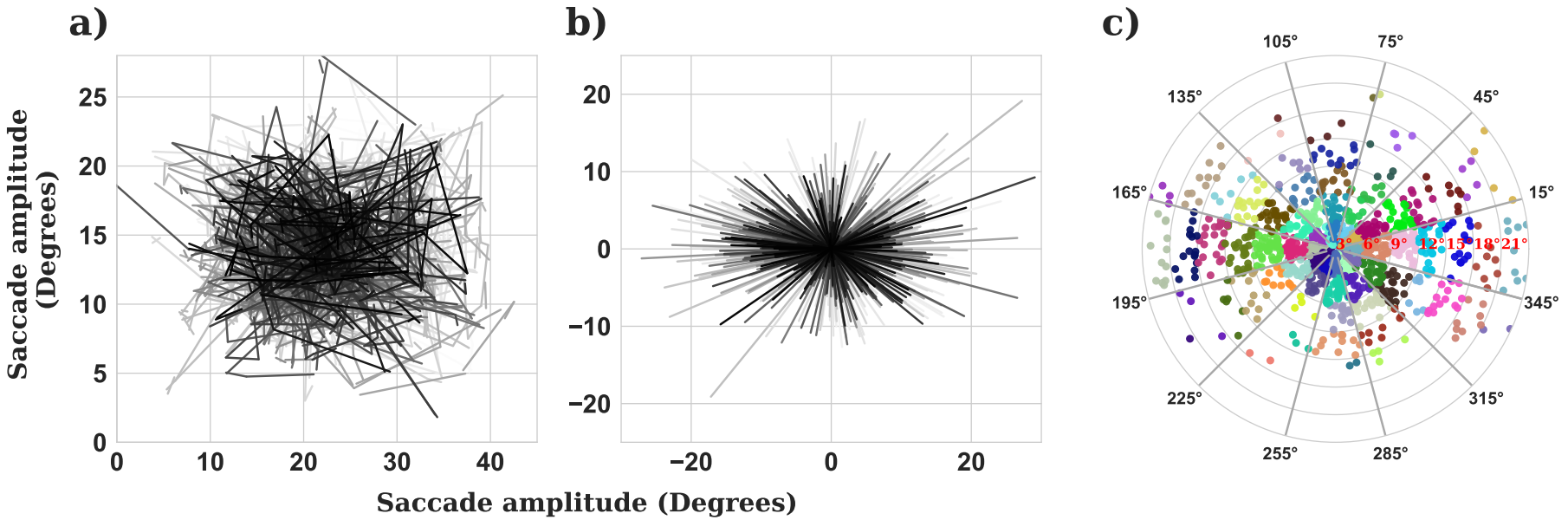

Figure B.3: Feature extraction from saccadic movements. (a) Example of a scanpath from a participant who watched VIDEO 2. (b) Each saccade is mapped to a new planned by setting their starting position to as(0,0) position. (c) Scatter plot of the end of the saccades in (b) shown in a polar plane. Saccades that landed in the same bin (sector) are shown using the same color. Histogram of the saccades both in the radial and angular directions are computed to extract the number of saccades landing in each bin. Each bin measures 3° (radial) and by 30° (angular). In total, there were 84 bins (resolution of seven in the radial direction and 12 in the angular direction). The extracted features represent the number of saccades that landed in each bin. For example, the first bin represents the saccades that were greater than 0° and less than 3° in amplitude and executed in a direction between 345° and 15°.

Appendix C

Supplemental material for Chapter 5

C.1 Analysis using summary eye movement measures for dataset in Chapter 5

Analysis using summary eye movement measures This section described analysis of the dataset described in Chapter 5 using summary statistics measures described in Chapters 3 and 4.

C.1.1 Saccade amplitude

As stated previously, saccade amplitude describes the size (in degrees visual angle) of the rapid eye movements that met the pre-defined 'saccadic' criteria (see data pre-processing), with the median value used as the summary measure for statistical analyses since the distribution of saccadic amplitudes is often non-Gaussian. One median saccade-amplitude value was computed per participant per video clip.

C.1.2 Saccade rate

As stated in a previous chapter, saccadic rate describes the average number of saccades made per second, with the mean value of the saccade rate used as the summary measure for statistical analyses. One mean saccade-rate value was computed per participant per video clip.

C.1.3 The spread of fixations: Bivariate contour ellipse area (BCEA)

As defined earlier, BCEA was computed to measure the spread of saccadic endpoints. To do this, the start of each saccade was translated to the centre (0,0) and the same transformation was applied to the corresponding saccade endpoint. This procedure of centralising saccades was described previously by Crabb et al. (2014). The BCEA was computed with a probability area of 95% and this process produced one BCEA value per participant per video clip.

C.1.4 Fixation duration

As described in before, fixation duration is the time (in milliseconds) between two successive saccades. The median value of fixation duration was used as the summary measure for statistical analyses since the distribution of fixation durations is often non-Gaussian. One median saccade amplitude value was computed per participant per video clip.

C.1.5 Kernel density estimate (KDE) of gaze fixations

This metric was computed, following a similar procedure proposed in chapter 4, as a way of classifying an observer as healthy or abnormal from their fixational eye movements. In other words, the KDE analysis measures the consistency between fixations of controls and patients, with a higher KDE score meaning the participant was looking in the same locations as most controls in each frame in the video. For controls, the KDE score was computed using a leave-one-out analysis. One KDE score value was computed per participant per video clip.

C.1.6 Saccadic reversal rate

This summary static measure was to measure the proportion of saccades that move in the opposite direction relative to the preceding saccade (see chapter 3). To calculate this rate, the angle between successive saccades was measured, with the saccadic reversal rate (SRR) being the proportion of angle differences that were between 165-195°. One SRR value was computed per person per video clip.

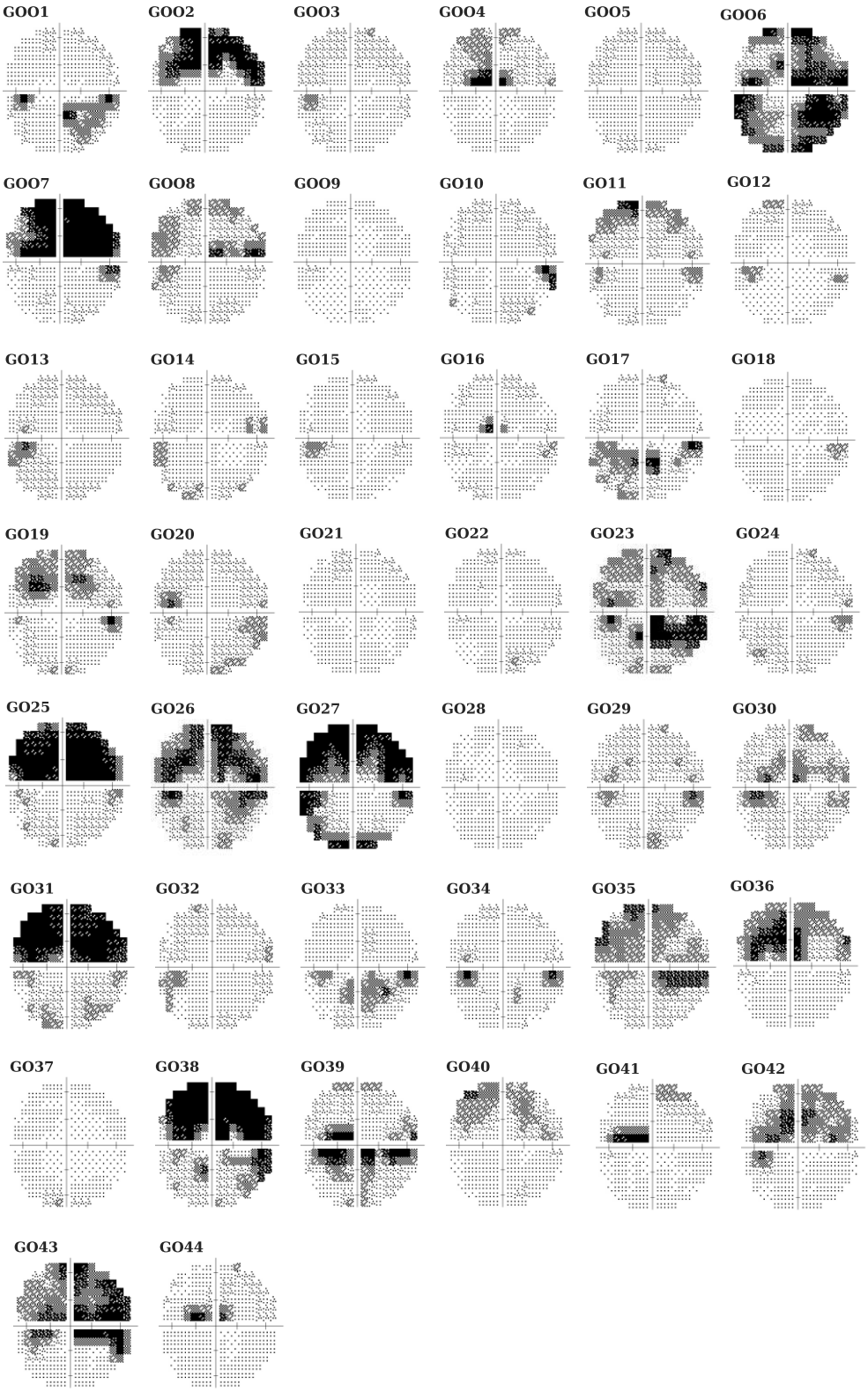

Figure C.1: Integrated VF (IVF) of the patients. IVF estimates of the binocular VF from the two monocular (left and right eye) VFs. The sensitivity values for each point in the IVF were computed by taking the maximum sensitivity from corresponding points in the left and right eye VFs. The IVF was generated with a bespoke computer program written in MATLAB (MATLAB R2017a (MathWorks, Inc., Natick, MA, USA).

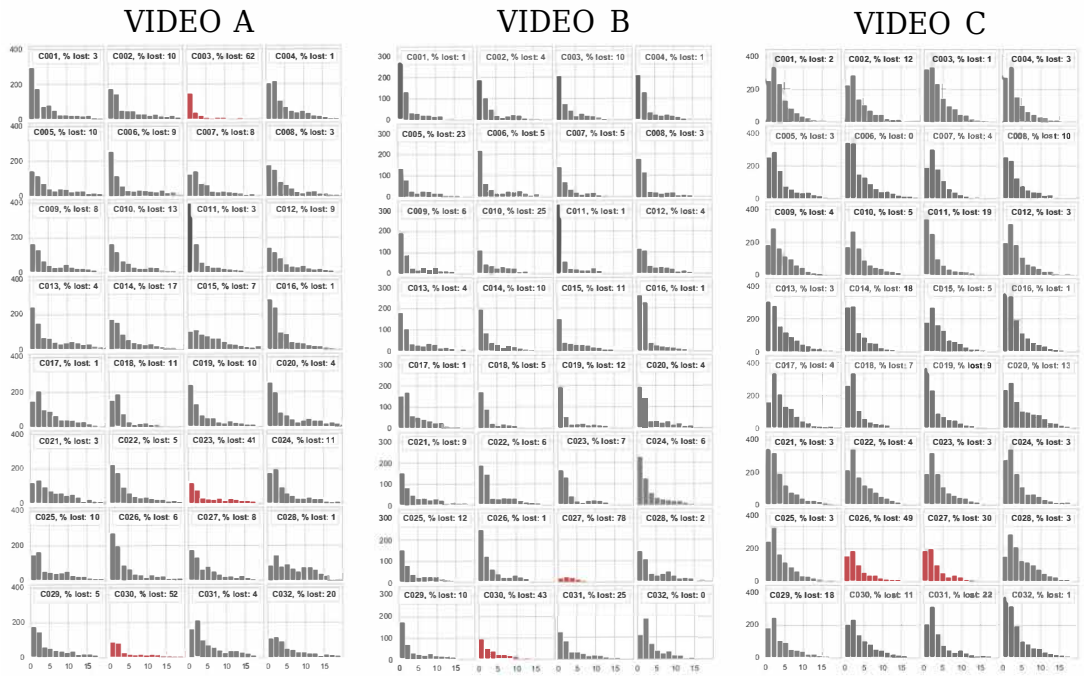

Figure C.2: Histogram of saccades for each video clip for each participant in the control group.

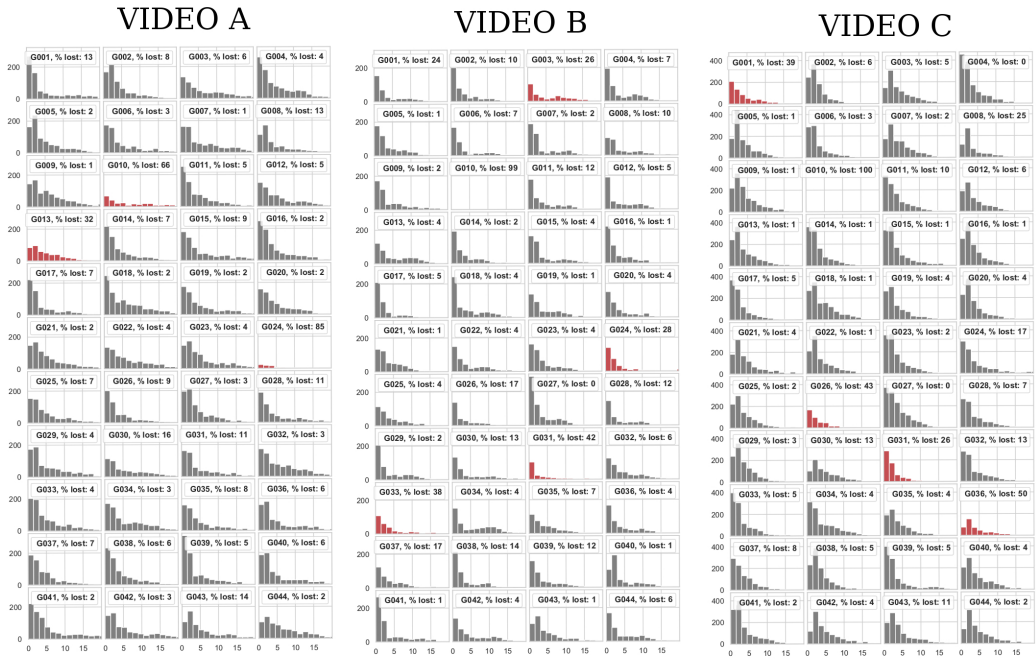

Figure C.3: Histogram of saccades for each video clip for each participant in the glaucoma group.

References

Akobeng, A. K. (2007). Understanding diagnostic tests 3: receiver operating characteristic curves. *Acta paediatrica*, 96(5):644–647.

Almutleb, E. S., Bradley, A., Jedlicka, J., and Hassan, S. E. (2018). Simulation of a central scotoma using contact lenses with an opaque centre. *Ophthalmic and physiological optics*, 38(1):76–87.

Altman, D. G. and Bland, J. M. (1994). Statistics notes: Diagnostic tests 2: predictive values. *Bmj*, 309(6947):102.

Amor, T. A., Reis, S. D., Campos, D., Herrmann, H. J., and Andrade Jr, J. S. (2016). Persistence in eye movement during visual search. *Scientific reports*, 6:20815.

Anderson, D., Ghate, D. A., Kedar, S., and Rizzo, M. (2019). Spatially biased eye movements in older drivers with glaucoma and visual field defects. In *Proceedings of the... international driving symposium on human factors in driver assessment, training and vehicle design*, volume 2019, pages 147–153. University of Iowa Public Policy Center.

Anderson, T. J. and MacAskill, M. R. (2013). Eye movements in patients with neurodegenerative disorders. *Nature reviews neurology*, 9(2):74.

Arden, G. and Jacobson, J. (1978). A simple grating test for contrast sensitivity: preliminary results indicate value in screening for glaucoma. *Investigative ophthalmology & visual science*, 17(1):23–32.

Arditi, A. (2005). Improving the design of the letter contrast sensitivity test. *Investigative ophthalmology & visual science*, 46(6):2225–2229.

Armstrong, T. and Olatunji, B. O. (2012). Eye tracking of attention in the affective disorders: A meta-analytic review and synthesis. *Clinical psychology review*, 32(8):704–723.

Asaoka, R., Crabb, D. P., Yamashita, T., Russell, R. A., Wang, Y. X., and Garway-Heath, D. F. (2011). Patients have two eyes!: binocular versus better eye visual field indices. *Investigative ophthalmology & visual science*, 52(9):7007–7011.

Asfaw, D. S., Jones, P. R., Mönter, V. M., Smith, N. D., and Crabb, D. P. (2018a). Does glaucoma alter eye movements when viewing images of natural scenes? a between-eye study. *Investigative ophthalmology & visual science*, 59(8):3189–3198.

Asfaw, D. S., Jones, P. R., Smith, N. D., and Crabb, D. P. (2018b). Data on eye movements in people with glaucoma and peers with normal vision. *Data in brief*.

Åsman, P. and Heijl, A. (1992). Glaucoma hemifield test: automated visual field evaluation. *Archives of ophthalmology*, 110(6):812–819.

Baddeley, R. J. and Tatler, B. W. (2006). High frequency edges (but not contrast) predict where we fixate: A bayesian system identification analysis. *Vision research*, 46(18):2824–2833.

Bahill, A. T. and Stark, L. (1975). The high-frequency burst of motoneuronal activity lasts about half the duration of saccadic eye movements. *Mathematical biosciences*, 26(3-4):319–323.

Bailey, I. L. and Lovie, J. E. (1976). New design principles for visual acuity letter charts. *American journal of optometry and physiological optics*, 53(11):740–745.

Bailey, I. L. and Lovie-Kitchin, J. E. (2013). Visual acuity testing. from the laboratory to the clinic. *Vision research*, 90:2–9.

Bair, W. and O'keefe, L. P. (1998). The influence of fixational eye movements on the response of neurons in area mt of the macaque. *Visual neuroscience*, 15(4):779–786.

Ballard, D. H., Hayhoe, M. M., and Pelz, J. B. (1995). Memory representations in natural tasks. *Journal of cognitive neuroscience*, 7(1):66–80.

Bambo, M. P., Ferrandez, B., Güerri, N., Fuertes, I., Cameo, B., Polo, V., Larrosa, J. M., and Garcia-Martin, E. (2016). Evaluation of contrast sensitivity, chromatic vision, and reading ability in patients with primary open angle glaucoma. *Journal of ophthalmology*, 2016.

Barkan, O. (1938). Glaucoma: Classification, causes, and surgical control*: Results of microgonioscopic research. *American journal of ophthalmology*, 21(10):1099–1117.

Barth, E., Zetzsche, C., and Rentschler, I. (1998). Intrinsic two-dimensional features as textons. *Optical society of america*, 15(7):1723–1732.

Beel, J., Gipp, B., Langer, S., and Breitinger, C. (2016). paper recommender systems: a literature survey. *International Journal on Digital Libraries*, 17(4):305–338.

Bellmann, C., Feely, M., Crossland, M. D., Kabanarou, S. A., and Rubin, G. S. (2004). Fixation stability using central and pericentral fixation targets in patients with age-related macular degeneration. *Ophthalmology*, 111(12):2265–2270.

Bennett, C. R., Bex, P. J., Bauer, C. M., and Merabet, L. B. (2019). The assessment of visual function and functional vision. In *Seminars in pediatric neurology*, volume 31, pages 30–40. Elsevier.

Bergstra, J. and Bengio, Y. (2012). Random search for hyper-parameter optimization. *Journal of machine learning research*, 13(Feb):281–305.

Bertera, J. H. and Rayner, K. (2000). Eye movements and the span of the effective stimulus in visual search. *Perception & psychophysics*, 62(3):576–585.

Beurskens, R. and Bock, O. (2012). Age-related decline of peripheral visual processing:

the role of eye movements. *Experimental brain research*, 217(1):117–124.

Biddyr, S. and Jones, A. (2015). Preventing sight loss in older people. a qualitative study exploring barriers to the uptake of regular sight tests of older people living in socially deprived communities in south wales. *Public Health*, 129(2):110–116.

Bindemann, M. (2010). Scene and screen center bias early eye movements in scene viewing. *Vision research*, 50(23):2577–2587.

Birmingham, E., Bischof, W. F., and Kingstone, A. (2008). Social attention and real-world scenes: The roles of action, competition and social content. *Quarterly journal of experimental psychology*, 61(7):986–998.

Black, A. A., Wood, J. M., and Lovie-Kitchin, J. E. (2011). Inferior visual field reductions are associated with poorer functional status among older adults with glaucoma. *Ophthalmic and physiological optics*, 31(3):283–291.

Bossuyt, P. M., Reitsma, J. B., Bruns, D. E., Gatsonis, C. A., Glasziou, P. P., Irwig, L. M., Lijmer, J. G., Moher, D., Rennie, D., and De Vet, H. C. (2003). Towards complete and accurate reporting of studies of diagnostic accuracy: the stard initiative. *Radiology*, 226(1):24–28.

Bowers, A., Peli, E., Elgin, J., McGWIN Jr, G., and Owsley, C. (2005). On-road driving with moderate visual field loss. *Optometry and vision science*, 82(8):657–667.

Brandt, J. D., Beiser, J. A., Kass, M. A., and Gordon, M. O. (2001). Central corneal thickness in the ocular hypertension treatment study (ohts). *Ophthalmology*, 108(10):1779–1788.

Brouwer, A.-M., Franz, V. H., and Gegenfurtner, K. R. (2009). Differences in fixations between grasping and viewing objects. *Journal of Vision*, 9(1):18–18.

Brown, P., de Souza, P., and Mercer, R. (1992). Della pietra, v., lai. *J.,"Class-based n-gram models of natural language.", Computational linguistics*, 467479.

Brusini, P. and Filacorda, S. (2006). Enhanced glaucoma staging system (gss 2) for classifying functional damage in glaucoma. *Journal of glaucoma*, 15(1):40–46.

Budenz, D. L., Rhee, P., Feuer, W. J., McSoley, J., Johnson, C. A., and Anderson, D. R. (2002). Sensitivity and specificity of the swedish interactive threshold algorithm for glaucomatous visual field defects. *Ophthalmology*, 109(6):1052–1058.

Buhmann, M. D. (2003). *Radial basis functions: theory and implementations*, volume 12. Cambridge university press.

Bulling, A., Ward, J. A., Gellersen, H., and Tröster, G. (2009). Eye movement analysis for activity recognition. In *Proceedings of the 11th international conference on Ubiquitous computing*, pages 41–50. ACM.

Bulling, A., Ward, J. A., Gellersen, H., and Troster, G. (2010). Eye movement analysis for activity recognition using electrooculography. *IEEE transactions on pattern analysis and machine intelligence*, 33(4):741–753.

Bulling, A., Ward, J. A., Gellersen, H., and Troster, G. (2011). Eye movement analysis for

activity recognition using electrooculography. *IEEE transactions on pattern analysis and machine intelligence*, 33(4):741–753.

Burton, R., Saunders, L. J., and Crabb, D. P. (2015). Areas of the visual field important during reading in patients with glaucoma. *Japanese journal of ophthalmology*, 59(2):94–102.

Burton, R., Smith, N. D., and Crabb, D. P. (2014). Eye movements and reading in glaucoma: observations on patients with advanced visual field loss. *Graefe's Archive for Clinical and Experimental Ophthalmology*, 252(10):1621–1630.

Busswell, G. (1935). How people look at pictures: A study of the psychology of perception in art.

Butt, T., Crossland, M. D., West, P., Orr, S. W., and Rubin, G. S. (2015). Simulation contact lenses for amd health state utility values in nice appraisals: A different reality. *British journal of ophthalmology*, 99(4):540–544.

Button, K. S., Ioannidis, J. P., Mokrysz, C., Nosek, B. A., Flint, J., Robinson, E. S., and Munafò, M. R. (2013). Power failure: why small sample size undermines the reliability of neuroscience. *Nature reviews neuroscience*, 14(5):365–376.

Cajar, A., Engbert, R., and Laubrock, J. (2016). Spatial frequency processing in the central and peripheral visual field during scene viewing. *Vision Research*, 127:186–197.

Carmi, R. and Itti, L. (2006a). The role of memory in guiding attention during natural vision. *Journal of vision*, 6(9):4–4.

Carmi, R. and Itti, L. (2006b). Visual causes versus correlates of attentional selection in dynamic scenes. *Vision research*, 46(26):4333–4345.

Casson, R. J., Chidlow, G., Wood, J. P., Crowston, J. G., and Goldberg, I. (2012). Definition of glaucoma: clinical and experimental concepts. *Clinical & experimental ophthalmology*, 40(4):341–349.

Cello, K. E., Nelson-Quigg, J. M., and Johnson, C. A. (2000). Frequency doubling technology perimetry for detection of glaucomatous visual field loss. *American journal of ophthalmology*, 129(3):314–322.

Cerf, M., Frady, E. P., and Koch, C. (2009). Faces and text attract gaze independent of the task: Experimental data and computer model. *Journal of vision*, 9(12):10–10.

Cerulli, A., Cesareo, M., Ciuffoletti, E., Montanaro, M. L., Mancino, R., Mirisola, C., Sorge, R., Cedrone, C., Nucci, C., and Cerulli, L. (2014). Evaluation of eye movements pattern during reading process in patients with glaucoma: a microperimeter study. *European journal of ophthalmology*, 24(3):358–363.

Chan, E. W., Chiang, P. P., Liao, J., Rees, G., Wong, T. Y., Lam, J. S., Aung, T., and Lamoureux, E. (2015). Glaucoma and associated visual acuity and field loss significantly affect glaucoma-specific psychosocial functioning. *Ophthalmology*, 122(3):494–501.

Chan, M. P., Broadway, D. C., Khawaja, A. P., Yip, J. L., Garway-Heath, D. F., Burr, J. M.,

Luben, R., Hayat, S., Dalzell, N., Khaw, K.-T., et al. (2017). Glaucoma and intraocular pressure in epic-norfolk eye study: cross sectional study. *bmj*, 358:j3889.

Cheong, A. M., Geruschat, D. R., and Congdon, N. (2008). Traffic gap judgment in people with significant peripheral field loss. *Optometry and vision science*, 85(1):26–36.

Cherici, C., Kuang, X., Poletti, M., and Rucci, M. (2012). Precision of sustained fixation in trained and untrained observers. *Journal of Vision*, 12(6):31–31.

Chuk, T., Chan, A. B., and Hsiao, J. H. (2017). Is having similar eye movement patterns during face learning and recognition beneficial for recognition performance? evidence from hidden markov modeling. *Vision research*, 141:204–216.

Coeckelbergh, T. R., Brouwer, W. H., Cornelissen, F. W., Van Wolffelaar, P., and Kooijman, A. C. (2002). The effect of visual field defects on driving performance: a driving simulator study. *Archives of ophthalmology*, 120(11):1509–1516.

Coleman, A. L., Cummings, S. R., Yu, F., Kodjebacheva, G., Ensrud, K. E., Gutierrez, P., Stone, K. L., Cauley, J. A., Pedula, K. L., Hochberg, M. C., et al. (2007). Binocular visual-field loss increases the risk of future falls in older white women. *Journal of the American Geriatrics Society*, 55(3):357–364.

Collewijn, H., Van der Mark, F., and Jansen, T. (1975). Precise recording of human eye movements. *Vision research*.

Cook, C. and Foster, P. (2012). Epidemiology of glaucoma: what's new? *Canadian journal of ophthalmology*, 47(3):223–226.

Cornelissen, F. W., Bruin, K. J., and Kooijman, A. C. (2005). The influence of artificial scotomas on eye movements during visual search. *Optometry and vision science*, 82(1):27–35.

Cornia, M., Baraldi, L., Serra, G., and Cucchiara, R. (2016). A deep multi-level network for saliency prediction. In *2016 23rd International conference on pattern recognition (ICPR)*, pages 3488–3493. IEEE.

Cornia, M., Baraldi, L., Serra, G., and Cucchiara, R. (2018). Predicting human eye fixations via an lstm-based saliency attentive model. *IEEE Transactions on Image Processing*, 27(10):5142–5154.

Cortes, C. and Vapnik, V. (1995). Support-vector networks. *Machine learning*, 20(3):273–297.

Coutrot, A., Binetti, N., Harrison, C., Mareschal, I., and Johnston, A. (2016). Face exploration dynamics differentiate men and women. *Journal of vision*, 16(14):16–16.

Coutrot, A. and Guyader, N. (2014). How saliency, faces, and sound influence gaze in dynamic social scenes. *Journal of vision*, 14(8):5–5.

Coutrot, A., Hsiao, J. H., and Chan, A. B. (2018). Scanpath modeling and classification with hidden markov models. *Behavior research methods*, 50(1):362–379.

Crabb, D. P., Fitzke, F., Hitchings, R., and Viswanathan, A. (2004). A practical approach to measuring the visual field component of fitness to drive. *British journal of*

ophthalmology, 88(9):1191–1196.

Crabb, D. P., Smith, N. D., Glen, F. C., Burton, R., and Garway-Heath, D. F. (2013). How does glaucoma look?: patient perception of visual field loss. *Ophthalmology*, 120(6):1120–1126.

Crabb, D. P., Smith, N. D., Rauscher, F. G., Chisholm, C. M., Barbur, J. L., Edgar, D. F., and Garway-Heath, D. F. (2010). Exploring eye movements in patients with glaucoma when viewing a driving scene. *Plos one*, 5(3):e9710.

Crabb, D. P., Smith, N. D., and Zhu, H. (2014). What's on tv? detecting age-related neurodegenerative eye disease using eye movement scanpaths. *Frontiers in aging neuroscience*, 6:312.

Crabb, D. P. and Viswanathan, A. C. (2005). Integrated visual fields: a new approach to measuring the binocular field of view and visual disability. *Graefe's archive for clinical and experimental ophthalmology*, 243(3):210–216.

Crabb, D. P., Viswanathan, A. C., McNaught, A. I., Poinoosawmy, D., Fitzke, F. W., and Hitchings, R. A. (1998). Simulating binocular visual field status in glaucoma. *British journal of ophthalmology*, 82(11):1236–1241.

Crane, H. D. (2018). The purkinje image eyetracker, image stabilization, and related forms of stimulus manipulation. In *Visual science and engineering*, pages 37–63. CRC Press.

Crouzet, S. M., Kirchner, H., and Thorpe, S. J. (2010). Fast saccades toward faces: face detection in just 100 ms. *Journal of vision*, 10(4):16–16.

Dalmaijer, E. S., Mathôt, S., and Van der Stigchel, S. (2014). Pygaze: An open-source, cross-platform toolbox for minimal-effort programming of eyetracking experiments. *Behavior research methods*, 46(4):913–921.

David, E. J., Le Callet, P., Perreira Da Silva, M., and Lebranchu, P. (2018). How are ocular behaviours affected by central and peripheral vision loss? a study based on artificial scotomas and gaze-contingent paradigm. *Electronic imaging*, 2018(14):1–6.

David, E. J., Lebranchu, P., Da Silva, M. P., and Le Callet, P. (2019). Predicting artificial visual field losses: a gaze-based inference study. *Journal of Vision*, 19(14):22–22.

Davis, B. M., Crawley, L., Pahlitzsch, M., Javaid, F., and Cordeiro, M. F. (2016). Glaucoma: the retina and beyond. *Acta neuropathologica*, 132(6):807–826.

Davis, J. R. and Shackel, B. (1960). Changes in the electro-oculogram potential level. *The British journal of ophthalmology*, 44(10):606.

De Fauw, J., Ledsam, J. R., Romera-Paredes, B., Nikolov, S., Tomasev, N., Blackwell, S., Askham, H., Glorot, X., O'Donoghue, B., Visentin, D., et al. (2018). Clinically applicable deep learning for diagnosis and referral in retinal disease. *Nature medicine*, 24(9):1342–1350.

Deco, G. and Rolls, E. T. (2004). A neurodynamical cortical model of visual attention and invariant object recognition. *Vision research*, 44(6):621–642.

Delabarre, E. B. (1898). A method of recording eye-movements. *The American journal of psychology*, 9(4):572–574.

Dielemans, I., Vingerling, J. R., Wolfs, R. C., Hofman, A., Grobbee, D. E., and de Jong, P. T. (1994). The prevalence of primary open-angle glaucoma in a population-based study in the netherlands: the rotterdam study. *Ophthalmology*, 101(11):1851–1855.

Ditchburn, R. and Ginsborg, B. (1952). Vision with a stabilized retinal image. *Nature*, 170(4314):36–37.

Dive, S., Rouland, J. F., Lenoble, Q., Szaffarczyk, S., McKendrick, A. M., and Boucart, M. (2016). Impact of peripheral field loss on the execution of natural actions: a study with glaucomatous patients and normally sighted people. *Journal of glaucoma*, 25(10):e889–e896.

Dodge, R. and Cline, T. S. (1901). The angle velocity of eye movements. *Psychological Review*, 8(2):145.

Dorr, M., Martinetz, T., Gegenfurtner, K. R., and Barth, E. (2010). Variability of eye movements when viewing dynamic natural scenes. *Journal of vision*, 10(10):28–28.

Dorr, M., Vig, E., and Barth, E. (2012). Eye movement prediction and variability on natural video data sets. *Visual cognition*, 20(4-5):495–514.

Duchowski, A. T. (2007). Eye tracking methodology. *Theory and practice*, 328(614):2–3.

Duchowski, A. T. (2017). Diversity and types of eye tracking applications. In *Eye Tracking Methodology*, pages 247–248. Springer.

Dueker, D. K., Singh, K., Lin, S. C., Fechtner, R. D., Minckler, D. S., Samples, J. R., and Schuman, J. S. (2007). Corneal thickness measurement in the management of primary open-angle glaucoma: a report by the american academy of ophthalmology. *Ophthalmology*, 114(9):1779–1787.

Eggert, T. (2007). Eye movement recordings: methods. In *Neuro-Ophthalmology*, volume 40, pages 15–34. Karger Publishers.

Einhäuser, W. and König, P. (2003). Does luminance-contrast contribute to a saliency map for overt visual attention? *European journal of neuroscience*, 17(5):1089–1097.

Einhäuser, W., Spain, M., and Perona, P. (2008). Objects predict fixations better than early saliency. *Journal of vision*, 8(14):18–18.

Engbert, R., Nuthmann, A., Richter, E. M., and Kliegl, R. (2005). Swift: a dynamical model of saccade generation during reading. *Psychological review*, 112(4):777.

Erdem, E. and Erdem, A. (2013). Visual saliency estimation by nonlinearly integrating features using region covariances. *Journal of vision*, 13(4):11–11.

Esterman, B. (1982). Functional scoring of the binocular field. *Ophthalmology*, 89(11):1226–1234.

Eusebi, P. (2013). Diagnostic accuracy measures. *Cerebrovascular diseases*, 36(4):267–272.

Fairclough, S. H. and Gilleade, K. (2014). *Advances in physiological computing*. Springer.

Flammer, J., Pache, M., and Resink, T. (2001). Vasospasm, its role in the pathogenesis

of diseases with particular reference to the eye. *Progress in retinal and eye research*, 20(3):319–349.

Foley-Fisher, J. and Murphy, K. S. J. (1987). Simulation of a retinal scotoma by a stabilized retinal image. *Ophthalmic and physiological optics*, 7(4):495–498.

Fortenbaugh, F. C., Hicks, J. C., Hao, L., and Turano, K. A. (2007). Losing sight of the bigger picture: Peripheral field loss compresses representations of space. *Vision research*, 47(19):2506–2520.

Foster, P. J., Buhrmann, R., Quigley, H. A., and Johnson, G. J. (2002). The definition and classification of glaucoma in prevalence surveys. *British journal of ophthalmology*, 86(2):238–242.

Foulsham, T. and Kingstone, A. (2012). Modelling the influence of central and peripheral information on saccade biases in gaze-contingent scene viewing. *Visual cognition*, 20(4-5):546–579.

Foulsham, T., Teszka, R., and Kingstone, A. (2011). Saccade control in natural images is shaped by the information visible at fixation: Evidence from asymmetric gaze-contingent windows. *Attention, perception, & psychophysics*, 73(1):266–283.

Freeman, E. E., Muñoz, B., West, S. K., Jampel, H. D., and Friedman, D. S. (2008). Glaucoma and quality of life: the salisbury eye evaluation. *Ophthalmology*, 115(2):233–238.

Freund, Y. and Schapire, R. E. (1995). A desicion-theoretic generalization of on-line learning and an application to boosting. In *European conference on computational learning theory*, pages 23–37. Springer.

Frey, H.-P., König, P., and Einhäuser, W. (2007). The role of first-and second-order stimulus features for human overt attention. *Perception & psychophysics*, 69(2):153–161.

Friedberg, M. H., Lee, S. M., and Ebner, F. F. (2004). The contribution of the principal and spinal trigeminal nuclei to the receptive field properties of thalamic vpm neurons in the rat. *Journal of neurocytology*, 33(1):75–85.

Fujita, K., Yasuda, N., Oda, K., and Yuzawa, M. (2006). Reading performance in patients with central visual field disturbance due to glaucoma. *Nippon ganka gakkai zasshi*, 110(11):914–918.

Gajewski, D. A., Pearson, A. M., Mack, M. L., Bartlett, F. N., and Henderson, J. M. (2004). Human gaze control in real world search. In *International Workshop on Attention and Performance in Computational Vision*, pages 83–99. Springer.

Gangeddula, V., Ranchet, M., Akinwuntan, A. E., Bollinger, K., and Devos, H. (2017). Effect of cognitive demand on functional visual field performance in senior drivers with glaucoma. *Frontiers in aging neuroscience*, 9:286.

Geringswald, F. and Pollmann, S. (2015). Central and peripheral vision loss differentially affects contextual cueing in visual search. *Journal of experimental psychology: learning, memory, and cognition*, 41(5):1485.

Geruschat, D. R., Hassan, S. E., Turano, K. A., Quigley, H. A., and Congdon, N. G. (2006). Gaze behavior of the visually impaired during street crossing. *Optometry and vision science*, 83(8):550–558.

Ginsburg, R. B. (1984). Some thoughts on autonomy and equality in relation to roe v. wade. *NCL Rev.*, 63:375.

Glen, F. C., Baker, H., and Crabb, D. P. (2014). A qualitative investigation into patients' views on visual field testing for glaucoma monitoring. *BMJ open*, 4(1):e003996.

Glen, F. C., Smith, N. D., and Crabb, D. P. (2013). Saccadic eye movements and face recognition performance in patients with central glaucomatous visual field defects. *Vision research*, 82:42–51.

Glen, F. C., Smith, N. D., and Crabb, D. P. (2015). Impact of superior and inferior visual field loss on hazard detection in a computer-based driving test. *British journal of ophthalmology*, 99(5):613–617.

Glen, F. C., Smith, N. D., Jones, L., and Crabb, D. P. (2016). 'i didn't see that coming': simulated visual fields and driving hazard perception test performance. *Clinical and experimental optometry*, 99(5):469–475.

Goldstein, R. B., Woods, R. L., and Peli, E. (2007). Where people look when watching movies: Do all viewers look at the same place? *Computers in biology and medicine*, 37(7):957–964.

González, E. G., Teichman, J., Lillakas, L., Markowitz, S. N., and Steinbach, M. J. (2006). Fixation stability using radial gratings in patients with age-related macular degeneration. *Canadian journal of ophthalmology/journal canadien d'ophtalmologie*, 41(3):333–339.

Gordon, M. O., Beiser, J. A., Brandt, J. D., Heuer, D. K., Higginbotham, E. J., Johnson, C. A., Keltner, J. L., Miller, J. P., Parrish, R. K., Wilson, M. R., et al. (2002). The ocular hypertension treatment study: baseline factors that predict the onset of primary open-angle glaucoma. *Archives of ophthalmology*, 120(6):714–720.

Greco, A., Rizzo, M. I., De Virgilio, A., Gallo, A., Fusconi, M., and de Vincentiis, M. (2016). Emerging concepts in glaucoma and review of the literature. *The American journal of medicine*, 129(9):1000–e7.

Greiner, M., Pfeiffer, D., and Smith, R. (2000). Principles and practical application of the receiver-operating characteristic analysis for diagnostic tests. *Preventive veterinary medicine*, 45(1-2):23–41.

Grillini, A., Ombelet, D., Soans, R. S., and Cornelissen, F. W. (2018). Towards using the spatio-temporal properties of eye movements to classify visual field defects. In *Proceedings of the 2018 ACM Symposium on Eye Tracking Research & Applications*, pages 1–5.

Halko, N., Martinsson, P.-G., and Tropp, J. A. (2011). Finding structure with randomness: Probabilistic algorithms for constructing approximate matrix decompositions.

SIAM review, 53(2):217–288.

Hartridge, H. and Thomson, L. (1948). Methods of investigating eye movements. *The British journal of ophthalmology*, 32(9):581.

Hastie, T., Rosset, S., Zhu, J., and Zou, H. (2009). Multi-class adaboost. *Statistics and its interface*, 2(3):349–360.

Hayhoe, M., Mennie, N., Sullivan, B., and Gorgos, K. (2005). The role of internal models and prediction in catching balls. In *Proceedings of the american association for artificial intelligence*, pages 1–5.

Henderson, J. M. (2003). Human gaze control during real-world scene perception. *Trends in cognitive sciences*, 7(11):498–504.

Henderson, J. M., Brockmole, J. R., Castelhano, M. S., and Mack, M. (2007). Visual saliency does not account for eye movements during visual search in real-world scenes. In *Eye movements*, pages 537–III. Elsevier.

Henson, D. B. et al. (2000). *Visual fields*, volume 457. Butterworth-Heinemann.

Hoppe, S., Loetscher, T., Morey, S. A., and Bulling, A. (2018). Eye movements during everyday behavior predict personality traits. *Frontiers in human neuroscience*, 12:105.

Hu, C. X., Zangalli, C., Hsieh, M., Gupta, L., Williams, A. L., Richman, J., and Spaeth, G. L. (2014). What do patients with glaucoma see? visual symptoms reported by patients with glaucoma. *The American journal of the medical sciences*, 348(5):403–409.

Hu, S., Smith, N. D., Saunders, L. J., and Crabb, D. P. (2015). Patterns of binocular visual field loss derived from large-scale patient data from glaucoma clinics. *Ophthalmology*, 122(12):2399–2406.

Huey, E. B. (1898). Preliminary experiments in the physiology and psychology of reading. *The American journal of psychology*, 9(4):575–586.

Hysi, P. G., Cheng, C.-Y., Springelkamp, H., Macgregor, S., Bailey, J. N. C., Wojciechowski, R., Vitart, V., Nag, A., Hewitt, A. W., Höhn, R., et al. (2014). Genome-wide analysis of multi-ancestry cohorts identifies new loci influencing intraocular pressure and susceptibility to glaucoma. *Nature genetics*, 46(10):1126.

Iester, M. and Zingirian, M. (2002). Quality of life in patients with early, moderate and advanced glaucoma. *Eye*, 16(1):44–49.

Ikeda, M. and Saida, S. (1978). Span of recognition in reading. *Vision research*, 18(1):83–88.

Irving, E. L., Zacher, J. E., Allison, R. S., and Callender, M. G. (2003). Effects of scleral search coil wear on visual function. *Investigative ophthalmology & visual science*, 44(5):1933–1938.

Ishii, M., Seki, M., Harigai, R., Abe, H., and Fukuchi, T. (2013). Reading performance in patients with glaucoma evaluated using the mnread charts. *Japanese journal of ophthalmology*, 57(5):471–474.

Itti, L. and Koch, C. (2000). A saliency-based search mechanism for overt and covert

shifts of visual attention. *Vision research*, 40(10-12):1489–1506.

Itti, L. and Koch, C. (2001). Computational modelling of visual attention. *Nature reviews neuroscience*, 2(3):194.

Itti, L., Koch, C., and Niebur, E. (1998). A model of saliency-based visual attention for rapid scene analysis. *IEEE Transactions on pattern analysis and machine intelligence*, 20(11):1254–1259.

Jampel, H. D., Singh, K., Lin, S. C., Chen, T. C., Francis, B. A., Hodapp, E., Samples, J. R., and Smith, S. D. (2011). Assessment of visual function in glaucoma: a report by the american academy of ophthalmology. *Ophthalmology*, 118(5):986–1002.

Jansen, L., Onat, S., and König, P. (2009). Influence of disparity on fixation and saccades in free viewing of natural scenes. *Journal of vision*, 9(1):29–29.

Javal, E. (1878). Essai sur la physiologie de la lecture. *Annales d'Ocilistique*, 80:61–73.

Johnson, E. C., Deppmeier, L. M., Wentzien, S. K., Hsu, I., and Morrison, J. C. (2000). Chronology of optic nerve head and retinal responses to elevated intraocular pressure. *Investigative ophthalmology & visual science*, 41(2):431–442.

Jones, K. S. (1972). A statistical interpretation of term specificity and its application in retrieval. *Journal of documentation*.

Jones, P. R., Smith, N. D., Bi, W., and Crabb, D. P. (2019). Portable perimetry using eye-tracking on a tablet computer—a feasibility assessment. *Translational vision science & technology*, 8(1):17–17.

Kaiser, P. K. (2009). Prospective evaluation of visual acuity assessment: a comparison of snellen versus etdrs charts in clinical practice (an aos thesis). *Transactions of the american ophthalmological society*, 107:311.

Kanjee, R., Yücel, Y. H., Steinbach, M. J., González, E. G., and Gupta, N. (2012). Delayed saccadic eye movements in glaucoma. *Eye and brain*, 4:63.

Kasneci, E., Black, A. A., and Wood, J. M. (2017). Eye-tracking as a tool to evaluate functional ability in everyday tasks in glaucoma. *Journal of ophthalmology*, 2017.

Kasneci, E., Sippel, K., Aehling, K., Heister, M., Rosenstiel, W., Schiefer, U., and Papageorgiou, E. (2014). Driving with binocular visual field loss? a study on a supervised on-road parcours with simultaneous eye and head tracking. *PloS one*, 9(2):e87470.

Kasper, H. and Hess, B. J. (1991). Magnetic search coil system for linear detection of three-dimensional angular movements. *IEEE transactions on biomedical engineering*, 38(5):466–475.

Klein, C. and Ettinger, U. (2019). *Eye Movement Research: An Introduction to Its Scientific Foundations and Applications*. Springer Nature.

Krafka, K., Khosla, A., Kellnhofer, P., Kannan, H., Bhandarkar, S., Matusik, W., and Torralba, A. (2016). Eye tracking for everyone. In *Proceedings of the IEEE conference on computer vision and pattern recognition*, pages 2176–2184.

Krauzlis, R. J. (2013). Eye movements. In *Fundamental neuroscience*, pages 697–714. Elsevier.

Krauzlis, R. J., Goffart, L., and Hafed, Z. M. (2017). Neuronal control of fixation and fixational eye movements. *Philosophical transactions of the royal society B: biological sciences*, 372(1718):20160205.

Krekelberg, B. (2011). Microsaccades. *Current biology*, 21(11):R416.

Kruthiventi, S. S., Ayush, K., and Babu, R. V. (2017). Deepfix: A fully convolutional neural network for predicting human eye fixations. *IEEE Transactions on image processing*, 26(9):4446–4456.

Kübler, T. C., Kasneci, E., Rosenstiel, W., Heister, M., Aehling, K., Nagel, K., Schiefer, U., and Papageorgiou, E. (2015). Driving with glaucoma: task performance and gaze movements. *Optometry and vision science*, 92(11):1037–1046.

Kwon, M. and Legge, G. E. (2012). Spatial-frequency requirements for reading revisited. *Vision research*, 62:139–147.

Lagun, D., Manzanares, C., Zola, S. M., Buffalo, E. A., and Agichtein, E. (2011). Detecting cognitive impairment by eye movement analysis using automatic classification algorithms. *Journal of neuroscience methods*, 201(1):196–203.

Lajoie, K., Miller, A. B., Strath, R. A., Neima, D. R., and Marigold, D. S. (2018). Glaucoma-related differences in gaze behavior when negotiating obstacles. *Translational vision science & technology*, 7(4):10–10.

Lalor, S. J., Formankiewicz, M. A., and Waugh, S. J. (2016). Crowding and visual acuity measured in adults using paediatric test letters, pictures and symbols. *Vision research*, 121:31–38.

Lamirel, C., Milea, D., Cochereau, I., Duong, M.-H., and Lorenceau, J. (2014). Impaired saccadic eye movement in primary open-angle glaucoma. *Journal of glaucoma*, 23(1):23–32.

Land, M., Mennie, N., and Rusted, J. (1999). The roles of vision and eye movements in the control of activities of daily living. *Perception*, 28(11):1311–1328.

Land, M. and Tatler, B. (2009). *Looking and acting: vision and eye movements in natural behaviour*. Oxford University Press.

Land, M. F. and Hayhoe, M. (2001). In what ways do eye movements contribute to everyday activities? *Vision research*, 41(25-26):3559–3565.

Land, M. F. and Lee, D. N. (1994). Where we look when we steer. *Nature*, 369(6483):742–744.

Land, M. F. and McLeod, P. (2000). From eye movements to actions: how batsmen hit the ball. *Nature neuroscience*, 3(12):1340–1345.

Larson, A. M. and Loschky, L. C. (2009). The contributions of central versus peripheral vision to scene gist recognition. *Journal of vision*, 9(10):6–6.

Le, A., Mukesh, B. N., McCarty, C. A., and Taylor, H. R. (2003). Risk factors asso-

ciated with the incidence of open-angle glaucoma: the visual impairment project. *Investigative ophthalmology & visual science*, 44(9):3783–3789.

Le Meur, O. and Liu, Z. (2015). Saccadic model of eye movements for free-viewing condition. *Vision research*, 116:152–164.

Lee, S. P., Badler, J. B., and Badler, N. I. (2002). Eyes alive. In *ACM transactions on graphics (TOG)*, volume 21, pages 637–644. ACM.

Lee, S. S.-Y., Black, A. A., and Wood, J. M. (2017). Effect of glaucoma on eye movement patterns and laboratory-based hazard detection ability. *PloS one*, 12(6).

Lee, S. S.-Y., Black, A. A., and Wood, J. M. (2018). Scanning behavior and daytime driving performance of older adults with glaucoma. *Journal of glaucoma*, 27(6):558–565.

Lee, S. S.-Y., Black, A. A., and Wood, J. M. (2019). Eye movements of drivers with glaucoma on a visual recognition slide test. *Optometry and Vision Science*, 96(7):484–491.

Legge, G. E., Klitz, T. S., and Tjan, B. S. (1997). Mr. chips: an ideal-observer model of reading. *Psychological review*, 104(3):524.

Leske, M. C., Connell, A., Schachat, A. P., and Hyman, L. (1994). The barbados eye study: prevalence of open angle glaucoma. *Archives of ophthalmology*, 112(6):821–829.

Leske, M. C., Heijl, A., Hussein, M., Bengtsson, B., Hyman, L., and Komaroff, E. (2003). Factors for glaucoma progression and the effect of treatment: the early manifest glaucoma trial. *Archives of ophthalmology*, 121(1):48–56.

Leske, M. C., Heijl, A., Hyman, L., Bengtsson, B., Dong, L., Yang, Z., Group, E., et al. (2007). Predictors of long-term progression in the early manifest glaucoma trial. *Ophthalmology*, 114(11):1965–1972.

Lewallen, S. and Courtright, P. (1998). Epidemiology in practice: case-control studies. *Community Eye Health*, 11(28):57.

Liu, F. T., Ting, K. M., and Zhou, Z.-H. (2008). Isolation forest. In *2008 Eighth IEEE international conference on data mining*, pages 413–422. IEEE.

Liversedge, S., Gilchrist, I., and Everling, S. (2011). *The Oxford handbook of eye movements*. Oxford University Press.

Loschky, L. C., Larson, A. M., Magliano, J. P., and Smith, T. J. (2015). What would jaws do? the tyranny of film and the relationship between gaze and higher-level narrative film comprehension. *PloS one*, 10(11).

Loschky, L. C., Sethi, A., Simons, D. J., Pydimarri, T. N., Ochs, D., and Corbeille, J. L. (2007). The importance of information localization in scene gist recognition. *Journal of experimental psychology: human perception and performance*, 33(6):1431.

Luo, G., Vargas-Martin, F., and Peli, E. (2008). The role of peripheral vision in saccade planning: learning from people with tunnel vision. *Journal of vision*, 8(14):25–25.

Mackworth, N. H. and Thomas, E. L. (1962). Head-mounted eye-marker camera. *JOSA*,

52(6):713–716.

Malik, R., Baker, H., Russell, R. A., and Crabb, D. P. (2013). A survey of attitudes of glaucoma subspecialists in england and wales to visual field test intervals in relation to nice guidelines. *BMJ open*, 3(5):e002067.

Manabe, H. and Fukumoto, M. (2006). Full-time wearable headphone-type gaze detector. In *CHI'06 extended abstracts on Human factors in computing systems*, pages 1073–1078.

Mannan, S., Ruddock, K., and Wooding, D. (1997). Fixation sequences made during visual examination of briefly presented 2d images. *Spatial vision*, 11(2):157–178.

Mannan, S. K., Ruddock, K. H., and Wooding, D. S. (1996). The relationship between the locations of spatial features and those of fixations made during visual examination of briefly presented images. *Spatial vision*, 10(3):165–188.

Manning, C. D., Raghavan, P., and Schütze, H. (2008). *Introduction to information retrieval*. Cambridge university press.

Marsman, J.-B. C., Cornelissen, F. W., Dorr, M., Vig, E., Barth, E., and Renken, R. J. (2016). A novel measure to determine viewing priority and its neural correlates in the human brain. *Journal of vision*, 16(6):3–3.

Martinez-Conde, S., Macknik, S. L., Troncoso, X. G., and Hubel, D. H. (2009). Microsaccades: a neurophysiological analysis. *Trends in neurosciences*, 32(9):463–475.

McIlreavy, L., Fiser, J., and Bex, P. (2012). Impact of simulated central scotomas on visual search in natural scenes. *Optometry and vision science: official publication of the American Academy of Optometry*, 89(9):1385.

McKendrick, A. M., Sampson, G. P., Walland, M. J., and Badcock, D. R. (2007). Contrast sensitivity changes due to glaucoma and normal aging: low-spatial-frequency losses in both magnocellular and parvocellular pathways. *Investigative ophthalmology & visual science*, 48(5):2115–2122.

Medeiros, F. A., Weinreb, R. N., Boer, E., and Rosen, P. N. (2012). Driving simulation as a performance-based test of visual impairment in glaucoma. *Journal of glaucoma*, 21(4):221.

Mihailovic, A., Swenor, B. K., Friedman, D. S., West, S. K., Gitlin, L. N., and Ramulu, P. Y. (2017). Gait implications of visual field damage from glaucoma. *Translational vision science & technology*, 6(3):23–23.

Miller, A. B., Lajoie, K., Strath, R. A., Neima, D. R., and Marigold, D. S. (2018). Coordination of gaze behavior and foot placement during walking in persons with glaucoma. *Journal of glaucoma*, 27(1):55–63.

Mills, R. P. and Drance, S. M. (1986). Esterman disability rating in severe glaucoma. *Ophthalmology*, 93(3):371–378.

Mital, P. K., Smith, T. J., Hill, R. L., and Henderson, J. M. (2011). Clustering of gaze during dynamic scene viewing is predicted by motion. *Cognitive Computation*, 3(1):5–

24.

Mitchell, P., Lee, A. J., Wang, J. J., and Rochtchina, E. (2005). Intraocular pressure over the clinical range of blood pressure: blue mountains eye study findings. *American journal of ophthalmology*, 140(1):131–132.

Moeller, G. U., Kayser, C., Knecht, F., and König, P. (2004). Interactions between eye movement systems in cats and humans. *Experimental brain research*, 157(2):215–224.

Momont, A. C. and Mills, R. P. (2013). Glaucoma screening: current perspectives and future directions. In *Seminars in ophthalmology*, volume 28, pages 185–190. Taylor & Francis.

Murata, N., Miyamoto, D., Togano, T., and Fukuchi, T. (2017). Evaluating silent reading performance with an eye tracking system in patients with glaucoma. *Plos one*, 12(1).

Murphy, K. S. J. and Foley-Fisher, J. (1989). Effect of a scotoma on eye movements during visual search. *Ophthalmic and physiological optics*, 9(3):317–321.

Najemnik, J. and Geisler, W. S. (2005). Optimal eye movement strategies in visual search. *Nature*, 434(7031):387.

Najjar, R. P., Sharma, S., Drouet, M., Leruez, S., Baskaran, M., Nongpiur, M. E., Aung, T., Fielding, J., White, O., Girard, M. J., et al. (2017). Disrupted eye movements in preperimetric primary open-angle glaucoma. *Investigative ophthalmology & visual science*, 58(4):2430–2437.

Noiret, N., Vigneron, B., Diogo, M., Vandel, P., and Laurent, É. (2017). Saccadic eye movements: what do they tell us about aging cognition? *Aging, neuropsychology, and cognition*, 24(5):575–599.

Nuthmann, A. (2014). How do the regions of the visual field contribute to object search in real-world scenes? evidence from eye movements. *Journal of experimental psychology: human perception and performance*, 40(1):342.

Nuthmann, A. and Henderson, J. M. (2010). Object-based attentional selection in scene viewing. *Journal of vision*, 10(8):20–20.

Onat, S., Libertus, K., and König, P. (2007). Integrating audiovisual information for the control of overt attention. *Journal of vision*, 7(10):11–11.

Owen, V. M., Crabb, D. P., White, E. T., Viswanathan, A. C., Garway-Heath, D. F., and Hitchings, R. A. (2008). Glaucoma and fitness to drive: using binocular visual fields to predict a milestone to blindness. *Investigative ophthalmology & visual science*, 49(6):2449–2455.

Owsley, C. and McGwin Jr, G. (2010). Vision and driving. *Vision research*, 50(23):2348–2361.

Parker, B. J., Günter, S., and Bedo, J. (2007). Stratification bias in low signal microarray studies. *BMC bioinformatics*, 8(1):326.

Parkhurst, D., Culurciello, E., and Niebur, E. (2000). Evaluating variable resolution displays with visual search: Task performance and eye movements. In *Proceedings*

of the 2000 symposium on Eye tracking research & applications, pages 105–109.

Parkhurst, D. J. and Niebur, E. (2003). Scene content selected by active vision. *Spatial vision*, 16(2):125–154.

Parkhurst, D. J. and Niebur, E. (2004). Texture contrast attracts overt visual attention in natural scenes. *European journal of neuroscience*, 19(3):783–789.

Pedregosa, F., Varoquaux, G., Gramfort, A., Michel, V., Thirion, B., Grisel, O., Blondel, M., Prettenhofer, P., Weiss, R., Dubourg, V., et al. (2011). Scikit-learn: Machine learning in python. *Journal of machine learning research*, 12(Oct):2825–2830.

Pelli, D., Robson, J., et al. (1988). The design of a new letter chart for measuring contrast sensitivity. In *Clinical vision sciences*. Citeseer.

Pelz, J. B. and Canosa, R. (2001). Oculomotor behavior and perceptual strategies in complex tasks. *Vision research*, 41(25-26):3587–3596.

Peng, F. and Schuurmans, D. (2003). Combining naive bayes and n-gram language models for text classification. In *European conference on information retrieval*, pages 335–350. Springer.

Penzel, T., Lo, C.-C., Ivanov, P., Kesper, K., Becker, H., and Vogelmeier, C. (2006). Analysis of sleep fragmentation and sleep structure in patients with sleep apnea and normal volunteers. In *2005 IEEE Engineering in medicine and biology 27th annual conference*, pages 2591–2594. IEEE.

Peters, R. J., Peters, R. J., Iyer, A., Itti, L., and Koch, C. (2005). Components of bottom-up gaze allocation in natural images. *Vision research*, 45(18):2397–2416.

Pezzullo, L., Streatfeild, J., Simkiss, P., and Shickle, D. (2018). The economic impact of sight loss and blindness in the uk adult population. *BMC health services research*, 18(1):63.

Pizzi, L. T., Waisbourd, M., Hark, L., Sembhi, H., Lee, P., Crews, J. E., Saaddine, J. B., Steele, D., and Katz, L. J. (2018). Costs of a community-based glaucoma detection programme: analysis of the philadelphia glaucoma detection and treatment project. *British journal of ophthalmology*, 102(2):225–232.

Porterfield, W. (1737). An essay concerning the motions of our eyes. part i. of their external motions. *Edinburgh medical essays and observations*, 3:160–263.

Prum, B. E., Rosenberg, L. F., Gedde, S. J., Mansberger, S. L., Stein, J. D., Moroi, S. E., Herndon, L. W., Lim, M. C., and Williams, R. D. (2016). Primary open-angle glaucoma preferred practice pattern® guidelines. *Ophthalmology*, 123(1):P41–P111.

Purves, D., Augustine, G. J., Fitzpatrick, D., Hall, W., LaMantia, A.-S., McNamara, J. O., and White, L. (2001). Neuroscience. sunderland. *MA: Sinauer Associates*.

Quartilho, A., Simkiss, P., Zekite, A., Xing, W., Wormald, R., and Bunce, C. (2016). Leading causes of certifiable visual loss in england and wales during the year ending 31 march 2013. *Eye*, 30(4):602.

Quigley, H. A. (1996). Number of people with glaucoma worldwide. *British journal of*

ophthalmology, 80(5):389–393.

Quigley, H. A. and Broman, A. T. (2006). The number of people with glaucoma worldwide in 2010 and 2020. *British journal of ophthalmology*, 90(3):262–267.

Quigley, H. A., West, S. K., Rodriguez, J., Munoz, B., Klein, R., and Snyder, R. (2001). The prevalence of glaucoma in a population-based study of hispanic subjects: Proyecto ver. *Archives of ophthalmology*, 119(12):1819–1826.

Rahimy, E. (2018). Deep learning applications in ophthalmology. *Current opinion in ophthalmology*, 29(3):254–260.

Ramdas, W. D., van Koolwijk, L. M., Lemij, H. G., Pasutto, F., Cree, A. J., Thorleifsson, G., Janssen, S. F., Jacoline, t. B., Amin, N., Rivadeneira, F., et al. (2011). Common genetic variants associated with open-angle glaucoma. *Human molecular genetics*, 20(12):2464–2471.

Ramulu, P. (2009). Glaucoma and disability: which tasks are affected, and at what stage of disease? *Current opinion in ophthalmology*, 20(2):92.

Rayner, K. (1998). Eye movements in reading and information processing: 20 years of research. *Psychological bulletin*, 124(3):372.

Robertson, S. (2004). Understanding inverse document frequency: on theoretical arguments for idf. *Journal of documentation*.

Robinson, D. A. (1963). A method of measuring eye movemnent using a scieral search coil in a magnetic field. *IEEE Transactions on bio-medical electronics*, 10(4):137–145.

Rothkopf, C. A., Ballard, D. H., and Hayhoe, M. M. (2007). Task and context determine where you look. *Journal of vision*, 7(14):16–16.

Rucci, M. and Poletti, M. (2015). Control and functions of fixational eye movements. *Annual review of vision science*, 1:499–518.

Rudnicka, A. R., Mt-Isa, S., Owen, C. G., Cook, D. G., and Ashby, D. (2006). Variations in primary open-angle glaucoma prevalence by age, gender, and race: a bayesian meta-analysis. *Investigative ophthalmology & visual science*, 47(10):4254–4261.

Saunders, D. R. and Woods, R. L. (2014). Direct measurement of the system latency of gaze-contingent displays. *Behavior research methods*, 46(2):439–447.

Scholes, S., Neave, A., et al. (2013). Health survey for england 2016: Physical activity in adults. *Health & Social Care Information Centre Retrieved from http://www. hscic. gov. uk/catalogue/PUB13218/HSE201*.

Schölkopf, B., Smola, A., and Müller, K.-R. (1998). Nonlinear component analysis as a kernel eigenvalue problem. *Neural computation*, 10(5):1299–1319.

Schütz, A. C., Braun, D. I., and Gegenfurtner, K. R. (2011). Eye movements and perception: A selective review. *Journal of vision*, 11(5):9–9.

Sethi, S., Fay, C., and Bollinger, K. E. (2013). Functional testing in glaucoma diagnosis. *Current ophthalmology reports*, 1(2):89–97.

Shabana, N., Pérès, V. C., Carkeet, A., and Chew, P. T. (2003). Motion perception in

glaucoma patients: a review. *Survey of ophthalmology*, 48(1):92–106.

Sippel, K., Kasneci, E., Aehling, K., Heister, M., Rosenstiel, W., Schiefer, U., and Papageorgiou, E. (2014). Binocular glaucomatous visual field loss and its impact on visual exploration-a supermarket study. *PloS one*, 9(8):e106089.

Smith, J. R., Cronin, M. J., and Karacan, I. (1971). A multichannel hybrid system for rapid eye movement detection (rem detection). *Computers and biomedical research*, 4(3):275–290.

Smith, N., Crabb, D., Glen, F., Burton, R., and Garway-Heath, D. (2012). Eye movements in patients with glaucoma when viewing images of everyday scenes. *Seeing and perceiving*, 25(5):471.

Smith, N., Rubin, G., Garway-Heath, D., and Crabb, D. (2008). Exploring eye movements in glaucomatous patients when viewing natural photographs. *Investigative ophthalmology & visual science*, 49(13):1110–1110.

Smith, N. D., Crabb, D. P., and Garway-Heath, D. F. (2011). An exploratory study of visual search performance in glaucoma. *Ophthalmic and physiological optics*, 31(3):225–232.

Smith, N. D., Glen, F. C., Mönter, V. M., and Crabb, D. P. (2014). Using eye tracking to assess reading performance in patients with glaucoma: a within-person study. *Journal of ophthalmology*, 2014.

Smith, T. J. (2013). Watching you watch movies: Using eye tracking to inform film theory.

Smith, T. J. and Mital, P. K. (2013). Attentional synchrony and the influence of viewing task on gaze behavior in static and dynamic scenes. *Journal of vision*, 13(8):16–16.

Sohn, J.-w. and Lee, D. (2006). Effects of reward expectancy on sequential eye movements in monkeys. *Neural networks*, 19(8):1181–1191.

Sommer, A., Tielsch, J. M., Katz, J., Quigley, H. A., Gottsch, J. D., Javitt, J., and Singh, K. (1991). Relationship between intraocular pressure and primary open angle glaucoma among white and black americans: the baltimore eye survey. *Archives of ophthalmology*, 109(8):1090–1095.

Springelkamp, H., Iglesias, A. I., Mishra, A., Höhn, R., Wojciechowski, R., Khawaja, A. P., Nag, A., Wang, Y. X., Wang, J. J., Cuellar-Partida, G., et al. (2017). New insights into the genetics of primary open-angle glaucoma based on meta-analyses of intraocular pressure and optic disc characteristics. *Human molecular genetics*, 26(2):438–453.

Tatham, A. J., Boer, E. R., Rosen, P. N., Della Penna, M., Meira-Freitas, D., Weinreb, R. N., Zangwill, L. M., and Medeiros, F. A. (2014). Glaucomatous retinal nerve fiber layer thickness loss is associated with slower reaction times under a divided attention task. *American journal of ophthalmology*, 158(5):1008–1017.

Tatler, B. W. (2007). The central fixation bias in scene viewing: Selecting an optimal

viewing position independently of motor biases and image feature distributions. *Journal of vision*, 7(14):4–4.

Tatler, B. W., Baddeley, R. J., and Gilchrist, I. D. (2005). Visual correlates of fixation selection: Effects of scale and time. *Vision research*, 45(5):643–659.

Tatler, B. W., Hayhoe, M. M., Land, M. F., and Ballard, D. H. (2011). Eye guidance in natural vision: Reinterpreting salience. *Journal of vision*, 11(5):5–5.

Tatler, B. W. and Vincent, B. T. (2009). The prominence of behavioural biases in eye guidance. *Visual Cognition*, 17(6-7):1029–1054.

Tham, Y.-C., Li, X., Wong, T. Y., Quigley, H. A., Aung, T., and Cheng, C.-Y. (2014). Global prevalence of glaucoma and projections of glaucoma burden through 2040: a systematic review and meta-analysis. *Ophthalmology*, 121(11):2081–2090.

Thorpe, S. J., Gegenfurtner, K. R., Fabre-Thorpe, M., and BuÈlthoff, H. H. (2001). Detection of animals in natural images using far peripheral vision. *European journal of neuroscience*, 14(5):869–876.

Torralba, A. and Oliva, A. (2003). Statistics of natural image categories. *Network: computation in neural systems*, 14(3):391–412.

Tseng, P.-H., Cameron, I. G., Pari, G., Reynolds, J. N., Munoz, D. P., and Itti, L. (2013). High-throughput classification of clinical populations from natural viewing eye movements. *Journal of neurology*, 260(1):275–284.

Tseng, P.-H., Carmi, R., Cameron, I. G., Munoz, D. P., and Itti, L. (2009). Quantifying center bias of observers in free viewing of dynamic natural scenes. *Journal of vision*, 9(7):4–4.

Turalba, A. V. and Grosskreutz, C. (2010). A review of current technology used in evaluating visual function in glaucoma. In *Seminars in ophthalmology*, volume 25, pages 309–316. Taylor & Francis.

Turano, K. A., Broman, A. T., Bandeen-Roche, K., Munoz, B., Rubin, G. S., West, S. K., Team, S. P., et al. (2004). Association of visual field loss and mobility performance in older adults: Salisbury eye evaluation study. *Optometry and vision science*, 81(5):298–307.

Vega, R. P., van Leeuwen, P. M., Vélez, E. R., Lemij, H. G., and de Winter, J. C. (2013). Obstacle avoidance, visual detection performance, and eye-scanning behavior of glaucoma patients in a driving simulator: a preliminary study. *PloS one*, 8(10):e77294.

Victor, T. W., Harbluk, J. L., and Engström, J. A. (2005). Sensitivity of eye-movement measures to in-vehicle task difficulty. *Transportation research part F: traffic psychology and behaviour*, 8(2):167–190.

Vig, E., Dorr, M., and Barth, E. (2009). Efficient visual coding and the predictability of eye movements on natural movies. *Spatial vision*, 22(5):397–408.

Vincent, B. T., Baddeley, R., Correani, A., Troscianko, T., and Leonards, U. (2009). Do we look at lights? using mixture modelling to distinguish between low-and high-level

factors in natural image viewing. *Visual cognition*, 17(6-7):856–879.

Wade, N., Tatler, B. W., et al. (2005). *The moving tablet of the eye: The origins of modern eye movement research*. Oxford University Press, USA.

Wang, H. X., Freeman, J., Merriam, E. P., Hasson, U., and Heeger, D. J. (2012). Temporal eye movement strategies during naturalistic viewing. *Journal of vision*, 12(1):16–16.

Wang, J. J., Mitchell, P., and Smith, W. (1997). Is there an association between migraine headache and open-angle glaucoma?: findings from the blue mountains eye study. *Ophthalmology*, 104(10):1714–1719.

Wang, X., Rumpel, H., Lim, W. E. H., Baskaran, M., Perera, S. A., Nongpiur, M. E., Aung, T., Milea, D., and Girard, M. J. (2016). Finite element analysis predicts large optic nerve head strains during horizontal eye movements. *Investigative ophthalmology & visual science*, 57(6):2452–2462.

Weinreb, R. N., Aung, T., and Medeiros, F. A. (2014). The pathophysiology and treatment of glaucoma: a review. *Jama*, 311(18):1901–1911.

Weinreb, R. N. and Khaw, P. T. (2004). Primary open-angle glaucoma. *The Lancet*, 363(9422):1711–1720.

Weinreb, R. N., Leung, C. K., Crowston, J. G., Medeiros, F. A., Friedman, D. S., Wiggs, J. L., and Martin, K. R. (2016). Primary open-angle glaucoma. *Nature reviews disease primers*, 2(1):1–19.

Wiecek, E. W., Pasquale, L. R., Fiser, J., Dakin, S., and Bex, P. J. (2012). Effects of peripheral visual field loss on eye movements during visual search. *Frontiers in psychology*, 3:472.

Willard, A. and Lueck, C. J. (2014). Ocular motor disorders. *Current opinion in neurology*, 27(1):75–82.

Williams, C. C. and Castelhano, M. S. (2019). The changing landscape: High-level influences on eye movement guidance in scenes. *Vision*, 3(3):33.

Wong, S. H. and Plant, G. T. (2015). How to interpret visual fields. *Practical neurology*, 15(5):374–381.

Wong, T.-T. (2015). Performance evaluation of classification algorithms by k-fold and leave-one-out cross validation. *Pattern recognition*, 48(9):2839–2846.

Wood, E. and Bulling, A. (2014). Eyetab: Model-based gaze estimation on unmodified tablet computers. In *Proceedings of the Symposium on Eye Tracking Research and Applications*, pages 207–210.

Wu, H. C., Luk, R. W. P., Wong, K. F., and Kwok, K. L. (2008). Interpreting tf-idf term weights as making relevance decisions. *ACM Transactions on Information Systems (TOIS)*, 26(3):1–37.

Yarbus, A. L. (1967). Eye movements during perception of complex objects. In *Eye movements and vision*, pages 171–211. Springer.

Zetzsche, C., Schill, K., Deubel, H., Krieger, G., Umkehrer, E., and Beinlich, S. (1998).

Investigation of a sensorimotor system for saccadic scene analysis: an integrated approach. In *Proc. 5th Int. Conf. Simulation Adaptive Behav*, volume 5, pages 120–126.

Zhao, Q. and Koch, C. (2013). Learning saliency-based visual attention: A review. *Signal Processing*, 93(6):1401–1407.

Zweig, M. H. and Campbell, G. (1993). Receiver-operating characteristic (roc) plots: a fundamental evaluation tool in clinical medicine. *Clinical chemistry*, 39(4):561–577.